Master's thesis

NTNU
Norwegian University of Science and Technology
Faculty of Natural Sciences

Johanne Bratland Tjernshaugen

Beyond the Chandrasekhar-Clogston limit in a spin-split superconductor driven out of equilibrium by a spin-accumulation

Master's thesis in Physics
Supervisor: Jacob Linder
Co-supervisor: Morten Amundsen
May 2023

NTNU
Norwegian University of
Science and Technology

Summary

A thin-film spin-split superconductor connected to normal metal reservoirs driven out of equilibrium by a spin dependent voltage is studied numerically in the quasi-classical Keldysh-Usadel framework. Two setups are considered: one in which the spin dependent chemical potentials are shifted oppositely in the reservoirs (setup A) and one where they are shifted in the same way in both reservoirs (setup B). Phase diagrams showing the regions of superconductivity, bistability and the normal state for various spin-voltages and spin-splitting fields are calculated for both setups. A bulk superconductor in equilibrium can only coexist with spin-splitting fields smaller than the Chandrasekhar-Clogston limit $m < \Delta_0/\sqrt{2}$, but when driven out of equilibrium this limit can be surpassed. In setup B, we find that superconductivity is recovered when $m - eV_s < \Delta_0$. This is attributed to how the spin-splitting field and the voltage shows up in the gap equation, demonstrating that the combined effect of a spin-splitting field and a voltage is an effective field $m_{eff} = m - eV_s$. In setup A, superconductivity is recovered when $m \approx eV_s$, but the gap is spatially inhomogeneous due to an increased effective spin-splitting field at one interface, and a decreased field at the other interface. This reveals the appearance of the FFLO state in the superconductor.

Sammendrag

En spinn-splittet superledende film koblet til normalmetall-reservoarer drevet ut av likevekt av en spinnavhengig spenning blir undersøkt numerisk ved å løse den kvasiklassiske Usadelligningen. To ulike oppsett blir undersøkt: ett hvor det spinnavhenginge kjemiske potensialet er forskjøvet på motsatt måte i de to reservoarene (oppsett A) og ett hvor det er forskjøvet på samme måte (oppsett B). Fasediagrammer som viser hvilke parametersett som gir superledning, bistabilitet og normaltilstand blir beregnet for begge oppsettene. En bulk superleder i likevekt kan eksistere sammen med et spinn-splittende felt mindre enn Chandrasekhar-Clogston-grensen $m < \Delta_0/\sqrt{2}$, men ute av likevekt er det mulig å overskride denne grensen. I oppsett B finner vi at superledning gjenopprettes når $m - eV_s < \Delta_0$. Dette forklares med at det spin-splittende feltet og spinn-spenningen opptrer som et effektivt spinn-splittende felt $m_{eff} = m - eV_s$ i gapligningen. I oppsett A opprettholdes den superledende tilstanden når $m \approx eV_s$, men det superledende gapet er romlig inhomogent grunnet et økt effektivt spinn-splittende felt på den ene siden av superlederen, og et minket felt på den andre siden. Dette demonstrerer at superlederen er i en tilstand kjent som FFLO-tilstanden.

Preface

This thesis was submitted after a two years' Master's degree in physics at the Norwegian University of Science and Technology (NTNU), and it amounts to 60 ECTS credits. The most time-consuming part of the work has been to write, test, and execute a program that solves the Usadel equation self-consistently and out of equilibrium. The resulting code is given in appendix A.

I want to thank my supervisor, Jacob Linder, for answering my endless amount of questions in our weekly meetings over the past two years. Our discussions have been inspiring and helpful, and I look forward to our continued collaboration. I also want to thank my co-supervisor, Morten Amundsen, for patiently helping me overcome my problems with the numerical code. Finally, I would like to thank my partner, Magnus, for your encouragement and support, and for reminding me from time to time that there exists a life outside physics as well.

Contents

1 Notation and conventions

This thesis uses natural units, where Planck's reduced constant $\hbar$, Boltzmann's constant k_B, the speed of light c, the vacuum permittivity ϵ_0 and permeability μ_0, and the gravitational constant $4\pi G$ are all normalized to unity. The electron charge is $e = -|e|$. Complex numbers are written $z = x + iy$ where i is the imaginary unit, and the superscript * is used for complex conjugation.

Three-dimensional vectors are written in bold typeface as $\mathbf{A}$. Cartesian unit vectors are denoted by $\mathbf{e}_x, \mathbf{e}_y, \mathbf{e}_z$. Partial derivatives are written $\partial_x \equiv \partial/\partial_x$, and the operator $\nabla = \partial_x \mathbf{e}_x + \partial_y \mathbf{e}_y + \partial_z \mathbf{e}_z$.

Many matrices of different dimensions will be encountered. For 2×2 matrices, no additional notation is introduced. 4×4 matrices are specified with a hat $\hat{A}$, and 8×8 matrices are denoted $\check{A}$. Commutators are written with square brackets $[A, B] = AB - BA$, and anticommutators with curly brackets $\{A, B\} = AB + BA$. The superscript † is used for Hermitian conjugation and ^{T} is used for the matrix transpose.

The multiplication of matrices with different dimensions is resolved by taking Kronecker products with appropriate identity matrices, for example

$$\hat{A}\check{B} = \begin{pmatrix} \hat{A} & 0 \\ 0 & \hat{A} \end{pmatrix} \check{B}. \tag{1.1}$$

The Pauli matrices are

$$\sigma_x = \begin{pmatrix} 0 & 1 \\ 1 & 0 \end{pmatrix} \qquad \sigma_y = \begin{pmatrix} 0 & -i \\ i & 0 \end{pmatrix} \qquad \sigma_z = \begin{pmatrix} 1 & 0 \\ 0 & -1 \end{pmatrix}, \tag{1.2}$$

and the Pauli matrix vector $\boldsymbol{\sigma} \equiv \sigma_x \mathbf{e}_x + \sigma_y \mathbf{e}_y + \sigma_z \mathbf{e}_z$.

The Dirac delta function $\delta(x)$ is defined by

$$\int_{-\infty}^{\infty} f(x)\delta(x)\mathrm{d}x = f(0). \tag{1.3}$$

2 Superconductivity

2.1 Introduction

Superconductivity is a remarkable phenomenon in which certain conductors exhibit zero electrical resistance and perfect diamagnetism when cooled below a critical temperature T_c. The discovery of superconductivity dates back to 1911, when Heike Onnes observed that mercury's electrical resistance vanished below 4.2 K [1]. At the time quantum mechanics was not yet born, and the underlying mechanism of the phenomenon remained a mystery. In 1933, a discovery was made by Meissner and Ochsenfeld. They realized that a superconductor is a perfect diamagnet and that magnetic flux can only penetrate a thin layer near the surface [2], and this became known as *the Meissner effect*. A fully microscopic theory for superconductivity explaining the phenomenon from first principles was published in 1957 by Bardeen, Cooper and Schrieffer [3]. The BCS theory proposed that a weak, attractive interaction between electrons caused the formation of Cooper pairs, which consist of two entangled electrons with opposite spin and momenta. A gap in the electronic band structure was also predicted.

Superconductors are divided into two categories depending on how they respond to an external magnetic field [4]. Type I superconductors switch abruptly from the Meissner state, corresponding to complete screening, to the normal state with full penetration of magnetic flux when the field reaches a critical strength h_c. Type II superconductors exhibit a phase in between the Meissner state and the normal state in which magnetic flux is allowed to partially penetrate the material through vortices. In the Meissner state, screening currents occur because the electrons moving in a magnetic field are affected by the Lorentz force. When the currents become large enough, the kinetic energy is too large to favor the superconducting state over the normal state. This is known as the orbital effect. In thin films with an in-plane magnetic field, the orbital effect can be neglected because the currents perpendicular to the plane are suppressed [5]. In such thin films, the magnetic field manifests as a spin-splitting field, causing the electronic bands for different spins to be split, which again causes pair breaking. This is known as the paramagnetic effect, and together with the orbital effect it is responsible for trying to prevent the coexistence of magnetism and superconductivity.

When a superconductor is in contact with a non-superconducting material, new phases can arise due to the proximity effect. The proximity effect is the process by which properties of adjacent materials leak into one another, creating a region with

properties derived from both materials. A phenomenon related to the proximity effect is Andreev reflection [6], which can be understood by considering a superconductor in contact with a normal metal. An electron in the normal metal with energy lower than the superconducting gap is approaching the interface to the superconductor. It cannot enter the superconductor because no quasiparticle states exist for such an energy. The electron has several possibilities to overcome this obstacle. It could for example be reflected at the interface, or it could tunnel through the superconductor. Another option is to be Andreev retroreflected as a hole. The electron then pairs up with another electron at the interface leaving a hole behind, and the electrons enter the superconductor as a Cooper pair. The reflected hole is phase coherent with the Cooper pair, and will therefore carry information about the superconducting correlations into the normal metal. The proximity effect is an essential ingredient in for example superconducting spintronics.

Superconducting spintronics is an emerging field that offers exciting possibilities for novel technology [7–10]. Spintronics is a field that utilizes the spin property of electrons to store, process, and manipulate information in electronic devices. Spin is an intrinsic angular momentum of electrons, and along a given quantization axis it can have two values: up or down. This binary structure makes the spin a natural choice for information carrier, as the fundamental building blocks in digital electronics consist of 0s and 1s. One common example of a device based on concepts from spintronics is the hard disk drive (HDD), which is a storage device used in most computers. The storage capacity of the HDD was increased drastically by the introduction of giant magnetoresistance [11, 12], which is the observation that the resistance of a ferromagnet/normal metal/ferromagnet junction depends on the relative orientation of the magnetization in the ferromagnets. Switching the alignment of the spins in one of the ferromagnets creates a different current signal, and this can be used to code information. The dissipationless currents in a superconductor have the potential to reduce the power consumption of electronic devices. The marriage of the energy efficient superconductors and the increased functionality of utilizing electronic spins as information carriers is therefore an intriguing idea. Superconducting order can enhance central effects in spintronics such as magnetoresistance and open up for more energy-efficient computing, and superconducting spintronics is an area of great research interest.

In electronic devices, there can be magnetic elements. Superconductivity is easily destroyed by magnetic fields, so for the realization of superconducting spintronics it is crucial to develop methods for restoring superconductivity in contact with magnetic materials. This thesis is dedicated to exploring how the superconducting

state can be restored for high spin-splitting fields. Additionally, the analytical and numerical framework established in this thesis sets the stage to explore further non-equilibrium effects in spin-split superconductors that have not been studied previously, such as crossed Andreev reflection [13].

In this chapter, we describe two fundamental objects in condensed matter physics, namely field operators and Green functions. We proceed to derive a mean-field Hamiltonian describing superconducting systems, and we explore how a spin-splitting field affects superconductivity. In chapter 3, the quasiclassical Keldysh-Usadel formalism is introduced and a transport equation for the relevant Green function is derived. In chapter 4, the non-equilibrium distribution function is introduced. In chapter 5, parametrized transport equations are derived, and the numerical framework for solving and interpreting the results of these equations are presented. Chapter 6 presents the exact setup used and the results obtained. The thesis is concluded with a summary and outlook in chapter 7.

2.2 Field operators and Green functions

In quantum mechanics, a system is described by a wave function that solves the relevant Schrödinger equation, and any quantum mechanical observable can be calculated from the wave function [14]. However, many systems are cumbersome or impossible to describe using quantum mechanics. In many-body systems, for example, it is close to impossible to keep track of the wave function of every single particle. In some systems, particles might be created or annihilated, and quantum mechanics does not account for that. This demonstrates the need for quantum field theory.

Quantum field theory introduces the operators $c_\alpha^\dagger$ and c_α which create and annihilate a particle in the state associated with the quantum numbers α, respectively. The quantum numbers contained in α could for example be momentum $\mathbf{k}$ and spin σ. The creation and annihilation operators act on vectors in Fock space, which houses all possible many-particle states. In superconducting systems, we are mostly concerned with electrons, which are fermions. Fermionic creation and annihilation operators satisfy the anticommutation relations

$$\left\{c_\alpha^\dagger, c_\alpha\right\} = \delta_{\alpha\alpha'}, \qquad \left\{c_\alpha, c_\alpha\right\} = \left\{c_\alpha^\dagger, c_\alpha^\dagger\right\} = 0. \tag{2.1}$$

The operators $c_{\mathbf{k}\sigma}, c_{\mathbf{k}\sigma}^\dagger$ can be Fourier transformed from the momentum basis to the

position basis, giving the field operators

$$\psi_\sigma^\dagger(\mathbf{r}) = \sum_{\mathbf{k}} c_{\mathbf{k}\sigma}^\dagger \, \mathrm{e}^{-i\mathbf{k}\cdot\mathbf{r}} \qquad \psi_\sigma(\mathbf{r}) = \sum_{\mathbf{k}} c_{\mathbf{k}\sigma} \, \mathrm{e}^{i\mathbf{k}\cdot\mathbf{r}} \, . \tag{2.2}$$

The field operators satisfy the same anticommutation relations as the creation and annihilation operators. $\psi_\sigma^\dagger(\mathbf{r})$ is interpreted as an operator that creates a particle with spin σ at the position $\mathbf{r}$, while $\psi_\sigma(\mathbf{r})$ destroys such a particle. In the Heisenberg picture, operators are time-dependent and their time evolution is governed by the Heisenberg equation,

$$i\frac{\partial \psi_\sigma^\dagger(\mathbf{r})}{\partial t} = \big[H, \psi_\sigma^\dagger(\mathbf{r})\big], \tag{2.3}$$

$$i\frac{\partial \psi_\sigma(\mathbf{r})}{\partial t} = [H, \psi_\sigma(\mathbf{r})], \tag{2.4}$$

where the right-hand side is a commutator between the second-quantized Hamilton operator H and the field operator.

Green functions can loosely be thought of as the quantum many-particle physics analogy to the wave functions in quantum mechanics, and they are a powerful tool. Green functions are correlation functions between two field operators, describing the evolution of one state into another state. There exist several versions of Green functions, but one with an easy interpretation is the time-ordered Green function,

$$G_{\sigma_1\sigma_2}(\mathbf{r}_1, t_1; \mathbf{r}_2, t_2) = -i\langle \mathcal{T}\psi_\sigma(\mathbf{r}_1, t_1)\psi_{\sigma_2}^\dagger(\mathbf{r}_2, t_2)\rangle. \tag{2.5}$$

The time ordering operator $\mathcal{T}$ ensures that the field operators act in chronological order. Assuming $t_1 > t_2$, the Green function is interpreted as the probability amplitude for finding a particle at $(\mathbf{r}_1, t_1)$, provided that a particle was inserted at $(\mathbf{r}_2, t_2)$.

Mathematically, a Green function $G(x, s)$ of a linear operator $\mathcal{L}(x)$ is a solution to

$$\mathcal{L}(x)G(x, s) = \delta(x - s). \tag{2.6}$$

Green functions are particularly useful when solving the inhomogeneous equation $\mathcal{L}(x)u(x) = f(x)$, because the solution can be expressed via a Green function: $u(x) = \int G(x, s)f(s)\mathrm{d}s$.

2.3 The superconducting Hamiltonian

The starting point for the BCS theory is that there exists an effective attractive interaction between electrons. The origin of this interaction was initially taken to be phonons, which are quasiparticles describing quantized lattice vibrations, but

superconductivity can be mediated by any interaction as long as it is attractive in a thin shell around the Fermi surface. The Hamiltonian describing a general attractive spin-independent electron-electron interaction is

$$H = \frac{1}{2}\int \mathrm{d}\mathbf{r}\mathrm{d}\mathbf{r}' V(\mathbf{r},\mathbf{r}') \sum_{\sigma\sigma'} \psi^\dagger_\sigma(\mathbf{r},t)\psi^\dagger_{\sigma'}(\mathbf{r}',t)\psi_{\sigma'}(\mathbf{r}',t)\psi_\sigma(\mathbf{r},t), \tag{2.7}$$

where the potential $V(\mathbf{r},\mathbf{r}') < 0$ for at least some positions $(\mathbf{r},\mathbf{r}')$. This describes a two-particle interaction, but it would be useful to rewrite it to a single-particle Hamiltonian in which the particle moves in a background field set up by the other electrons. This is conducted by the mean-field approximation, in which it is assumed that the product of two field operators is close to the expectation value of the product. The product of two field operators in the mean-field approximation is

$$\psi_{\sigma'}(\mathbf{r}')\psi_\sigma(\mathbf{r}) = \phi_{\sigma\sigma'}(\mathbf{r},\mathbf{r}') + \varphi(\mathbf{r},\mathbf{r}'), \tag{2.8}$$

where $\phi_{\sigma\sigma'}(\mathbf{r},\mathbf{r}') \equiv \langle\psi_{\sigma'}(\mathbf{r}')\psi_\sigma(\mathbf{r})\rangle$ and $\varphi(\mathbf{r},\mathbf{r}')$ is a small fluctuation field. The time dependence of the field operators is suppressed for brevity in the notation. Next, define the order parameter

$$\Delta_{\sigma\sigma'}(\mathbf{r},\mathbf{r}') = -V(\mathbf{r},\mathbf{r}')\phi_{\sigma\sigma'}(\mathbf{r},\mathbf{r}'). \tag{2.9}$$

The absolute value $|\Delta_{\sigma\sigma'}(\mathbf{r},\mathbf{r}')|$ is referred to as the superconducting gap, while the phase of the order parameter is referred to as the superconducting phase. To first order in the fluctuation field, the mean-field version of the Hamiltonian (2.7) becomes

$$\begin{aligned} H = -\frac{1}{2}\iint \mathrm{d}\mathbf{r}\mathrm{d}\mathbf{r}' \sum_{\sigma\sigma'} [&\Delta_{\sigma\sigma'}(\mathbf{r},\mathbf{r}')\psi^\dagger_\sigma(\mathbf{r})\psi^\dagger_{\sigma'}(\mathbf{r}') + \Delta^*_{\sigma\sigma'}(\mathbf{r},\mathbf{r}')\psi_{\sigma'}(\mathbf{r}')\psi_\sigma(\mathbf{r}) \\ &-\Delta_{\sigma\sigma'}(\mathbf{r},\mathbf{r}')\phi^*_{\sigma\sigma'}(\mathbf{r},\mathbf{r}')]. \end{aligned} \tag{2.10}$$

This Hamiltonian describes superconductivity. We will proceed from 2.10 in two different ways. Firstly, the Hamiltonian for a contact interaction $V(\mathbf{r}-\mathbf{r}') = -\lambda(\mathbf{r})\delta(\mathbf{r}-\mathbf{r}')$ will be considered, and the resulting Hamiltonian will be used when deriving equations of motion for superconducting hybrid systems. Secondly, we will consider the Hamiltonian for a bulk superconductor with a short-range interaction and use this to obtain an expression for the free energy. The free energy will be used to derive the BCS gap equation and the Chandrasekhar-Clogston limit, which is an upper limit on the spin-splitting field that can coexist with a superconductor in equilibrium.

2.3.1 Contact interaction

If the particles that mediate the attractive electron-electron interaction are very short-ranged, the potential can be approximated by $V(\mathbf{r},\mathbf{r}') = -\lambda(\mathbf{r})\delta(\mathbf{r},\mathbf{r}')$. Due

to the Pauli principle, the two electrons that now are located at the same position must have opposite spins. The order parameter therefore satisfies

$$\Delta_{\sigma\sigma'}(\mathbf{r},\mathbf{r}') = \lambda(\mathbf{r})\langle\psi_{-\sigma}(\mathbf{r})\psi_{\sigma}(\mathbf{r})\rangle\delta(\mathbf{r}-\mathbf{r}')\delta_{-\sigma,\sigma'}, \tag{2.11}$$

where the anticommutation rules of fermionic field operators with different quantum numbers were applied. Define a new order parameter

$$\Delta(\mathbf{r}) \equiv \Delta_{\uparrow\downarrow}(\mathbf{r},\mathbf{r}) = -\Delta_{\uparrow\downarrow}(\mathbf{r},\mathbf{r}). \tag{2.12}$$

Performing the sum over the spins in (2.10) and inserting the definition of $\Delta(\mathbf{r})$ yields

$$H = -\int \mathrm{d}\mathbf{r}\left(\Delta(\mathbf{r})\psi^{\dagger}_{\uparrow}(\mathbf{r})\psi^{\dagger}_{\downarrow}(\mathbf{r}) + \Delta^{*}(\mathbf{r})\psi_{\downarrow}(\mathbf{r})\psi_{\uparrow}(\mathbf{r}) + \right) + \int \mathrm{d}\mathbf{r}\Delta(\mathbf{r})\phi_{\uparrow\downarrow}(\mathbf{r}). \tag{2.13}$$

In calculations that do not depend on constant terms in the Hamiltonian, the second integral can be set to zero. This is the case for the Hamiltonian that we will use to describe superconducting hybrid systems, but it is not the case when for example deriving free energies.

2.3.2 Bulk superconductor

In bulk and homogeneous materials, operators and observables depend on the relative coordinate $\boldsymbol{\rho} = \mathbf{r} - \mathbf{r}'$, and they do not depend on the direction or absolute position. We assume interactions between the fermions to be short-ranged so that their spins must be opposite, but we do not assume the interaction to be a delta-function. In this case, the order parameter (2.9) reduces to

$$\Delta_{\sigma,-\sigma}(\boldsymbol{\rho}) = -V(\boldsymbol{\rho})\langle\psi_{-\sigma}(0)\psi_{\sigma}(\boldsymbol{\rho})\rangle, \tag{2.14}$$

and we define the order parameter

$$\Delta(\boldsymbol{\rho}) = \Delta_{\uparrow\downarrow}(\boldsymbol{\rho}) = -\Delta_{\downarrow\uparrow}(\boldsymbol{\rho}) = \sum_{\mathbf{q}} \Delta_{\mathbf{q}}\, \mathrm{e}^{i\mathbf{q}\cdot\boldsymbol{\rho}}\,. \tag{2.15}$$

Inserting the Fourier transformed expressions for the field operators $\psi_{\sigma}(\mathbf{r}) = \sum_{\mathbf{k}} c_{\mathbf{k}\sigma}\, \mathrm{e}^{i\mathbf{k}\cdot\mathbf{r}}$ and the order parameter into (2.10) gives the Hamiltonian

$$H = -\sum_{\mathbf{q}}\left(\Delta_{\mathbf{q}} c^{\dagger}_{\mathbf{q}\uparrow} c^{\dagger}_{-\mathbf{q}\downarrow} + \Delta^{*}_{\mathbf{q}} c_{-\mathbf{q}\downarrow} c_{\mathbf{q}\uparrow}\right) + H_0, \tag{2.16}$$

where

$$H_0 = \sum_{\mathbf{q}} \Delta_{\mathbf{q}} \langle c^{\dagger}_{-\mathbf{q}\downarrow} c^{\dagger}_{\mathbf{q}\uparrow}\rangle. \tag{2.17}$$

Next, we want to diagonalize the Hamiltonian because that will explain why $|\Delta|$ is termed "the superconducting gap", and it is also a convenient starting point for deriving an expression for free energy. We consider a superconducting system in the presence a spin-splitting field $\mathbf{m} = m\mathbf{e}_z$, for which the full Hamiltonian is

$$H = \sum_{\mathbf{k},\sigma} \epsilon_{\mathbf{k},\sigma} c^\dagger_{\mathbf{k},\sigma} c_{\mathbf{k},\sigma} - \sum_{\mathbf{k}} \left(\Delta_{\mathbf{k}} c^\dagger_{\mathbf{k},\uparrow} c^\dagger_{-\mathbf{k},\downarrow} + \Delta^*_{\mathbf{k}} c_{-\mathbf{k},\downarrow} c_{\mathbf{k},\uparrow} \right) + H_0. \tag{2.18}$$

Here, $\epsilon_{\mathbf{k},\sigma} = \epsilon_{\mathbf{k}} - \sigma m$ and $\epsilon_{\mathbf{k}}$ is the free electron energy relative to the Fermi energy. The diagonalization is performed via a Boglioubov-transformation [15] by introducing new fermion operators $\gamma_{\mathbf{k},\sigma}$ that are linear combinations of $c_{\mathbf{k},\sigma}$ and $c^\dagger_{\mathbf{k},\sigma}$,

$$\begin{pmatrix} c_{\mathbf{k}\uparrow} \\ c^\dagger_{-\mathbf{k}\downarrow} \end{pmatrix} = \begin{pmatrix} v_{\mathbf{k}} & u_{\mathbf{k}} \\ -u_{\mathbf{k}} & v_{\mathbf{k}} \end{pmatrix} \begin{pmatrix} \gamma_{\mathbf{k}\uparrow} \\ \gamma^\dagger_{-\mathbf{k}\downarrow} \end{pmatrix}. \tag{2.19}$$

In the gauge where $\Delta_{\mathbf{k}}$ is real, the constants $v_{\mathbf{k}}$ and $u_{\mathbf{k}}$ are chosen to be [16]

$$v_{\mathbf{k}} = \frac{1}{\sqrt{2}} \sqrt{1 + \frac{\epsilon_{\mathbf{k}}}{\sqrt{\epsilon^2_{\mathbf{k}} + \Delta^2_{\mathbf{k}}}}}, \tag{2.20}$$

$$u_{\mathbf{k}} = \frac{1}{\sqrt{2}} \sqrt{1 - \frac{\epsilon_{\mathbf{k}}}{\sqrt{\epsilon^2_{\mathbf{k}} + \Delta^2_{\mathbf{k}}}}}, \tag{2.21}$$

and this makes the Hamiltonian diagonal:

$$\begin{aligned} H = H_0 + \sum_{\mathbf{k}\sigma} \left(\sqrt{\epsilon^2_{\mathbf{k}} + \Delta^2_{\mathbf{k}}} - \sigma m \right) \gamma^\dagger_{\mathbf{k}\sigma} \gamma_{\mathbf{k}\sigma} + \sum_{\mathbf{k}} \left(\epsilon_{\mathbf{k}} - \sqrt{\epsilon^2_{\mathbf{k}} + \Delta^2_{\mathbf{k}}} \right) \\ \equiv H_0 + \sum_{\mathbf{k}\sigma} E_{\mathbf{k}\sigma} \gamma^\dagger_{\mathbf{k}\sigma} \gamma_{\mathbf{k}\sigma} + \sum_{\mathbf{k}} \left(\epsilon_{\mathbf{k}} - E_{\mathbf{k}} \right). \end{aligned} \tag{2.22}$$

The quasiparticle energy was defined as $E_{\mathbf{k}\sigma} = E_{\mathbf{k}} - \sigma m = \sqrt{\epsilon^2_{\mathbf{k}} + \Delta^2_{\mathbf{k}}} - \sigma m$. It is clear that $\Delta_{\mathbf{k}}$ appears as a gap in the quasiparticle energy spectrum, and this is why it is referred to as the superconducting gap.

We now derive the free energy associated with this diagonal Hamiltonian. This derivation, as well as the soon-to-come derivation of the Chandrasekhar-Clogston limit, is based on Ref. [16]. Free energy is defined as

$$F = -\frac{1}{\beta} \ln(Z), \tag{2.23}$$

where Z is the grand canonical partition function,

$$Z = \mathrm{Tr}\left(\mathrm{e}^{-\beta H}\right) = \sum_{\{n_s\}} \langle \{n_s\} | \, \mathrm{e}^{-\beta H} \, | \{n_s\} \rangle \,. \tag{2.24}$$

Here, $|\{n_s\}\rangle$ is a many-particle state with n_1 particles in state (k_1, σ_1), n_2 particles in state (k_2, σ_2) etc. The many-particle states can be chosen to be the eigenstates of the diagonal Hamiltonian, and the partition function is then

$$\begin{aligned} Z &= \mathrm{e}^{-\beta(H_0+\sum_{\mathbf{k}}(\epsilon_{\mathbf{k}}-E_{\mathbf{k}}))} \sum_{\{n_s\}} \langle\{n_s\}| \sum_i \frac{1}{i!} \left(-\beta \sum_j E_{\mathbf{k}_j\sigma_j} n_j\right)^i |\{n_{k,\sigma}\}\rangle \\ &= \mathrm{e}^{-\beta(H_0+\sum_{\mathbf{k}}(\epsilon_{\mathbf{k}}-E_{\mathbf{k}}))} \sum_{\{n_s\}} \prod_j \mathrm{e}^{E_{\mathbf{k}_j\sigma_j} n_j} \\ &= \mathrm{e}^{-\beta(H_0+\sum_{\mathbf{k}}(\epsilon_{\mathbf{k}}-E_{\mathbf{k}}))} \sum_{n_1=0}^{1} \sum_{n_2=0}^{1} \cdots \sum_{n_M=0}^{1} \mathrm{e}^{E_{\mathbf{k}_1\sigma_1} n_1} \mathrm{e}^{E_{\mathbf{k}_2\sigma_j} n_2} \cdots \mathrm{e}^{E_{\mathbf{k}_M\sigma_M} n_M} . \end{aligned} \tag{2.25}$$

Here, n_j is the occupation number for the single-particle state $(\mathbf{k}_j\sigma_j)$ in the many-particle state $|\{n_s\}\rangle$, which has to be either zero or one due to the particle being fermions. The free energy of the Hamiltonian (2.22) therefore becomes

$$F = H_0 + \sum_{\mathbf{k}} (\epsilon_{\mathbf{k}} - E_{\mathbf{k}}) - \frac{1}{\beta} \sum_{\mathbf{k}\sigma} \ln\bigl(1 + \mathrm{e}^{-\beta E_{\mathbf{k}\sigma}}\bigr), \tag{2.26}$$

where the sum runs over all single-particle states. Differentiating the free energy with respect to the order parameter $\Delta_{\mathbf{k}}$ and demanding this derivative to be zero gives the BCS gap equation

$$\Delta_{\mathbf{k}} = -\sum_{\mathbf{k}'} V_{\mathbf{k},\mathbf{k}'} \Delta_{\mathbf{k}'} \frac{\tanh\bigl(\frac{\beta}{2}(E_{\mathbf{k}'} - m)\bigr) + \tanh\bigl(\frac{\beta}{2}(E_{\mathbf{k}'} + m)\bigr)}{4E_{\mathbf{k}'}} \tag{2.27}$$

in the presence of a spin-splitting field.

2.4 The Chandrasekhar-Clogston limit

Looking back at the gap equation (2.27), we realize that there might exist several solutions for the order parameter. For example, the normal metal state with $\Delta = 0$ is always a solution to the gap equation, but from experiment we know that superconductors exist and that the normal state is not always the ground state. It is the free energy given by (2.26) that determines whether the system is in the superconducting or the normal state, as the free energy is always minimized in equilibrium. By comparing the free energy of the normal state and the superconducting state for increasing spin-splitting fields, we can find a limit on the magnitude of the spin-splitting field that can coexist with bulk superconductivity in equilibrium. This limit is known as the Chandrasekhar-Clogston limit [17, 18].

First of all, note that the term on the second line of the mean-field Hamiltonian (2.10) is zero when $V(\mathbf{r}, \mathbf{r}') = 0$, and otherwise it can be rewritten to

$$H_0 = \frac{1}{2} \iint \mathrm{d}\mathbf{r}\mathrm{d}\mathbf{r}' \Delta_{\sigma\sigma'}(\mathbf{r}, \mathbf{r}') \phi^*_{\sigma\sigma'}(\mathbf{r}, \mathbf{r}') = -\frac{1}{2} \iint \mathrm{d}\mathbf{r}\mathrm{d}\mathbf{r}' \frac{|\Delta_{\sigma\sigma'}(\mathbf{r}, \mathbf{r}')|^2}{V(\mathbf{r}, \mathbf{r}')}. \tag{2.28}$$

Neglecting any dependence on absolute position, using the definition (2.15) and Fourier transforming the relative coordinate gives

$$H_0 = -\sum_{\mathbf{kq}} \frac{\Delta_{\mathbf{k}}\Delta^*_{\mathbf{k}-\mathbf{q}}}{V_{\mathbf{q}}}, \tag{2.29}$$

where $\mathbf{k}$ and $\mathbf{q}$ are measured relative to the Fermi momentum. We assume that the potential is non-zero and constantly equal to $-V$ in a thin shell $|\epsilon_{\mathbf{k}}| < \omega$ around the Fermi surface, and zero otherwise .This corresponds to a constant potential in real space, meaning $\Delta(\boldsymbol{\rho})$ also is a constant in real space. Therefore, in $\mathbf{k}$-space the gap is present only in the thin shell around the Fermi surface, which we will use later to constrict some $\mathbf{k}$-space sums. The constant term becomes

$$H_0 = \frac{\Delta^2}{V}. \tag{2.30}$$

For a superconductor, the free energy is

$$F^{SC}(m) = \frac{\Delta^2}{V} + \sum_{\mathbf{k}}(\epsilon_{\mathbf{k}} - E_{\mathbf{k}}) - \frac{1}{\beta}\sum_{\mathbf{k}\sigma} \ln\bigl(1 + \mathrm{e}^{-\beta(E_{\mathbf{k}} - \sigma m)}\bigr). \tag{2.31}$$

The normal state has the free energy

$$F^{N}(m) = \sum_{\mathbf{k}}(\epsilon_{\mathbf{k}} - |\epsilon_{\mathbf{k}}|) - \frac{1}{\beta}\sum_{\mathbf{k}\sigma} \ln\bigl(1 + \mathrm{e}^{-\beta(|\epsilon_{\mathbf{k}}| - \sigma m)}\bigr). \tag{2.32}$$

From now on, the temperature is set to zero. As seen from the gap equation (2.27), the gap is unaffected by a spin-splitting field $m < \Delta_0$ when the temperature is zero. In the derivation $m < \Delta_0$ is assumed, and this should be self-consistently checked at the end of the derivation.

In the case without a spin-splitting field, the free energies are

$$F^{N}(0) = \sum_{\mathbf{k}}(\epsilon_{\mathbf{k}} - |\epsilon_{\mathbf{k}}|), \tag{2.33}$$

$$F^{SC}(0) = \frac{\Delta_0^2}{V} + \sum_{\mathbf{k}}(\epsilon_{\mathbf{k}} - E_{\mathbf{k}}), \tag{2.34}$$

and $F^N > F^{SC}$ because we consider a material that is superconducting at low temperatures.

In the presence of a spin-splitting field $m > 0$, the free energy of the normal state decreases to

$$\begin{aligned} F^{N}(m) &= \sum_{\mathbf{k}}(\epsilon_{\mathbf{k}} - |\epsilon_{\mathbf{k}}|) - \frac{1}{\beta}\sum_{\mathbf{k}} \Big(\ln\bigl(1 + \mathrm{e}^{-\beta(|\epsilon_{\mathbf{k}}| - m)}\bigr) + \ln\bigl(1 + \mathrm{e}^{-\beta(|\epsilon_{\mathbf{k}}| + m)}\bigr)\Big) \\ &= \sum_{\mathbf{k}}(\epsilon_{\mathbf{k}} - |\epsilon_{\mathbf{k}}|) - \sum_{\mathbf{k}}^{|\epsilon_{\mathbf{k}}|<m} (m - |\epsilon_{\mathbf{k}}|)\,. \end{aligned} \tag{2.35}$$

Similarly, the free energy of the superconducting state in the presence of a spin-splitting field can be expressed as

$$F^{SC}(m) = \frac{\Delta_0^2}{V} + \sum_{\mathbf{k}}(\epsilon_{\mathbf{k}} - E_{\mathbf{k}}) - \sum_{\mathbf{k}}^{E_{\mathbf{k}}<m} (m - E_{\mathbf{k}})\,. \tag{2.36}$$

The last sum is zero because we assumed $m < \Delta_0$ and the free energy is therefore unaffected by the spin-splitting field.

When increasing the strength of the spin-splitting field, the system will remain superconducting until the free energy of the normal state has decreased to $F^N = F^{SC}$. At this critical value m_c of the spin-splitting field a phase transition will occur, and for any field $m > m_c$ the normal state will be the ground state of the system. The equation to be solved is therefore

$$\sum_{\mathbf{k}}(\epsilon_{\mathbf{k}} - |\epsilon_{\mathbf{k}}|) - \sum_{\mathbf{k}}^{|\epsilon_{\mathbf{k}}|<m_c} (m_c - |\epsilon_{\mathbf{k}}|) = \frac{\Delta_0^2}{V} + \sum_{\mathbf{k}}(\epsilon_{\mathbf{k}} - E_{\mathbf{k}}). \tag{2.37}$$

In the thermodynamic limit, which is the limit where the particle number N and the volume of the system $\mathcal{V}$ go to infinity while the ratio $N/\mathcal{V}$ stays constant, the $\mathbf{k}$-space sum is replaced by an integral,

$$\sum_{\mathbf{k}} \to \int D(\epsilon)\mathrm{d}\epsilon. \tag{2.38}$$

Here, $D(\epsilon)$ is the density of states for particles with energy ϵ. The density of states is approximated by the density of states at the Fermi level N_0 because the temperature is zero and the electrons under consideration are close to the Fermi surface. This gives

$$\sum_{\mathbf{k}}^{|\epsilon_{\mathbf{k}}|<m_c} (m_c - |\epsilon_{\mathbf{k}}|) = 2N_0 \int_0^{m_c} (m_c - \epsilon)\mathrm{d}\epsilon = N_0 m_c^2. \tag{2.39}$$

For the term Δ_0^2/V, return to the gap equation and substitute one of the Δ_0s:

$$\frac{\Delta_0^2}{V} = \sum_{\mathbf{k}}^{|\epsilon_{\mathbf{k}}|<\omega} \Delta_0^2 \frac{\tanh\big(\frac{\beta}{2}(E_{\mathbf{k}} - m)\big) + \tanh\big(\frac{\beta}{2}(E_{\mathbf{k}} + m)\big)}{4E_{\mathbf{k}}} \tag{2.40}$$

Because the temperature is zero, $\tanh\big(\frac{\beta}{2}(E_{\mathbf{k}} \pm m)\big) = 1$. Therefore,

$$\begin{aligned} \frac{\Delta_0^2}{V} &= \frac{\Delta_0^2 N_0}{2} \int_{-\omega}^{\omega} \frac{\mathrm{d}\epsilon}{\sqrt{\epsilon^2 + \Delta_0^2}} \\ &= \Delta_0^2 N_0 \sinh^{-1}(\frac{\omega}{\Delta_0}). \end{aligned} \tag{2.41}$$

The last term in the equation for m_c is

$$Q \equiv \sum_{\mathbf{k}} (E_{\mathbf{k}} - |\epsilon_{\mathbf{k}}|) = N_0 \int_{-\omega}^{\omega} \left(\sqrt{\epsilon^2 + \Delta_0^2} - |\epsilon| \right) \mathrm{d}\epsilon. \tag{2.42}$$

The integral was constricted to $[-\omega, \omega]$ because Δ_0 is zero outside this thin shell around the Fermi level. Using the approximation $\Delta_0/\omega \ll 1$ gives

$$\begin{aligned} Q &= -N_0\omega^2 + N_0\omega\Delta_0\sqrt{\frac{\omega^2}{\Delta_0^2} + 1} + N_0\Delta_0^2 \sinh^{-1}\left(\frac{\omega}{\Delta_0}\right) \\ &\approx \frac{1}{2}N_0\Delta_0^2 + N_0\Delta_0^2 \sinh^{-1}\left(\frac{\omega}{\Delta_0}\right). \end{aligned} \tag{2.43}$$

Inserting all this into the equation for m_c gives

$$m_c = \frac{\Delta_0}{\sqrt{2}}, \tag{2.44}$$

which is consistent with the assumption $m < \Delta_0$. This is known as the Chandrasekhar-Clogston limit.

2.5 The FFLO state

In the previous section, we derived a limit on the spin-splitting field that can coexist with BCS superconductivity. However, there exist possibilities for the Cooper pair to survive even beyond the Chandrasekhar-Clogston limit in systems where the paramagnetic effect suppresses the orbital effect. One option is to become an equal-spin triplet Cooper pair [19]. Another option is to keep the spins anti-parallel and instead acquire a non-zero center of mass momentum $2\mathbf{q}$, as shown in figure 1. Such a state was predicted in 1964 by two independent groups: Fulde and Ferrel [20], as well as Larkin and Ovchinnikov [21], and the state is known as the FFLO state in the western literature and the LOFF state in the eastern literature. The FFLO state appears for certain strengths of the spin-splitting field when the temperature is lower than a critical value T^* [22, 23]. In clean superconductors, $T^* < 0.56T_c$. The critical temperature is sensitive to impurities [24, 25], so in a dirty superconductor the critical temperature has to satisfy $T^* < -\Delta_0/2\ln(\tau\Delta_0)$ where τ is a parameter related to the time between collisions with impurities.

In an FFLO state, the superconducting order parameter is spatially modulated. The electrons with spin-up are modeled as plane waves, and because their Fermi surface is shifted by $\mathbf{q}$ they acquire an extra phase factor $\mathrm{e}^{\pm i\mathbf{q}\cdot\mathbf{r}}$. The Fermi surface of the

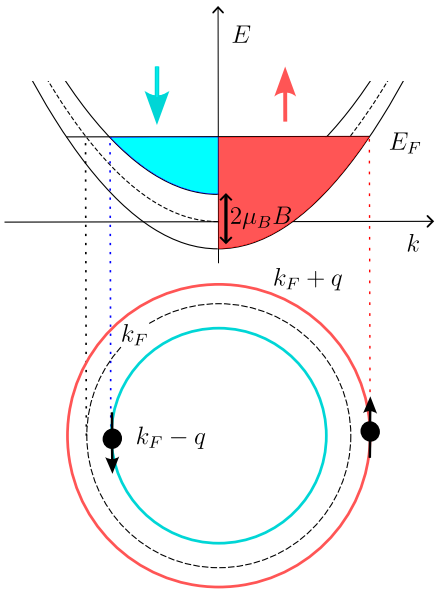

Figure 1: Due to a spin-splitting field, the electronic bands for spin-up and spin-down are shifted relative to each other by $2\mu_B B$. In the FFLO state, this shifts the Fermi momenta to $\mathbf{k}_{F\sigma} = \mathbf{k}_F + \sigma\mathbf{q}$, leading to the Cooper pair in the figure (black dots) gaining a center-of-mass momentum $2\mathbf{q}$.

spin-down electrons is shifted by $-\mathbf{q}$ giving an extra phase factor $\mathrm{e}^{\pm i\mathbf{q}\cdot\mathbf{r}}$. Therefore, the singlet Cooper pair changes to [19]

$$\begin{aligned}(\uparrow\downarrow - \downarrow\uparrow) &\to (\uparrow \mathrm{e}^{i\mathbf{q}\cdot\mathbf{r}} \downarrow \mathrm{e}^{i\mathbf{q}\cdot\mathbf{r}} - \downarrow \mathrm{e}^{-i\mathbf{q}\cdot\mathbf{r}} \uparrow \mathrm{e}^{-i\mathbf{q}\cdot\mathbf{r}}) \\ &= (\uparrow\downarrow - \downarrow\uparrow)\cos(2\mathbf{q}\cdot\mathbf{r}) + i(\uparrow\downarrow + \downarrow\uparrow)\sin(2\mathbf{q}\cdot\mathbf{r}).\end{aligned} \tag{2.45}$$

The singlet superconducting correlations, and thus the order parameter, as well as the triplet correlations are therefore seen to oscillate in space.

The FFLO state is quite sensitive to impurity scattering and hardly exists in dirty superconductors [26], and is therefore hard to detect experimentally. The existence of an FFLO-like state is established in superconductor/ferromagnet hybrid structures [8]. Evidence have been claimed in some organic quasi-2D superconductors and heavy fermion superconductors, but there is no undisputed experimental verification in such systems yet [23, 27–30].

3 The Usadel equation

As discussed earlier, Green functions are one of the cornerstones in quantum field theory, and it is desirable to find the Green function for our system. To find the Green function we need a transport equation and suitable boundary conditions, and

this is what we will accomplish in this section. The derivation follows closely the derivation in Ref. [31].

Firstly, we will write down the Hamiltonian for the system and derive transport equations for the field operators. Then the Keldysh Green function formalism will be introduced, and an equation of motion for the Keldysh Green function will be derived. Next, we introduce appropriate approximations, which in our case are the quasiclassical approximation, the dirty limit and the diffusive limit. The resulting transport equation is a second order partial differential equation known as the Usadel equation [32].

3.1 The Hamiltonian

We will now introduce an ultimate Hamiltonian for a superconductive, ferromagnetic system with magnetic and non-magnetic impurity scattering. In the end, the magnetic spin-flip scattering will be neglected and the electromagnetic fields $\mathbf{A}$ and ϕ will be set to zero, but we nevertheless include them for generality in the derivations.

The Hamiltonian consists of five parts,

$$H(t) = H_0(t) + H_{SC}(t) + H_M(t) + H_{imp}(t) + H_{sf}(t). \tag{3.1}$$

H_0 is the Hamiltonian for non-interacting particles, given by

$$H_0(t) = \sum_\sigma \int d\mathbf{r} \psi_\sigma^\dagger(\mathbf{r},t) \left[\frac{1}{2m} \left(\frac{\hbar}{i}\nabla - e\mathbf{A}(\mathbf{r},t) \right)^2 + e\varphi(\mathbf{r},t) - \mu \right] \psi_\sigma(\mathbf{r},t). \tag{3.2}$$

Here, $\mathbf{A}(\mathbf{r},t)$ and $\varphi(\mathbf{r},t)$ are the electromagnetic fields, and μ is the chemical potential. H_{SC} is the superconducting Hamiltonian given by equation (2.13), and H_M describes the effect of the spin-splitting field $\mathbf{m}$,

$$H_M(t) = -\sum_{\sigma\sigma'} \int d\mathbf{r} \psi_\sigma^\dagger(\mathbf{r},t) (\boldsymbol{\sigma}\cdot\mathbf{m})_{\sigma\sigma'} \psi_{\sigma'}(\mathbf{r},t). \tag{3.3}$$

Here, $\boldsymbol{\sigma}$ is the Pauli matrix vector. Scattering events are taken into account by the non-magnetic impurity scattering Hamiltonian

$$H_{imp}(t) = \sum_\sigma \int d\mathbf{r} \psi_\sigma^\dagger(\mathbf{r},t) V_{imp}(\mathbf{r}) \psi_\sigma(\mathbf{r},t), \tag{3.4}$$

and by the magnetic, spin-flip scattering Hamiltonian

$$H_{sf}(t) = \sum_{\sigma\sigma'} \int d\mathbf{r} \psi_\sigma^\dagger(\mathbf{r},t) V_{sf} (\boldsymbol{\sigma}\cdot\mathbf{S}(\mathbf{r}))_{\sigma\sigma'} \psi_{\sigma'}(\mathbf{r},t). \tag{3.5}$$

3.2 Equation of motion for field operators

The starting point for deriving the transport equations is the Heisenberg equation of motion for the field operators and their adjoints,

$$i\frac{\partial\psi_\sigma^{(\dagger)}(\mathbf{r},t)}{\partial t} = \left[\psi_\sigma^{(\dagger)}(\mathbf{r},t), H(t)\right] \tag{3.6}$$

It is therefore necessary to calculate the commutator between the field operators $\psi_\sigma(\mathbf{r},t)$ and $\psi_\sigma^\dagger(\mathbf{r},t)$ and all five constituents of the Hamiltonian. All the components of H except the superconducting part have the form

$$H'(t) = \sum_{\sigma''\sigma'}\int \mathrm{d}\mathbf{r}'\psi_{\sigma''}^\dagger(\mathbf{r}',t)\mathcal{H}_{\sigma''\sigma'}(\mathbf{r}',t)\psi_{\sigma'}(\mathbf{r}',t). \tag{3.7}$$

Note that the operators denoted with $\mathcal{H}$ are neither Hamiltonians nor Hermitian in general, and that they depend on $\mathbf{r}$ in contrast to the Hamiltonian. It can be shown that the commutator between the constituents of the Hamiltonian and the field operator is

$$[\psi_\sigma(\mathbf{r},t), H'(t)] = \sum_{\sigma'}\mathcal{H}_{\sigma\sigma'}(\mathbf{r},t)\psi_{\sigma'}(\mathbf{r},t). \tag{3.8}$$

In the derivation, the anticommutation rules of the field operators were used as well as the commutation relation $[A,BC] = \{A,B\}C - B\{A,C\}$. We also note that $\mathcal{H}_{\sigma''\sigma'}(\mathbf{r}')$ and $\psi_\sigma(\mathbf{r},t)$ commute because they depend on different coordinates. The contributions to the equation of motion for the field operator $\psi_\sigma(\mathbf{r},t)$ are conclusively

$$\begin{aligned}
[\psi_\sigma(\mathbf{r},t), H_0(t)] &= \left(-\frac{1}{2m}\left(\hbar\nabla - ie\mathbf{A}(\mathbf{r},t)\right)^2 + e\varphi(\mathbf{r},t) - \mu\right)\delta_{\sigma'\sigma''}\psi_\sigma(\mathbf{r},t) && (3.9)\\
&\equiv \mathcal{H}_0(\mathbf{r},t)\psi_\sigma(\mathbf{r},t),\\
[\psi_\sigma(\mathbf{r},t), H_M(t)] &= -\sum_{\sigma'}[\boldsymbol{\sigma}\cdot\mathbf{m}]_{\sigma\sigma'}\psi_{\sigma'}(\mathbf{r},t), && (3.10)\\
[\psi_\sigma(\mathbf{r},t), H_{imp}] &= V(\mathbf{r})\psi_\sigma(\mathbf{r}), && (3.11)\\
[\psi_\sigma(\mathbf{r},t), H_{sf}(t)] &= V_{sf}\sum_{\sigma'}[\boldsymbol{\sigma}\cdot\mathbf{S}(\mathbf{r})]_{\sigma\sigma'}\psi_{\sigma'}(\mathbf{r},t). && (3.12)
\end{aligned}$$

The commutator with the superconducting part of the Hamiltonian has to be computed separately, and the result is

$$[\psi_\sigma(\mathbf{r},t), H_{SC}(t)] = -\delta_{\sigma\uparrow}\Delta(\mathbf{r},t)\psi_\downarrow^\dagger(\mathbf{r},t) + \delta_{\sigma\downarrow}\Delta(\mathbf{r},t)\psi_\uparrow^\dagger(\mathbf{r},t). \tag{3.13}$$

Now that we have found the equation of motion for the field operators, we also need the equations of motion for the adjoint field operators $\psi_\sigma^\dagger(\mathbf{r},t)$. Calculating the commutator between the adjoint field operator and the constituents of the Hamiltonian

is straightforward for the superconducting, spin-splitting and scattering Hamiltonians, as we can simply take the adjoint of equations (3.10), (3.11), (3.12) and (3.13):

$$-\left[\psi_\sigma^\dagger(\mathbf{r},t), H_M(t)\right] = -\sum_{\sigma'}[(\boldsymbol{\sigma}\cdot\mathbf{m})^T]_{\sigma\sigma'}\psi_{\sigma'}^\dagger(\mathbf{r},t), \tag{3.14}$$

$$-\left[\psi_\sigma^\dagger(\mathbf{r},t), H_{sf}(t)\right] = V_{sf}\sum_{\sigma'}[(\boldsymbol{\sigma}\cdot\mathbf{S}(\mathbf{r}))^T]_{\sigma\sigma'}\psi_{\sigma'}^\dagger(\mathbf{r},t), \tag{3.15}$$

$$-\left[\psi_\sigma^\dagger(\mathbf{r},t), H_{imp}(t)\right] = V(\mathbf{r})\psi_\sigma^\dagger(\mathbf{r}), \tag{3.16}$$

$$-\left[\psi_\sigma^\dagger(\mathbf{r},t), H_{BCS}(t)\right] = -\delta_{\sigma\uparrow}\Delta^*(\mathbf{r},t)\psi_\downarrow(\mathbf{r},t) + \delta_{\sigma\downarrow}\Delta^*(\mathbf{r},t)\psi_\uparrow(\mathbf{r},t) \tag{3.17}$$

The commutator with H_0 has to be calculated in the same way as when deriving (3.8) because of the spatial derivative. A calculation similar to the calculation of (3.8) gives

$$\left[\psi_\sigma^\dagger(\mathbf{r},t), H_0(t)\right] = -\sum_{\sigma''\sigma'}\int d\mathbf{r}'\psi_{\sigma''}^\dagger(\mathbf{r}',t)\mathcal{H}_{\sigma''\sigma'}(\mathbf{r}',t)\delta_{\sigma\sigma'}\delta(\mathbf{r}-\mathbf{r}') \tag{3.18}$$

It would be convenient to swap the field operator $\psi_{\sigma''}^\dagger(\mathbf{r}',t)$ and $\delta(\mathbf{r}-\mathbf{r}')$ to get the commutator on the same form as the previous commutators. This is managed by partial integration and discarding surface terms, and the result is

$$\begin{aligned}\left[\psi_\sigma^\dagger(\mathbf{r},t), H_0\right] &= -\left[-\frac{1}{2m}\left(\hbar\nabla + ie\mathbf{A}(\mathbf{r},t)\right)^2 + e\varphi(\mathbf{r},t) - \mu\right]\psi_\sigma^\dagger(\mathbf{r},t) \\ &= \mathcal{H}_0^\dagger(\mathbf{r},t)\psi_\sigma^\dagger(\mathbf{r},t).\end{aligned} \tag{3.19}$$

3.3 Equation of motion in spin $\otimes$ Nambu space

Instead of working with the field operators for different spins and their adjoints, it is convenient to introduce a vector that describes both particles and holes and their spin. The vector and its adjoint are defined as

$$\begin{aligned}\psi(\mathbf{r},t) &= \begin{pmatrix}\psi_\uparrow(\mathbf{r},t) & \psi_\downarrow(\mathbf{r},t) & \psi_\uparrow^\dagger(\mathbf{r},t) & \psi_\downarrow^\dagger(\mathbf{r},t)\end{pmatrix}^T, \\ \psi^\dagger(\mathbf{r},t) &= \begin{pmatrix}\psi_\uparrow^\dagger(\mathbf{r},t) & \psi_\downarrow^\dagger(\mathbf{r},t) & \psi_\uparrow(\mathbf{r},t) & \psi_\downarrow(\mathbf{r},t),\end{pmatrix}\end{aligned} \tag{3.20}$$

and they live in a vector space named spin $\otimes$ Nambu space. We proceed to write down an equation of motion for the vector $\psi(\mathbf{r},t)$ based on the equations of motions for each of the components $\psi_\sigma^{(\dagger)}(\mathbf{r},t)$ from the previous section:

$$\begin{aligned}i\partial_t\hat{\rho}_4\psi(\mathbf{r},t) &= \left(\hat{\xi}(\mathbf{r}) + V_{imp}(\mathbf{r}) - \hat{\Delta} + \hat{S}(\mathbf{r}) - \hat{M}\right)\psi(\mathbf{r},t) \\ &\equiv \mathcal{H}(\mathbf{r},t)\psi(\mathbf{r},t).\end{aligned} \tag{3.21}$$

Here, the following matrices were defined:

$$\hat{\rho}_4 = \begin{pmatrix} 1 & 0 & 0 & 0 \\ 0 & 1 & 0 & 0 \\ 0 & 0 & -1 & 0 \\ 0 & 0 & 0 & -1 \end{pmatrix},$$

$$\hat{\xi}(\mathbf{r}) = -\frac{1}{2m}(\nabla_{\mathbf{r}} - ie\mathbf{A}(\mathbf{r})\hat{\rho}_4)^2 + \hat{\rho}_4(e\phi(\mathbf{r}) - \mu),$$

$$\hat{\Delta} = \begin{pmatrix} 0 & 0 & 0 & \Delta \\ 0 & 0 & -\Delta & 0 \\ 0 & \Delta^* & 0 & 0 \\ -\Delta^* & 0 & 0 & 0 \end{pmatrix},$$

$$\hat{S}(\mathbf{r}) = \begin{pmatrix} \boldsymbol{\sigma} \cdot \mathbf{S}(\mathbf{r}) & 0 \\ 0 & [\boldsymbol{\sigma} \cdot \mathbf{S}(\mathbf{r})]^T \end{pmatrix} V_{sf},$$

$$\hat{M} = \begin{pmatrix} \boldsymbol{\sigma} \cdot \mathbf{m} & 0 \\ 0 & [\boldsymbol{\sigma} \cdot \mathbf{m}]^T \end{pmatrix}.$$

Note that the components of $\hat{S}$ and $\hat{M}$ are 2×2 matrices.

The equation of motion for the adjoint vector $\psi^\dagger(\mathbf{r}, t)$ is found by adjugating the equation of motion (3.21), which switches the order of the vector and the matrices. However, the matrix $\hat{\xi}$ contains operators which should act on $\psi^\dagger$, which makes the notation inconvenient because then we cannot simply switch the order of this matrix and the field operator. A notational solution is to let the operators in the following equation work towards the left, whereas matrix multiplication is performed in the usual way:

$$\begin{aligned} \psi^\dagger(\mathbf{r}, t)(-i\partial_t\hat{\rho}_4) &= \psi^\dagger(\mathbf{r}, t)\left(\hat{\xi}^*(\mathbf{r}) + V_{imp}(\mathbf{r}) + \hat{\Delta} + \hat{S}(\mathbf{r}) - \hat{Z}\right) \\ &= \psi^\dagger(\mathbf{r}, t)\mathcal{H}^\dagger(\mathbf{r}, t). \end{aligned} \tag{3.22}$$

3.4 Keldysh space formalism

As foreshadowed at the beginning of this chapter, we will soon introduce and use the quasiclassical theory of superconductivity. In quantum field theory, there are many ways to define Green functions, and in the quasiclassical theory there are two main Green function formalisms: the Keldysh real-time formalism [33] and the Matsubara imaginary-time formalism [34]. The Matsubara imaginary-time formalism is less general than the Keldysh-space formalism, and it is not valid out of equilibrium. Therefore we will stick to the Keldysh space formalism, which has proven useful in the description of superconductors out of equilibrium.

The Green function in this formalism is an 8×8 matrix in Keldysh space defined as

$$\check{G}(1,2) = \begin{pmatrix} \hat{G}^R(1,2) & \hat{G}^K(1,2) \\ 0 & \hat{G}^A(1,2) \end{pmatrix}. \tag{3.23}$$

Here, $\hat{G}^R$, $\hat{G}^A$ and $\hat{G}^K$ are termed the retarded, the advanced and the Keldysh Green function respectively, and the coordinates $(1,2)$ are short for $(\mathbf{r}_1, t_1; \mathbf{r}_2, t_2)$.

The retarded Green function describes electrons, and its definition is

$$\hat{G}^R(1,2) = -i\theta(t_1 - t_2)\hat{\rho}_4\langle\{\psi(1), \psi^\dagger(2)\}\rangle. \tag{3.24}$$

The anticommutator should be interpreted as

$$\{\psi(1), \psi^\dagger(2)\} = \psi(1)\psi^\dagger(2) + ((\psi^\dagger(2))^T(\psi(1))^T)^T. \tag{3.25}$$

T denotes matrix transpose, and the commutator between $\psi(1)$ and $\psi^\dagger(2)$ is defined similarly. The advanced Green function describes holes and is defined as

$$\hat{G}^A(1,2) = +i\theta(t_2 - t_1)\hat{\rho}_4\langle\{\psi(1), \psi^\dagger(2)\}\rangle, \tag{3.26}$$

while the Keldysh Green function,

$$\hat{G}^K(1,2) = -i\hat{\rho}_4\langle[\psi(1), \psi^\dagger(2)]\rangle, \tag{3.27}$$

contains information about the non-equilibrium effects in the system. The 2×2 diagonal blocks of these three Green functions are termed normal Green functions G while the off-diagonal blocks are termed anomalous Green functions F.

It is possible to show that $\hat{G}^R$ and $\hat{G}^A$ are related by

$$\hat{G}^A = -(\hat{\rho}_4\hat{G}^R\hat{\rho}_4)^\dagger, \tag{3.28}$$

which means that if we know one of them, we can calculate the other [31, 35].

The equation of motion for the retarded Green function is found by multiplying with $i\hat{\rho}_4$ and differentiating with respect to t_1, and using the equation of motion (3.21) for the vector $\psi(1)$:

$$\begin{aligned} i\partial_t\hat{\rho}_4\hat{G}^R(1,2) =& -i(i\partial_{t_1}\hat{\rho}_4\theta(t_1 - t_2))\hat{\rho}_4\langle\{\psi(1), \psi^\dagger(2)\}\rangle \\ & - i\theta(t_1 - t_2)\hat{\rho}_4\langle\{i\partial_{t_1}\hat{\rho}_4\psi(1), \psi^\dagger(2)\}\rangle \\ =& \ \delta(t_1 - t_2)\langle\{\psi(\mathbf{r}_1, t_1), \psi^\dagger(\mathbf{r}_2, t_1)\}\rangle \\ & - i\theta(t_1 - t_2)\hat{\rho}_4\langle\{\mathcal{H}(1)\psi(1), \psi^\dagger(2)\}\rangle \\ =& \ \delta(1-2) + \hat{\rho}_4\mathcal{H}(1)\hat{\rho}_4\hat{G}^R(1,2). \end{aligned} \tag{3.29}$$

The advanced Green function satisfies the same equation of motion. The Keldysh Green function satisfies almost the same equation, but there is no delta-function because there is no step function in the definition of $\hat{G}^K$. Thus, for the full Green function,

$$(i\partial_{t_1}\hat{\rho}_4 - \hat{\rho}_4\mathcal{H}(1)\hat{\rho}_4)\,\check{G}(1,2) = \delta(1-2)\check{1}. \tag{3.30}$$

We will label this equation the *right-handed* equation of motion. Recall that the products $\hat{A}\check{B}$ of a 4×4 matrix $\hat{A}$ and a 8×8 matrix $\check{B}$ should be understood as

$$\hat{A}\check{B} \equiv \begin{pmatrix} \hat{A} & 0 \\ 0 & \hat{A} \end{pmatrix}\check{B}. \tag{3.31}$$

In the same way, we can find a *left-handed* equation of motion for the Green function using the equation of motion (3.22) for the adjoint vector $\psi^\dagger(2)$. Again we let operators work towards the left while matrix multiplication is performed in the usual way, and we multiply the Green functions with $i\partial_{t_2}\hat{\rho}_4$ from the right. The left-handed equation of motion reads

$$\check{G}(1,2)\left(i\partial_{t_2}\hat{\rho}_4 - \check{H}(2)\right)^\dagger = \delta(1-2)\check{1}. \tag{3.32}$$

Subtracting the left-handed equation of motion from the right-handed equation of motion gives the single transport equation

$$\left(i\partial_{t_1}\hat{\rho}_4 - \hat{\rho}_4\check{H}(1)\hat{\rho}_4\right)\check{G}(1,2) - \check{G}(1,2)\left(i\partial_{t_2}\hat{\rho}_4 - \check{H}(2)\right)^\dagger = 0. \tag{3.33}$$

Instead of continuing working with the coordinates $(1,2)$, we now switch to the center of mass and the relative coordinates defined by

$$\begin{aligned} \mathbf{R} = \frac{1}{2}(\mathbf{r_1} + \mathbf{r_2}), \quad T = \frac{1}{2}(t_1 + t_2), \\ \mathbf{r} = \mathbf{r_1} - \mathbf{r_2}, \quad t = t_1 - t_2. \end{aligned} \tag{3.34}$$

This is called the *mixed representation* or the *Wigner representation*. For more compact notation, we also introduce the notation

$$X = (\mathbf{R}, T), \quad x = (\mathbf{r}, t). \tag{3.35}$$

The quasiclassical theory is expressed in terms of $p = (\mathbf{p}, E)$, where $\mathbf{p}$ is the momentum and E is the energy, instead of the relative coordinates x. Therefore, we will Fourier transform the transport equation (3.33) by acting on it with $\int \mathrm{d}x\, \mathrm{e}^{-ipx}$, where $px \equiv \mathbf{p}\cdot\mathbf{r} - Et$. We also introduce a convolution $A\otimes B$ between two functions A, B in the mixed representation,

$$\begin{aligned} A(X,p)\otimes B(X,p) &= \int \mathrm{d}x\, \mathrm{e}^{-ipx}\int \mathrm{d}3 A(1,3)B(3,2) \\ &= \mathrm{e}^{i(\partial_{X_A}\partial_{p_B} - \partial_{p_A}\partial_{X_B})/2}\, A(X,p)B(X,p), \end{aligned} \tag{3.36}$$

where $\partial_{X_A}\partial_{p_B} = \nabla_{\mathbf{R}_A}\nabla_{\mathbf{p}_B} - \partial_{T_A}\partial_{E_B}$. The exponential is to be understood as a Taylor expansion, and the A and B subscripts indicate which of the functions A and B the derivatives act at. The convolution (3.36) product is introduced because the notation proves convenient for the gradient approximation, which will be introduced later. In the case of tranlationally invariant systems in time the partial derivatives with respect to the center of mass time T and energy E will fall out.

Note that the functions encountered here are expressed in different coordinates, for example $(\mathbf{r_1}, t_1; \mathbf{r_2}, t_2)$, $(\mathbf{R}, T; \mathbf{r}, t)$ and $(\mathbf{R}, T; \mathbf{p}, E)$. Strictly speaking, the function is not the same when we switch coordinates and it should be given a new name, for example $A(\mathbf{r_1}, t_1; \mathbf{r_2}, t_2) = A'(\mathbf{R}, T; \mathbf{r}, t)$. However, to ease the notation we omit the primes and keep the name of the function regardless of the coordinates.

Now we are ready to Fourier transform (3.33). Term by term, the left-hand side of the equation is

$$i\partial_{t_1}\hat{\rho}_4\check{G}(1,2) + i\partial_{t_2}\check{G}(1,2)\hat{\rho}_4 \tag{3.37}$$

$$-\hat{\xi}(\mathbf{r_1})\check{G}(\mathbf{r_1}, t_1; \mathbf{r_2}, t_2) + \check{G}(\mathbf{r_1}, t_1; \mathbf{r_2}, t_2)\hat{\xi}^*(\mathbf{r_2}) \tag{3.38}$$

$$-V_{imp}(\mathbf{r_1})\check{G}(\mathbf{r_1}, t_1; \mathbf{r_2}, t_2) + \check{G}(\mathbf{r_1}, t_1; \mathbf{r_2}, t_2)V_{imp}(\mathbf{r_2}) \tag{3.39}$$

$$-\hat{S}(\mathbf{r_1})\check{G}(\mathbf{r_1}, t_1; \mathbf{r_2}, t_2) + \check{G}(\mathbf{r_1}, t_1; \mathbf{r_2}, t_2)\hat{S}(\mathbf{r_2}) \tag{3.40}$$

$$\begin{aligned}\hat{\rho}_4\hat{\Delta}\hat{\rho}_4\check{G}(\mathbf{r_1}, t_1; \mathbf{r_2}, t_2) - \check{G}(\mathbf{r_1}, t_1; \mathbf{r_2}, t_2)\hat{\Delta}^\dagger \\ = -\hat{\Delta}\check{G}(\mathbf{r_1}, t_1; \mathbf{r_2}, t_2) + \check{G}(\mathbf{r_1}, t_1; \mathbf{r_2}, t_2)\hat{\Delta}\end{aligned} \tag{3.41}$$

$$\hat{M}\check{G}(\mathbf{r_1}, t_1; \mathbf{r_2}, t_2) - \check{G}(\mathbf{r_1}, t_1; \mathbf{r_2}, t_2)\hat{M}. \tag{3.42}$$

and each of these terms will be considered separately now.

The time derivatives in the mixed representation is given by $\partial_{t_1} = \partial_t + \partial_T/2$ and $\partial_{t_2} = -\partial_t + \partial_T/2$, and the Green function in the mixed representation is $\check{G}(X, x)$. The Fourier transform of the first term (3.37) becomes

$$\int \mathrm{d}x\, \mathrm{e}^{-ipx}\left[i(\partial_t + \frac{1}{2}\partial_T)\hat{\rho}_4\check{G}(X,x) + i(-\partial_t + \frac{1}{2}\partial_T)\check{G}(X,x)\hat{\rho}_4\right]. \tag{3.43}$$

The integration variable $x = (\mathbf{r}, t)$ is independent of T, thus we can take the ∂_Ts outside the integral. The ∂_t-parts can be rewritten using integration by parts. After setting a surface term to zero, inserting $\partial_t\, \mathrm{e}^{-ipx} = iE\, \mathrm{e}^{ipx}$ and using the definition of

the convolution $A \otimes B$ we get the final expression

$$\begin{aligned}
&\left(\frac{1}{2}\partial_T - iE\right)\int \mathrm{d}x\, \mathrm{e}^{-ipx}\left(i\hat{\rho}_4\check{G}(X,x) - \check{G}(X,x)i\hat{\rho}_4\right)\\
=&\left(\frac{i}{2}\partial_T + E\right)\left[\hat{\rho}_4, \check{G}(X,p)\right]\\
=&\left[E\hat{\rho}_4, \check{G}(X,p)\right] + \frac{i}{2}\{(\partial_E E\hat{\rho}_4)\partial_T(\check{G}(X,p)) - \partial_T(\check{G}(X,p))(\partial_E E\hat{\rho}_4)\}\\
=&E\hat{\rho}_4 \otimes \check{G}(X,p) - \check{G}(X,p)\otimes E\hat{\rho}_4 \equiv \left[E\hat{\rho}_4, \check{G}(X,p)\right]_{\otimes}.
\end{aligned} \tag{3.44}$$

The commutator is defined as $[A,B]_{\otimes} = A\otimes B - B\otimes A$.

Continue with the second term (3.38), and remember that the operators in $\hat{\xi}^*(\mathbf{r})$ work towards the left. Explicitly written out, the second term is

$$\begin{aligned}
&-\xi(\mathbf{r_1})\check{G}(1,2) + \check{G}(1,2)\xi^*(\mathbf{r_2}) = \frac{1}{2m}(\nabla_1^2 - \nabla_2^2)\check{G}(1,2)\\
&+\left[\left(\frac{e^2}{2m}\mathbf{A}^2(\mathbf{r_2}) + e\phi(\mathbf{r_2})\right) - \left(\frac{e^2}{2m}\mathbf{A}^2(\mathbf{r_1}) + e\phi(\mathbf{r_1})\right)\right]\check{G}(1,2)\\
&-\frac{ie}{2m}\left[\nabla_{\mathbf{r_1}}\mathbf{A}(\mathbf{r_1})\hat{\rho}_4\check{G}(1,2) + \nabla_{\mathbf{r_2}}\check{G}(1,2)\mathbf{A}(\mathbf{r_2})\hat{\rho}_4\right]\\
&-\frac{ie}{2m}\left[\mathbf{A}(\mathbf{r_1})\hat{\rho}_4\nabla_{\mathbf{r_1}}\check{G}(1,2) + (\nabla_{\mathbf{r_2}}\check{G}(1,2))\mathbf{A}(\mathbf{r_2})\hat{\rho}_4\right].
\end{aligned} \tag{3.45}$$

We will now Fourier transform each of these four terms. In the mixed representation, the derivatives are given by $\nabla_{\mathbf{r_1}} = \nabla_{\mathbf{r}} + \nabla_{\mathbf{R}}/2$ and $\nabla_{\mathbf{r_2}} = -\nabla_{\mathbf{r}} + \nabla_{\mathbf{R}}/2$. The first term of (3.45) becomes

$$\begin{aligned}
&\frac{1}{2m}\int \mathrm{d}x\, \mathrm{e}^{-ipx}\left[(\nabla_{\mathbf{r}} + \frac{1}{2}\nabla_{\mathbf{R}})^2 - (-\nabla_{\mathbf{r}} + \frac{1}{2}\nabla_{\mathbf{R}})^2\right]\check{G}(1,2)\\
&\qquad = \frac{1}{2m}\int \mathrm{d}x\, \mathrm{e}^{-ipx}\left[2\nabla_{\mathbf{r}}\nabla_{\mathbf{R}}\right]\check{G}(1,2) = i\frac{\mathbf{p}}{m}\nabla_{\mathbf{R}}\check{G}(X,p).
\end{aligned} \tag{3.46}$$

For calculation of the second term, define $f(\mathbf{r_i}) = \frac{e^2}{2m}\mathbf{A}^2(\mathbf{r_i}) + e\phi(\mathbf{r_i})$. The function f commutes with $\check{G}$ because it is a scalar. Taylor expanding the functions f around $\mathbf{R}$ gives

$$\begin{aligned}
&\int \mathrm{d}x\, \mathrm{e}^{-ipx}\left(f(\mathbf{R} - \frac{\mathbf{r}}{2}) - f(\mathbf{R} + \frac{\mathbf{r}}{2})\right)\check{G}(X,x)\\
=&\int \mathrm{d}x\, \mathrm{e}^{-ipx}\sum_{n=0}^{\infty}\frac{1}{n!}\left[\left(-\frac{1}{2}\right)^n - \left(\frac{1}{2}\right)^n\right]\frac{\partial^n f(\mathbf{R})}{\partial \mathbf{R}^n}\mathbf{r}^n\check{G}(X,x)\\
=&\left(\mathrm{e}^{-\frac{i}{2}\nabla_{\mathbf{R}_f}\nabla_{\mathbf{P}}} - \mathrm{e}^{\frac{i}{2}\nabla_{\mathbf{R}_f}\nabla_{\mathbf{P}}}\right)f(\mathbf{R})\check{G}(X,p) = -\left[f(\mathbf{R}), \check{G}(X,p)\right]_{\otimes}\\
&\qquad = -\left[\frac{e^2}{2m}\mathbf{A}^2(\mathbf{R}) + e\phi(\mathbf{R}), \check{G}(X,p)\right]_{\otimes}
\end{aligned} \tag{3.47}$$

From keeping track of the two terms $f(\mathbf{R}\pm\mathbf{r}/2)$ in this calculation, we also conclude that for general matrices A and B the following relations hold:

$$\int \mathrm{d}x\, \mathrm{e}^{-ipx}\, A\left(\mathbf{R}+\frac{\mathbf{r}}{2}\right) B(X,x) = A(\mathbf{R})\otimes B(X,p), \tag{3.48}$$

$$\int \mathrm{d}x\, \mathrm{e}^{-ipx}\, B(X,x) A\left(\mathbf{R}-\frac{\mathbf{r}}{2}\right) = B(X,p)\otimes A(\mathbf{R}). \tag{3.49}$$

For the third term, these two relations are applied and some surface terms are discarded, and we find

$$\begin{aligned}
&-\frac{ie}{2m}\int \mathrm{d}x\, \mathrm{e}^{-ipx}(\nabla_{\mathbf{r}}+\frac{1}{2}\nabla_{\mathbf{R}})\mathbf{A}(\mathbf{R}+\frac{\mathbf{r}}{2})\hat{\rho}_4\check{G}(X,x)\\
&\qquad +\mathrm{e}^{-ipx}(-\nabla_{\mathbf{r}}+\frac{1}{2}\nabla_{\mathbf{R}})\check{G}(X,x)\mathbf{A}(\mathbf{R}-\frac{\mathbf{r}}{2})\hat{\rho}_4\\
=&-\frac{ie}{2m}\left(-(-i\mathbf{p})+\frac{1}{2}\nabla_{\mathbf{R}}\right)\int \mathrm{d}x\, \mathrm{e}^{-ipx}\, \mathbf{A}(\mathbf{R}+\frac{\mathbf{r}}{2})\hat{\rho}_4\check{G}(X,x)\\
&-\frac{ie}{2m}\left(+(-i\mathbf{p})+\frac{1}{2}\nabla_{\mathbf{R}}\right)\int \mathrm{d}x\, \mathrm{e}^{-ipx}\, \check{G}(X,x)\mathbf{A}(\mathbf{R}-\frac{\mathbf{r}}{2})\hat{\rho}_4\\
=&-\frac{ie}{2m}\left(\frac{1}{2}\nabla_{\mathbf{R}}\big\{\hat{\rho}_4\mathbf{A}(\mathbf{R}),\check{G}(X,p)\big\}_{\otimes}+i\mathbf{p}\big[\hat{\rho}_4\mathbf{A}(\mathbf{R}),\check{G}(X,p)\big]_{\otimes}\right).
\end{aligned} \tag{3.50}$$

Split the fourth term of (3.45) into two parts. Consider the first part ignoring the prefactor $-\frac{ie}{2m}$ for brevity.

$$\begin{aligned}
&\int \mathrm{d}x\, \mathrm{e}^{-ipx}\, \mathbf{A}(\mathbf{R}+\frac{\mathbf{r}}{2})\hat{\rho}_4(\nabla_{\mathbf{r}}+\frac{1}{2}\nabla_{\mathbf{R}})\check{G}(X,x)\\
=&\sum_{n=0}^{\infty}\frac{1}{n!}\left(\frac{1}{2}\right)^n(\nabla_{\mathbf{R}}^n\mathbf{A}(\mathbf{R}))\hat{\rho}_4(i\nabla_{\mathbf{p}})^n\int \mathrm{d}x\, \mathrm{e}^{-ipx}(\nabla_{\mathbf{r}}+\frac{1}{2}\nabla_{\mathbf{R}})\check{G}(X,x)\\
=&\sum_{n=0}^{\infty}\frac{1}{n!}\left(\frac{1}{2}\right)^n(\nabla_{\mathbf{R}}^n\mathbf{A}(\mathbf{R}))\hat{\rho}_4(i\nabla_{\mathbf{p}})^n\left(i\mathbf{p}+\frac{1}{2}\nabla_{\mathbf{R}}\right)\check{G}(X,p)=\sum_{n=0}^{\infty}\frac{1}{n!}\left(\frac{i}{2}\right)^n\cdot\\
&(\nabla_{\mathbf{R}}^n\mathbf{A}(\mathbf{R}))\hat{\rho}_4\left(i\mathbf{p}\nabla_{\mathbf{p}}^n\check{G}(X,p)+in\nabla_{\mathbf{p}}^{n-1}\check{G}(X,p)+\frac{1}{2}\nabla_{\mathbf{R}}\nabla_{\mathbf{p}}^n\check{G}(X,p)\right)\\
=&i\mathbf{p}\left(\mathbf{A}(\mathbf{R})\hat{\rho}_4\otimes\check{G}(X,p)\right)-\frac{1}{2}\nabla_{\mathbf{R_A}}(\mathbf{A}(\mathbf{R})\hat{\rho}_4\otimes\check{G}(X,p))\\
&+\frac{1}{2}\nabla_{\mathbf{R}_G}(\mathbf{A}(\mathbf{R})\hat{\rho}_4\otimes\check{G}(X,p)).
\end{aligned} \tag{3.51}$$

The calculation of the second part is similar to the calculation of the first part and gives

$$\begin{aligned}
&\int \mathrm{d}x\, \mathrm{e}^{-ipx}[(-\nabla_{\mathbf{r}}+\frac{1}{2}\nabla_{\mathbf{R}})\check{G}(X,x)]\mathbf{A}(\mathbf{R}-\frac{\mathbf{r}}{2})\hat{\rho}_4\\
=&-i\mathbf{p}\left(\check{G}(X,p)\otimes\mathbf{A}(\mathbf{R})\hat{\rho}_4\right)-\frac{1}{2}\nabla_{\mathbf{R_A}}\left(\check{G}(X,p)\otimes\mathbf{A}(\mathbf{R})\hat{\rho}_4\right)\\
&+\frac{1}{2}\nabla_{\mathbf{R}_G}\left(\check{G}(X,p)\otimes\mathbf{A}(\mathbf{R})\hat{\rho}_4\right).
\end{aligned} \tag{3.52}$$

In total, the fourth term of (3.45) is

$$\begin{aligned} -\frac{ie}{2m} i\mathbf{p}\big[\mathbf{A}(\mathbf{R}), \check{G}(X,p)\big]_\otimes + \frac{ie}{2m}\frac{1}{2}\big\{\nabla_{\mathbf{R}}\mathbf{A}(\mathbf{R})\hat{\rho}_4, \check{G}(X,p)\big\}_\otimes \\ -\frac{ie}{2m}\frac{1}{2}\big\{\mathbf{A}(\mathbf{R})\hat{\rho}_4, \nabla_{\mathbf{R}}\check{G}(X,p)\big\}, \end{aligned} \tag{3.53}$$

and the Fourier transformed version of the entire equation (3.38) is

$$\begin{aligned} i\frac{\mathbf{p}}{m}\nabla_{\mathbf{R}}\check{G}(X,p) - \left[\frac{e^2}{2m}\mathbf{A}^2(\mathbf{R}) + e\phi(\mathbf{R}), \check{G}(X,p)\right]_\otimes \\ -i\frac{\mathbf{p}}{m}\big[ie\mathbf{A}(\mathbf{R})\hat{\rho}_4, \check{G}(X,p)\big]_\otimes - \frac{1}{2m}\big\{ie\mathbf{A}(\mathbf{R})\hat{\rho}_4, \nabla_{\mathbf{R}}\check{G}(X,p)\big\}. \end{aligned} \tag{3.54}$$

For (3.39) and (3.40), respectively, the relations (3.48) and (3.49) are applied and the results are

$$\big[-V_{imp}(\mathbf{R}), \check{G}(X,p)\big]_\otimes, \tag{3.55}$$

$$\Big[-\hat{S}(\mathbf{R}), \check{G}(X,p)\Big]_\otimes. \tag{3.56}$$

For the last two terms (3.41) and (3.42) the matrices $\hat{\Delta}$ and $\hat{M}$ are constants with respect to the coordinate x, and in that case the convolution $A \otimes B$ is equivalent with matrix multiplication. The terms therefore become

$$\Big[-\hat{\Delta} + \hat{M}, G(X,p)\Big]_\otimes. \tag{3.57}$$

The Fourier transformed version of the transport equation (3.33) finally takes the form

$$\begin{aligned} \Big[E\hat{\rho}_4 - e\phi(\mathbf{R}) - V_{imp}(\mathbf{R}) - \hat{S}(\mathbf{R}) - \hat{\Delta} + \hat{Z}, \check{G}(X,p)\Big]_\otimes \\ -i\frac{\mathbf{p}}{m}\big[ie\mathbf{A}(\mathbf{R})\hat{\rho}_4, \check{G}(X,p)\big]_\otimes + i\frac{\mathbf{p}}{m}\nabla_{\mathbf{R}}\check{G}(X,p) \\ -\frac{e^2}{2m}\big[\mathbf{A}^2(\mathbf{R}), \check{G}(X,p)\big]_\otimes - \frac{1}{2m}\big\{ie\mathbf{A}(\mathbf{R})\hat{\rho}_4, \nabla_{\mathbf{R}}\check{G}(X,p)\big\}_\otimes = 0. \end{aligned} \tag{3.58}$$

To shorten the notation, we introduce

$$\hat{\Sigma} = \hat{\Sigma}(X,p) = e\phi(\mathbf{R}) + \hat{S}(\mathbf{R}) + \hat{\Delta} - \hat{M}. \tag{3.59}$$

In our system, there is no $\mathbf{p}$- or E-dependence in $\hat{\Sigma}$, but in general there could exist terms in the Hamiltonian giving rise to a $\mathbf{p}$- and E-dependence. Therefore, $\hat{\Sigma}$ will be assumed to depend on (X,p) for generality. With this notation, the commutator on the first line of (3.58) reduces to

$$\Big[E\hat{\rho}_4 - \hat{\Sigma} - V_{imp}(\mathbf{R}), \check{G}(X,p)\Big]. \tag{3.60}$$

The transport equation (3.58) is still exact, and practically impossible to solve in most systems of interest. The next sections will be dedicated to introducing approximations that makes the equation solvable.

3.5 The quasiclassical approximation

Green functions are powerful for computing observables in condensed matter physics, but in most cases it is impossible to find an exact expression. Therefore, approximations are necessary. In superconductivity, the *quasiclassial approximation* has turned out to be very successful.

The assumption in the quasiclassical theory is that the Fermi wavelength λ_F is the shortest length scale in the system, or equivalently, that the Fermi energy is the greatest energy scale of the system. This means that λ_F is smaller than the system length, the impurity scattering length, the superconducting coherence length and any other relevant length scale in the system. The exact Green function of such a system consists of a part that oscillates rapidly on a length scale λ_F and an envelope function that varies on other length scales in the system. The rapid oscillations are on a length scale much shorter than typical relevant length scales in superconductivity, and for many applications it is desirable to integrate out these oscillations [36, 37]. Effects such as weak localization and persistent currents cannot be described when integrating away the oscillations, but usually the effects related to superconductivity are much more important. The quasiclassical theory provides a method for integrating out the irrelevant oscillations, which makes calculations a lot easier.

In the quasiclassical theory, only contributions close to the Fermi level are kept in the Green function because the Green function is strongly peaked at the Fermi level [36, 38, 39]. A simplified mathematical justification for this follows. In a homogeneous system, the Green function depends only on the relative coordinate $\mathbf{r}$, and for energies close to the Fermi level one finds

$$\check{G}(\mathbf{r}) \simeq \mathrm{e}^{-i\mathbf{p}_F\cdot\mathbf{r}}\,\check{f}(\mathbf{r}), \tag{3.61}$$

where $\check{f}$ is the envelope function that varies slowly compared to the oscillating exponential factor. In momentum space,

$$\check{G}(\mathbf{p}) = \int \mathrm{d}\mathbf{r}\,\mathrm{e}^{-i\mathbf{p}\cdot\mathbf{r}}\,\mathrm{e}^{-i\mathbf{p}_F\cdot\mathbf{r}}\,\check{f}(\mathbf{r}) = \check{f}(\mathbf{p}_F - \mathbf{p}). \tag{3.62}$$

Because $\check{f}$ varies slowly in real space, it is sharply peaked in momentum space at $\mathbf{p} \approx \mathbf{p}_F$. This demonstrates that $\check{G}(\mathbf{p})$ is strongly peaked at the Fermi level

$\mathbf{p}_F$. Constraining the quasiparticle momentum to the Fermi surface is equivalent to defining the *quasiclassical Green function*

$$\check{g}(\mathbf{R}, T, \mathbf{p}_F, E) = \frac{i}{\pi} \int_{-\omega_c}^{\omega_c} d\xi_p \check{G}(X, p), \tag{3.63}$$

where $\xi_p = \frac{\mathbf{p}^2}{2m} - \mu = \frac{\mathbf{p}^2 - \mathbf{p_F}^2}{2m}$. Even though the quasiclassical Green function does not depend on $|\mathbf{p}|$, the notation $\check{g}(X, \mathbf{p}_F, E) = \check{g}(X, p)$ will be kept for brevity. The cutoff energy ω_c must be there for the integral to converge [37]. It has no physical meaning and should disappear in any expression for physical observables.

The transition from the Green function $\check{G}$ to the quasiclassical Green function $\check{g}$ will not be carried out quite yet. Before doing it, it is convenient to rewrite the equation of motion utilizing the peakedness of $\check{G}$ around the Fermi level, which justifies neglecting the third line of (3.58) and the utilization of the gradient approximation. Additionally, a diffusive approximation of the impurity scattering will be applied.

3.5.1 The quasiclassical Green function in a bulk superconductor

We derive the quasiclassical Green function in a bulk superconductor. In a clean superconductor with no electromagnetic fields, the right-handed equation of motion (3.30) reads

$$(i\partial_{t_1}\hat{\rho}_4 + \frac{1}{2m}\nabla^2_{\mathbf{r}_1}\hat{1} - \hat{\Delta})\check{G}(1,2) = \delta(1-2)\check{1}. \tag{3.64}$$

Inside a bulk material, the Green function only depends on the relative coordinates $(\mathbf{r}_1 - \mathbf{r}_2, t_1 - t_2) = (\mathbf{r}, t)$. Fourier transforming the equation of motion gives

$$\left(E\hat{\rho}_4 - \frac{p^2}{2m}\hat{1} - \hat{\Delta}\right)\check{G}(\mathbf{p}, E) = \check{1}. \tag{3.65}$$

The solution to the retarded component of the Green function is therefore

$$\hat{G}^R(\mathbf{p}, E) = \left(E\hat{\rho}_4 - \frac{\mathbf{p}^2}{2m}\hat{1} - \hat{\Delta}\right)^{-1} = \frac{E\hat{\rho}_4 + \frac{p^2}{2m} - \hat{\Delta}}{E^2 - (\frac{p^2}{2m})^2 - |\Delta|^2}. \tag{3.66}$$

The isotropic quasiclassical Green function is then

$$\begin{aligned}
\hat{g}^R(E) &= \frac{i}{\pi}\int \frac{\mathrm{d}\Omega_p}{4\pi}\int_{-\omega_c}^{\omega_c} \mathrm{d}\xi_p \hat{G}^R(\mathbf{p}, E) \\
&= \frac{i}{\pi}\int_{-\omega_c-\mu}^{\omega_c+\mu} \mathrm{d}\left(\frac{p^2}{2m}\right) \frac{E\hat{\rho}_4 + \frac{p^2}{2m} - \hat{\Delta}}{E^2 - (\frac{p^2}{2m})^2 - |\Delta|^2} \\
&\approx \frac{i}{\pi}\int_{-\infty}^{\infty} \mathrm{d}\xi \frac{E\hat{\rho}_4 + \xi - \hat{\Delta}}{E^2 - \xi^2 - |\Delta|^2} = \frac{i}{\pi}\int_{-\infty}^{\infty} \mathrm{d}\xi \frac{E\hat{\rho}_4 - \hat{\Delta}}{E^2 - \xi^2 - |\Delta|^2}.
\end{aligned} \tag{3.67}$$

This integral is proportional to $\int_{-\infty}^{\infty} \frac{\mathrm{d}x}{1-x^2}$, which does not converge. However, from a physical perspective, the Green function cannot diverge because physical observables, such as the density of states and the superconducting gap, depend on it. This is resolved by adding a small, imaginary convergence factor $i\delta$ to the energy. The integral we need to solve is

$$I = \frac{i}{\pi}\int_{-\infty}^{\infty} \mathrm{d}\xi \frac{1}{(E+i\delta)^2 - \xi^2 - |\Delta|^2} \approx \frac{i}{\pi}\int_{-\infty}^{\infty} \frac{\mathrm{d}\xi}{E^2 - \xi^2 - |\Delta|^2 + 2i\delta E}. \tag{3.68}$$

This integral can be calculated in the two cases $E^2 > |\Delta|^2$ and $E^2 < |\Delta|^2$ by the residue theorem. This is thoroughly done in Ref. [31], and the result is

$$\hat{g}^R(E) = \begin{cases} \frac{sgn(E)}{\sqrt{E^2-|\Delta|^2}}(E\hat{\rho}_4 - \hat{\Delta}) & E^2 > |\Delta|^2 \\ \frac{-i}{\sqrt{|\Delta|^2-E^2}}(E\hat{\rho}_4 - \hat{\Delta}) & E^2 < |\Delta|^2 \end{cases}. \tag{3.69}$$

3.5.2 Symmetries of the quasiclassical Green function

Not all elements of the Green function are independent. Therefore, when solving the equations of motion, the Green function can be parametrized and thus reduce the complexity of the problem. In this section, we derive symmetry relations for the quasiclassical retarded, advanced and Keldysh Green functions.

The definition of the retarded Green function was given in equation (3.24), or written out on matrix form, $\hat{G}^R(1,2)$ equals

$$-i\theta(t_1-t_2)\begin{pmatrix} \langle\left\{\psi_\uparrow(1),\psi_\uparrow^\dagger(2)\right\}\rangle & \langle\left\{\psi_\uparrow(1),\psi_\downarrow^\dagger(2)\right\}\rangle & \langle\{\psi_\uparrow(1),\psi_\uparrow(2)\}\rangle & \langle\{\psi_\uparrow(1),\psi_\downarrow(2)\}\rangle \\ \langle\left\{\psi_\downarrow(1),\psi_\uparrow^\dagger(2)\right\}\rangle & \langle\left\{\psi_\downarrow(1),\psi_\downarrow^\dagger(2)\right\}\rangle & \langle\{\psi_\downarrow(1),\psi_\uparrow(2)\}\rangle & \langle\{\psi_\downarrow(1),\psi_\downarrow(2)\}\rangle \\ -\langle\left\{\psi_\uparrow^\dagger(1),\psi_\uparrow^\dagger(2)\right\}\rangle & -\langle\left\{\psi_\uparrow^\dagger(1),\psi_\downarrow^\dagger(2)\right\}\rangle & -\langle\left\{\psi_\uparrow^\dagger(1),\psi_\uparrow(2)\right\}\rangle & -\langle\left\{\psi_\uparrow^\dagger(1),\psi_\downarrow(2)\right\}\rangle \\ -\langle\left\{\psi_\downarrow^\dagger(1),\psi_\uparrow^\dagger(2)\right\}\rangle & -\langle\left\{\psi_\downarrow^\dagger(1),\psi_\downarrow^\dagger(2)\right\}\rangle & -\langle\left\{\psi_\downarrow^\dagger(1),\psi_\uparrow(2)\right\}\rangle & -\langle\left\{\psi_\downarrow^\dagger(1),\psi_\downarrow(2)\right\}\rangle \end{pmatrix}.$$

We see that the retarded Green function has the symmetry

$$\hat{G}^R(1,2) = \begin{pmatrix} G^R(1,2) & F^R(1,2) \\ (F^R)^*(1,2) & (G^R)^*(1,2) \end{pmatrix}. \tag{3.70}$$

Fourier transforming introduces a complex conjugate and a minus sign,

$$\begin{aligned} \hat{G}^R(X,p) &= \int \mathrm{d}\mathbf{r}\mathrm{d}t\, \mathrm{e}^{i(\mathbf{r}\cdot\mathbf{p}-Et)}\, \hat{G}^R(X,\mathbf{r},t) \\ &= \begin{pmatrix} G^R(X,p) & F^R(X,p) \\ (F^R(X,-p))^* & (G^R(X,-p))^* \end{pmatrix}. \end{aligned} \tag{3.71}$$

The quasiclassical Green function is found by $\frac{i}{\pi}\int \mathrm{d}\xi_p$. For the lower right block, this gives

$$\begin{aligned}\frac{i}{\pi}\int \mathrm{d}\xi_p (G^R(X,-p))^* &= -\left(\frac{i}{\pi}\int \mathrm{d}\xi_p G^R(X,-p)\right)^* \\ &= -(g^R(X,-\hat{\mathbf{p}}_F,-E))^* \equiv -\tilde{g}^R(X,\hat{\mathbf{p}}_F,E).\end{aligned} \tag{3.72}$$

In the last line, *tilde conjugation* was defined as complex conjugation and $E \to -E$. This shows that the quasiclassical retarded Green function has the symmetry

$$\hat{g}^R(X,\hat{\mathbf{p}}_F,E) = \begin{pmatrix} g^R(X,E) & f^R(X,E) \\ -\tilde{f}^R(X,E) & -\tilde{g}^R(X,E) \end{pmatrix} \tag{3.73}$$

The advanced Green function has the same symmetry. The symmetry of the Keldysh Green function is slightly different because there is a commutator instead of an anticommutator in the definition of the Keldysh Green function. Therefore, the minus signs on the lower row vanish, and

$$\hat{g}^K(X,\hat{\mathbf{p}}_F,E) = \begin{pmatrix} g^K(X,E) & f^K(X,E) \\ \tilde{f}^K(X,E) & \tilde{g}^K(X,E). \end{pmatrix} \tag{3.74}$$

3.5.3 Limits on the spatial variation of the vector potential and the Green function

The Green function is strongly peaked around the Fermi level. Therefore, the $\mathbf{p}$ in the transport equation (3.58) can be replaced by the Fermi momentum $\mathbf{p}_F$. The other assumption in the quasiclassical theory is that the Fermi energy is the greatest energy scale of the system. This means that for example $|\mathbf{p}_F| \gg |e\mathbf{A}(\mathbf{R})|$. The envelope function part of the Green function varies slowly on the Fermi wavelength, meaning $\nabla_{\mathbf{R}}\check{G}$ is small compared to the Fermi momentum:

$$\begin{aligned}\nabla_{\mathbf{R}}\check{G}(\mathbf{R})\lambda_F \approx \check{G}(\mathbf{R}+\lambda_F\mathbf{e}_F) - \check{G}(\mathbf{R}) \ll 1 \\ \implies \nabla_{\mathbf{R}}\check{G}(\mathbf{R}) \ll \frac{1}{\lambda_F} \propto p_F.\end{aligned} \tag{3.75}$$

It can now be seen why the third line of (3.58) is negligible. The first line has no assumptions on it, while the second line contains two terms with a large value ($\mathbf{p}_F$) times a small value ($ie\mathbf{A}$ and $\nabla_{\mathbf{R}}G$). The third line contains first a small term squared ($(-ie\mathbf{A})^2$), then small ($ie\mathbf{A}$) times small ($\nabla_{\mathbf{R}}G$), so these terms are negligibly small compared to the other terms in the equation.

3.5.4 The gradient approximation

We introduce the notation

$$A \circ B = \mathrm{e}^{i(\partial_{T_A}\partial_{E_B} - \partial_{E_A}\partial_{T_B})/2}\, AB \tag{3.76}$$

between two matrices $A = A(X,p)$ and $B = B(X,p)$. With this notation, the convolution can be written

$$A \otimes B = \mathrm{e}^{i(\nabla_{\mathbf{R}_A}\nabla_{\mathbf{p}_B} - \nabla_{\mathbf{p}_A}\nabla_{\mathbf{R}_B})/2}\, A \circ B. \tag{3.77}$$

In the gradient approximation, the quasiclassical assumption that all quantities vary slowly compared to the Fermi wavelength is applied. Therefore, spatial derivatives are only kept up to first order, and the rapid oscillations of the Green function disappear. The first order gradient approximation is given by

$$\mathrm{e}^{i(\nabla_{\mathbf{R}_A}\nabla_{\mathbf{p}_B} - \nabla_{\mathbf{p}_A}\nabla_{\mathbf{R}_B})/2} \approx 1 + \frac{i}{2}\left(\nabla_{\mathbf{R}_A}\nabla_{\mathbf{p}_B} - \nabla_{\mathbf{p}_A}\nabla_{\mathbf{R}_B}\right), \tag{3.78}$$

which implies

$$A \otimes B \approx A \circ B + \frac{i}{2}(\nabla_{\mathbf{R}} A) \circ (\nabla_{\mathbf{p}} B) - \frac{i}{2}(\nabla_{\mathbf{p}} A) \circ (\nabla_{\mathbf{R}} B). \tag{3.79}$$

Moreover, commutators in the gradient approximation are

$$[A,B]_{\otimes} \approx [A,B]_{\circ} + \frac{i}{2}\{\nabla_{\mathbf{R}} A, \nabla_{\mathbf{p}} B\}_{\circ} - \frac{i}{2}\{\nabla_{\mathbf{p}} A, \nabla_{\mathbf{R}} B\}_{\circ} \tag{3.80}$$

$$\{A,B\}_{\otimes} \approx \{A,B\}_{\circ} + \frac{i}{2}[\nabla_{\mathbf{R}} A, \nabla_{\mathbf{p}} B]_{\circ} - \frac{i}{2}[\nabla_{\mathbf{p}} A, \nabla_{\mathbf{R}} B]_{\circ}. \tag{3.81}$$

As before, the subscript on the commutators and anticommutators denotes what kind of multiplication to use.

Using the gradient approximation and neglecting any terms higher than first order in $\nabla_{\mathbf{R}}$ reduce the two first lines of the equation of motion (3.58) to

$$\begin{aligned} &\left[E\hat{\rho}_4 - \hat{\Sigma}(X,p) - V_{imp}(\mathbf{R}), \check{G}(X,p)\right]_{\circ} - i\frac{\mathbf{p}_F}{m}\tilde{\nabla}\check{G}(X,p) \\ &+\frac{i}{2}\left\{\nabla_{\mathbf{R}}\hat{\Sigma}'(X,p), \nabla_{\mathbf{p}}\check{G}(X,p)\right\}_{\circ} - \frac{i}{2}\left\{\nabla_{\mathbf{p}}\hat{\Sigma}'(X,p), \nabla_{\mathbf{R}}\check{G}(X,p)\right\}_{\circ} = 0, \end{aligned} \tag{3.82}$$

where the notation

$$\tilde{\nabla}\check{G} \equiv \nabla_{\mathbf{R}}\check{G} - \left[ie\mathbf{A}(X)\hat{\rho}_4, \check{G}\right]_{\circ} \tag{3.83}$$

was introduced as well as the short-hand notation

$$\hat{\Sigma}'(X,p) = E\hat{\rho}_4 - \hat{\Sigma} - V_{imp}(\mathbf{R}) - i\frac{\mathbf{p}_F}{m}ie\mathbf{A}(X)\hat{\rho}_4. \tag{3.84}$$

3.6 Impurity averaging

The impurity potential $V_{imp}(\mathbf{r})$ is modelled as a sum over N identical impurities:

$$V_{imp}(\mathbf{r}) = \sum_j U(\mathbf{r} - \mathbf{R}_j), \tag{3.85}$$

where $\mathbf{R}_j$ are the impurity positions. The impurity positions are denoted with capital $\mathbf{R}$s, and they are assumed to be random, uncorrelated and numerous. Superconductors satisfying these requirements are termed *dirty superconductors*. Dealing with this potential in the transport equation is hard because there is such a large number of impurities. Additionally, what matters is the average effect of the impurities, and the exact impurity configuration of the system is uninteresting. It is therefore reasonable to average over all possible configurations of the impurity positions. The average over all impurity positions is an integral over all possible impurity positions $\mathbf{R}_j$,

$$\langle X \rangle_{imp} = \frac{1}{\mathcal{V}^N} \int \mathrm{d}\mathbf{R}_1 \int \mathrm{d}\mathbf{R}_2 \ldots \int \mathrm{d}\mathbf{R}_N. \tag{3.86}$$

The volume of the system is $\mathcal{V}$, and X is the variable that is averaged over.

Explicitly extract the impurity scattering from the right-handed equation of motion (3.30), and use the subscript 0 for the part with no (non-magnetic) impurities:

$$(i\partial_{t_1}\hat{\rho}_4 - \hat{\rho}_4 \mathcal{H}_0(1)\hat{\rho}_4 - V_{imp}(1))\check{G}(1,2) = \delta(1-2)\check{1}. \tag{3.87}$$

Denote the Green function solving this equation without any impurities $\check{G}_0$. Define a function $F(1,2)$ such that

$$\int \mathrm{d}3 \check{G}_0(1,3)F(3,2) = \delta(1-2). \tag{3.88}$$

Then the Green function can be written

$$\check{G}(1,2) = \int \mathrm{d}3 \int \mathrm{d}4 \check{G}_0(1,4)F(4,3)G(3,2). \tag{3.89}$$

Insert this into (3.87) to obtain

$$\int \mathrm{d}3 F(1,3)\check{G}(3,2) - \int \mathrm{d}3 \delta(1-3)V_{imp}(3)\check{G}(3,2) = \delta(1-2). \tag{3.90}$$

Multiply this equation by $\int \mathrm{d}1 \check{G}_0(5,1)$:

$$\begin{aligned} &\int \mathrm{d}3 \int \mathrm{d}1 \check{G}_0(5,1)F(1,3)\check{G}(3,2) - \int \mathrm{d}3 \int \mathrm{d}1 \check{G}_0(5,1)\delta(1-3)V_{imp}(3)\check{G}(3,2) \\ &= \check{G}(5,2) - \int \mathrm{d}3 \check{G}_0(5,3)V_{imp}(3)\check{G}(3,2) = \int \mathrm{d}1 \check{G}_0(5,1)\delta(1-2) = \check{G}_0(5,2) \end{aligned}$$

$$\implies \check{G}(1,2) = \check{G}_0(1,2) + \int \mathrm{d}3\check{G}_0(1,3)V_{imp}(3)\check{G}(3,2) \tag{3.91}$$

This equation is known as the *Dyson equation*, and it is the integral equivalent to the differential equation of motion for the Green function (3.82) that we have considered up to now.

The goal now is to perform an approximation to Dyson's equation known as the *self-consistent Born approximation*. Before doing this, introduce the notation $AVB = \int \mathrm{d}3A(1,3)V(3)B(3,2)$ for convolution integrals to ease the notation. Iterating the Dyson equation gives

$$\begin{aligned} G(1,2) = \quad & G_0(1,2) + \int \mathrm{d}3G_0(1,3)V(3)G_0(3,2) \\ & + \iint \mathrm{d}3\mathrm{d}4G_0(1,3)V(3)G_0(3,4)V(4)G_0(4,2) + \dots \end{aligned} \tag{3.92}$$

which in the short-hand notation for convolution integrals is

$$G = G_0 + G_0VG = G_0 + G_0VG_0 + G_0VG_0VG_0 + \dots \tag{3.93}$$

Now we do an impurity average the way we defined in equation (3.86). G_0 does not depend on the impurity positions and can therefore be taken out of the integrals. Denote the impurity averaged Green function by $\langle G \rangle = G_{av}$. Then,

$$\begin{aligned} G_{av} &= G_0 + G_0\langle VG \rangle \\ &= G_0 + G_0\langle V \rangle G_0 + G_0\langle VG_0V \rangle G_0 + G_0\langle VG_0VG_0V \rangle G_0 + \dots \end{aligned} \tag{3.94}$$

Usually, we take $\langle V \rangle = 0$, meaning that on average the potential has the same strength at each point. If $\langle V \rangle \neq 0$ we can include the constant in the chemical potential which, effectively is the same as $\langle V \rangle = 0$. If the potential is sufficiently weak, we can do an approximation in orders of V. The first order approximation to G_{av} is called the Born approximation:

$$G_{av} = G_0 + G_0\langle VG_0V \rangle G_0 = G_0 + G_0\Sigma G_0. \tag{3.95}$$

We introduced an impurity self-energy Σ, which is defined as

$$\Sigma(3,4) = \langle V(3)G_0(3,4)V(4) \rangle. \tag{3.96}$$

With coordinates and integrals written explicitly, we get

$$\begin{aligned} G_{av}(1,2) &= G_0(1,2) + \int \mathrm{d}3G_0(1,3) \int \mathrm{d}4\langle V(3)G_0(3,4)V(4) \rangle G_0(4,2) \\ &= G_0(1,2) + \int \mathrm{d}3 \int \mathrm{d}4G_0(1,3)\Sigma(3,4)G_0(4,2). \end{aligned} \tag{3.97}$$

The Born approximation catches the first two terms of the exact expression for G_{av}.

Next, we introduce the self-consistent Born approximation,

$$G_{av} = G_0 + G_0 \langle V G_{av} V \rangle G_{av}. \tag{3.98}$$

Compared to the Born approximation, we switched two of the G_0s with G_{av}. The self-energy in the self-consistent Born approximation is

$$\Sigma(3,4) = \langle V(3) G_{av}(3,4) V(4) \rangle. \tag{3.99}$$

The point of doing this is that this approximation is closer to the exact expression than the Born approximation. The self-consistent Born approximation contains not only the zeroth and second order terms of G_{av} but also some (but not all) fourth order terms. This is seen by iterating (3.98), writing out the integrals and the sums in the Vs and comparing it to the exact expression.

The Dyson equation in the self-consistent Born approximation is

$$G_{av}(1,2) = G_0(1,2) + \int \mathrm{d}3 G_0(1,3) \int \mathrm{d}4 \Sigma(3,4) G_{av}(4,2). \tag{3.100}$$

Acting with $(i\partial_{t_1}\hat{\rho}_4 - \hat{\rho}_4 \mathcal{H}_{ni}(1)\hat{\rho}_4)$ on this equation gives the equivalent equation written with derivatives instead of integrals:

$$(i\partial_{t_1}\hat{\rho}_4 - \hat{\rho}_4 \mathcal{H}_{ni}(1)\hat{\rho}_4) G_{av}(1,2) - \int \mathrm{d}3 \Sigma(1,3) G_{av}(3,2) = \delta(1-2). \tag{3.101}$$

Compared to the right-handed equation of motion (3.30), this equation has the same form except for the impurity scattering part and that the Green function is the impurity averaged one. A similar argument as above can be executed for the left-handed equation of motion. This means that the only change we need to do to the transport equation (3.58) is to change the Green function to the impurity averaged one, and to recalculate the effect of impurity scattering.

3.6.1 Calculation of the impurity self energy

In the self-consistent Born approximation, we had

$$\Sigma(1,2) = \langle V(1) G_{av}(1,2) V(2) \rangle. \tag{3.102}$$

The potential V can be written

$$V(\mathbf{r}) = \sum_{\mathbf{q},\mathbf{R}_j} \frac{1}{\mathcal{V}} v(\mathbf{q})\, \mathrm{e}^{i\mathbf{q}\cdot(\mathbf{r}-\mathbf{R}_j)}, \tag{3.103}$$

where $v(\mathbf{q})$ is the Fourier transformed impurity potential belonging to one of the impurities. We assume V to be real, therefore v must satisfy $v(-\mathbf{q}) = v^*(\mathbf{q})$.

Writing out the self-energy and splitting it into one part where the impurity position from $V(1)$ and $V(2)$ is the same and one where it is not gives

$$\begin{aligned}\Sigma(1,2) = \langle \sum_{\mathbf{R}_j} \frac{1}{\mathcal{V}^2} \sum_{\mathbf{q}\mathbf{q}'} v(\mathbf{q})v(\mathbf{q}')\, \mathrm{e}^{-i\mathbf{R}_j(\mathbf{q}+\mathbf{q}')}\, \mathrm{e}^{i\mathbf{q}\mathbf{r}_1 + i\mathbf{q}'\mathbf{r}_2}\, \check{G}(1,2)\rangle \\ + \langle \sum_{\mathbf{R}_i \neq \mathbf{R}_j} \frac{1}{\mathcal{V}^2} \sum_{\mathbf{q}\mathbf{q}'} v(\mathbf{q})v(\mathbf{q}')\, \mathrm{e}^{i\mathbf{q}(\mathbf{r}_1 - \mathbf{R}_i)}\, \mathrm{e}^{i\mathbf{q}'(\mathbf{r}_2 - \mathbf{R}_j)}\, \check{G}(1,2)\rangle.\end{aligned} \tag{3.104}$$

If in the second line we consider specific impurity positions $\mathbf{R}_i \neq \mathbf{R}_j$ and perform the impurity averaging $\langle ... \rangle$, we find that these term vanishes due to the random locations of the impurities unless $\mathbf{q} = \mathbf{q}' = 0$. We assume that this contribution to the impurity self energy is so small that we can disregard it. If we consider the jth term in the first line and perform the average $\langle ... \rangle$, again we find that this is zero unless $\mathbf{q} + \mathbf{q}' = 0$ due to the integral $\int \mathrm{d}\mathbf{R}_i\, \mathrm{e}^{-i\mathbf{R}_i(\mathbf{q}+\mathbf{q}')} = \mathcal{V}\delta(\mathbf{q} + \mathbf{q}')$. This implies

$$\Sigma(1,2) = \frac{N}{\mathcal{V}^2} \sum_{\mathbf{q}} v(\mathbf{q})v(-\mathbf{q})\, \mathrm{e}^{i\mathbf{q}(\mathbf{r}_1 - \mathbf{r}_2)}\, \check{G}(1,2). \tag{3.105}$$

Now we approximate the sum over $\mathbf{q}$ with an integral,

$$\Sigma(1,2) = n \int \frac{\mathrm{d}\mathbf{q}'}{(2\pi)^3} |v(\mathbf{q}')|^2\, \mathrm{e}^{i\mathbf{q}(\mathbf{r}_1 - \mathbf{r}_2)}\, \check{G}(1,2), \tag{3.106}$$

where $n = N/\mathcal{V}$. In the equation of motion, it is the Fourier transformed version of the impurity self energy that shows up, so we need an expression for the Fourier transformed self-energy. After a a change of variables from $\mathbf{q}'$ to $\mathbf{q} = \mathbf{p} - \mathbf{q}'$, the self energy is

$$\Sigma(X,p) = \int \mathrm{d}x\, \mathrm{e}^{ipx}\, \Sigma(1,2) = n \int \frac{\mathrm{d}\mathbf{q}'}{(2\pi)^3} |v(\mathbf{p} - \mathbf{q})|^2 \check{G}(\mathbf{R}, T, \mathbf{q}, E). \tag{3.107}$$

We need an approximation for the integral to continue. In the quasiclassical approximation, integrals act on Green functions that are strongly peaked near the Fermi level. If we are in the quasiclassical regime and particle-hole symmetry applies, meaning that the density of states is approximately the same for particles and holes equally distanced from the Fermi level, the following integral approximation is valid:

$$\begin{aligned}\int \frac{\mathrm{d}\mathbf{p}}{(2\pi)^3} = \int \frac{\mathrm{d}\Omega_{\mathbf{p}}}{4\pi} \int_0^\infty \frac{\mathrm{d}p}{2\pi^2} p^2 = \frac{m}{2\pi^2} \int \frac{\mathrm{d}\Omega_{\mathbf{p}}}{4\pi} \int_{-\mu}^\infty \mathrm{d}\xi_{\mathbf{p}} p \\ \approx \frac{m}{2\pi^2} p_F \int \frac{\mathrm{d}\Omega_{\mathbf{p}}}{4\pi} \int_{-\infty}^\infty \mathrm{d}\xi_{\mathbf{p}} = N_0 \int \frac{\mathrm{d}\Omega_{\mathbf{p}}}{4\pi} \int_{-\infty}^\infty \mathrm{d}\xi_{\mathbf{p}}.\end{aligned} \tag{3.108}$$

N_0 is the density of states in a 3D free electron gas. With this approximation, the impurity self-energy becomes

$$\Sigma(X,p) = nN_0 \int \frac{\mathrm{d}\Omega_{\mathbf{q}}}{4\pi} \int \mathrm{d}\xi_{\mathbf{q}} |v(\mathbf{p}-\mathbf{q})|^2 \check{G}(\mathbf{R},T,\mathbf{q},E). \tag{3.109}$$

In our equations, $\Sigma(\mathbf{R},T,\mathbf{p},E)$ will always appear in combination with $\check{G}(\mathbf{R},T,\mathbf{p},E)$, which is strongly peaked near the Fermi level. It is therefore reasonable to approximate the self-energy with $\Sigma(\mathbf{R},T,\mathbf{p}_F,E)$, meaning that $\mathbf{p} \to \mathbf{p}_F$ in the above equation. In the same way, $\check{G}(\mathbf{R},T,\mathbf{q},E)$ is strongly peaked close to $\mathbf{p}_F$, so we can approximate $v(\mathbf{p}-\mathbf{q}) \approx v(0)$.

Lastly, we incorporate the *diffusive* or *dirty* limit in the equations. The superconductor is assumed to be dirty, which means that there are many impurities and consequently that the mean free path is small. The consequence of this assumption is that the momentum direction of the particles in the superconductor changes often. Diffusion is manifested in the theory in two assumptions. The first assumption is that the quasiclassical Green function can be Taylor expanded to first order in the momentum direction $\mathbf{e}_F$,

$$\check{g} \approx \check{g}_s + \mathbf{e}_F \cdot \check{\mathbf{g}}_p, \tag{3.110}$$

and that this is a good approximation. All the direction dependence of the Green function is now in $\mathbf{e}_F$. The first term $\check{g}_s = \check{g}_s(X,|\mathbf{p}_F|,E)$ is the isotropic part of the quasiclassical Green function, and the anisotropic part $\check{\mathbf{g}}_p = \check{\mathbf{g}}_p(X,|\mathbf{p}_F|,E)$ is small compared to the isotropic part. The second assumption is that the impurity potential part of the Hamiltonian dominates over the other parts.

After performing the angular integral, we then find that the self-energy can be written

$$\Sigma(\mathbf{R},T,\mathbf{p}_F,E) = -\frac{i}{2\tau}\check{g}_s(\mathbf{R},T,|\mathbf{p}_F|,E) \equiv \check{\sigma}(X,p), \tag{3.111}$$

where we changed notation from Σ to σ to emphasize that the self energy is a functional of $\check{g}$ and not $\check{G}$. We defined the constant relaxation time

$$\frac{1}{\tau} \equiv 2\pi n N_0 |v(0)|^2. \tag{3.112}$$

3.6.2 Equation of motion with the impurity self energy

When deriving the transport equation (3.58), we started by subtracting the left-handed equation of motion from the right-handed equation of motion. We then got a bunch of terms that we Fourier transformed and rewrote. The contribution to the right- minus left-handed equation from the impurity self-energy is

$$-\int \mathrm{d}3\Sigma(1,3)G_{av}(3,2) + \int \mathrm{d}3 G_{av}(1,3)\Sigma(3,2). \tag{3.113}$$

Fourier transforming gives

$$\begin{aligned} -\int \mathrm{d}3 \int \mathrm{d}x\, \mathrm{e}^{-ipx} \left(\Sigma(1,3)G_{av}(3,2) - G_{av}(1,3)\Sigma(3,2)\right) \\ = -\big[\Sigma(X,p), \check{G}(X,p)\big]_\otimes = -\big[\check{\sigma}(X,p), \check{G}(X,p)\big]_\otimes \end{aligned} \tag{3.114}$$

This followed from the definition (3.36) of the convolution in the mixed representation. Performing the gradient approximation gives the following contribution to the equation of motion:

$$\begin{aligned} -\big[\check{\sigma}(\mathbf{R},p), \check{G}(X,p)\big]_\otimes \approx -\big[\check{\sigma}(X,p), \check{G}(X,p)\big]_\circ \\ -\frac{i}{2}\big\{\nabla_{\mathbf{R}}\check{\sigma}(X,p), \nabla_{\mathbf{p}}\check{G}(X,p)\big\}_\circ + \frac{i}{2}\big\{\nabla_{\mathbf{p}}\check{\sigma}(X,p), \nabla_{\mathbf{R}}\check{G}(X,p)\big\}_\circ. \end{aligned} \tag{3.115}$$

Finally, the impurity averaged equation of motion in the self-consistent Born approximation and the first order gradient approximation is

$$\begin{aligned} \Big[E\hat{\rho}_4 - \hat{\Sigma}(X,p) - \check{\sigma}(X,p), \check{G}_{av}(X,p)\Big]_\circ + i\frac{\mathbf{p}_F}{m}\tilde{\nabla}\check{G}_{av}(X,p) \\ +\frac{i}{2}\big\{\nabla_{\mathbf{R}}\Sigma'(X,p), \nabla_{\mathbf{p}}\check{G}_{av}(X,p)\big\}_\circ - \frac{i}{2}\big\{\nabla_{\mathbf{p}}\Sigma'(X,p), \nabla_{\mathbf{R}}\check{G}_{av}(X,p)\big\}_\circ = 0. \end{aligned} \tag{3.116}$$

where

$$\Sigma'(X,p) = E\hat{\rho}_4 - \hat{\Sigma}(X,p) - \check{\sigma}(X,p) - i\frac{\mathbf{p}_F}{m}ie\mathbf{A}(X)\hat{\rho}_4. \tag{3.117}$$

3.7 The Usadel equation

We are now in the position to find the Usadel equation. The Usadel equation is the quasiclassical and diffusive version of (3.116) averaged over all momentum directions. The quasiclassical limit is found by performing the integral $\frac{i}{\pi}\int \mathrm{d}\xi_{\mathbf{p}}$. The diffusive limit is found by Taylor expanding the Green function as in (3.110) and by assuming that the impurity self energy dominates over the other parts of the Hamiltonian. The angular average is the integral $\int \mathrm{d}\Omega_{\mathbf{e}_F}/4\pi$.

Terms arising from the second line of (3.116) are usually neglected in the quasiclassical theory for superconductors. The first commutator is small due to the nearly isotropic nature of the Green function and the slow variation of all self-energies in the system, while the second commutator is small due to the spatial variation $\nabla_{\mathbf{R}}\check{G}_{av}$ being small. Neglecting the second line and performing the integral over the magnitude of the momentum $\frac{i}{\pi}\int \mathrm{d}\xi_{\mathbf{p}}$ gives

$$\Big[E\hat{\rho}_4 - \hat{\Sigma}(X,p) - \check{\sigma}(X,p), \check{g}(X,p)\Big]_\circ + i\mathbf{v}_F\tilde{\nabla}\check{g}(X,p) = 0, \tag{3.118}$$

where $\mathbf{v}_F = \mathbf{p}_F/m$ and $\check{g}$ is the impurity averaged quasiclassical Green function. This equation is known as the *Eilenberger equation* [40].

The Eilenberger equation does not uniquely determine the Green function because $\check{g}$ could be multiplied with any constant and still satisfy the transport equation. An additional normalization condition is therefore necessary:

$$\check{g} \circ \check{g} = \check{1}. \tag{3.119}$$

One way to see that this condition is valid is to first note that it is valid in a bulk, homogeneous superconductor in equilibrium. The quasiclassical, retarded Green function in such a system was given in equation (3.69). Returning to the beginning of the derivation of the transport equation, one can show that $\check{g} \circ \check{g}$ satisfies the same equation as $\check{g}$. The Green function is normalized to a constant $\check{g} \circ \check{g} = A\check{1}$, meaning A must equal one to join up smoothly with the equilibrium solution [41]. However, this argument is not particularly rigorous. A more rigorous derivation of the normalization can be found by an alternative derivation of the Eilenberger equation in Ref. [42].

To first order in the anisotropy, the normalization condition yields

$$\check{g}_s \circ \check{g}_s + \check{g}_s \circ \mathbf{e}_F \cdot \check{\mathbf{g}}_p + \mathbf{e}_F \cdot \check{\mathbf{g}}_p \circ \check{g}_s = 1. \tag{3.120}$$

Performing the angular average over this equation gives

$$\check{g}_s \circ \check{g}_s = 1, \tag{3.121}$$

which in turn implies that

$$\check{g}_s \circ \check{\mathbf{g}}_p + \check{\mathbf{g}}_p \circ \check{g}_s = 0. \tag{3.122}$$

These equations will soon be useful, as they will be used to express $\check{\mathbf{g}}_p$ in terms of $\check{g}_s$.

The Eilenberger equation together with the normalization condition makes it possible to express $\check{\mathbf{g}}_p$ in terms of $\check{g}_s$. This is seen by first multiplying Eilenberger with $\mathbf{e}_F$, and then performing the angular average, which gives

$$\frac{1}{3}\Big[E\hat{\rho}_4 - \hat{\Sigma} - \check{\sigma}, \check{\mathbf{g}}_p\Big]_\circ + \frac{1}{3}i|\mathbf{v}_F|\tilde{\nabla}\check{g}_s = 0. \tag{3.123}$$

The intermediate step

$$\left[\int \frac{\mathrm{d}\Omega}{4\pi}\mathbf{e}_F\tilde{\nabla}\check{g}\right]_x = \int \frac{\mathrm{d}\Omega}{4\pi}\mathbf{e}_{F_x}e_{F_i}\tilde{\nabla}_i(\check{g}_s + e_{F_k}\check{g}_{F_k}) = \frac{1}{3}\mathbf{e}_x\tilde{\nabla}_x\check{g}_s \tag{3.124}$$

and similarly for the y- and z-direction was used for the calculation of the second term. Note the Einstein summation convention in this equation.

In the diffusive limit, the magnitude of the content in $E\hat{\rho}_4 - \hat{\Sigma}$ is much smaller than the magnitude of $\hat{\sigma}$, so these terms are neglected in the commutator. Multiplying (3.123) with $\check{g}_s\circ$ from the left and using the normalization condition (3.122) gives

$$\check{\mathbf{g}}_p = -\tau|\mathbf{v}_F|\check{g}_s\tilde{\nabla}\check{g}_s. \tag{3.125}$$

In the final step of deriving the Usadel equation, an angular average over the momentum $\mathbf{p}_F$ will be performed on the equation of motion. The following two integrals, where the first order Taylor expansion has been applied, are therefore useful.

$$\int \frac{\mathrm{d}\Omega_{\mathbf{e}_F}}{4\pi}\check{g} = \check{g}_s, \tag{3.126}$$

$$\begin{aligned}\int \frac{\mathrm{d}\Omega_{\mathbf{e}_F}}{4\pi}\mathbf{e}_F\check{g} &= \int \frac{\mathrm{d}\Omega_{\mathbf{e}_F}}{4\pi}\left(e_{F_x}\mathbf{e}_x + e_{F_y}\mathbf{e}_y + e_{F_z}\mathbf{e}_z\right)\left(e_{F_x}\check{g}_{p_x} + e_{F_y}\check{g}_{p_y} + e_{F_z}\check{g}_{p_z}\right)\\ &= \frac{1}{3}\check{\mathbf{g}}_p.\end{aligned} \tag{3.127}$$

We now integrate the Eilenberger equation over all momentum directions. Note that $E\hat{\rho}_4 - \hat{\Sigma} - \hat{\sigma}$ and $i|\mathbf{v}_F|\tilde{\nabla}$ have no momentum dependence and can be pulled outside the averaging integral $\int \frac{\mathrm{d}\Omega}{4\pi}$. The result is

$$\left[E\hat{\rho}_4 - \hat{\Sigma}(X,p) - \sigma(X,p), \check{g}_s(X,p)\right]_\circ + i|\mathbf{v}_F|\tilde{\nabla}\frac{1}{3}\check{\mathbf{g}}_p(X,p) = 0. \tag{3.128}$$

The impurity self energy $\check{\sigma} = \check{g}_s/2\tau$ commutes with $\check{g}_s$, so it disappears from the equation. Defining the diffusion constant $D = \tau v_F^2/3$ and inserting the expression (3.125) for $\check{\mathbf{g}}_p$, the result is finally

$$D\tilde{\nabla}(\check{g}_s\tilde{\nabla}\check{g}_s) + i\left[E\hat{\rho}_4 - \hat{\Sigma}, \check{g}_s\right]_\circ = 0. \tag{3.129}$$

This equation is known as the *Usadel equation*. For the rest of this thesis, the isotropic Green function $\check{g}_s$ will be denoted $\check{g}$ unless stated otherwise.

It is not always a good approximation to omit the anticommutators on the second line of (3.116), for example if one wants to study spin Hall effects [43]. In that case, obtaining the Eilenberger equation is not straightforward due to the $\nabla_{\mathbf{p}}$s. The solution is to go straight from (3.116) to the Usadel equation by performing the integral over the magnitude and direction of the momentum at the same time. Partial integration can then be used in the anticommutators.

3.8 Boundary conditions

The Usadel equation is a second order differential equation, which means that two additional conditions are needed to uniquely determine the solution. These boundary conditions are applied at the edges of the material we solve for. If we want to solve the Usadel equation in several materials in a hybrid system, we must solve in each of them separately and apply boundary conditions at the interfaces. The reason for this is that the length scales associated with boundaries are not larger than the Fermi wavelength, as assumed in the quasiclassical theory. A derivation of general boundary conditions for the diffusive, quasiclassical theory is beyond the scope of this thesis but can be found in Ref. [44].

In the tunneling limit, the boundary conditions reduce to the *Kupriyanov-Lukichev boundary conditions* [45],

$$\check{g}\partial_x\check{g} = \pm\frac{1}{2L\zeta}\left[\underline{\check{g}},\check{g}\right]. \tag{3.130}$$

$\check{g}$ is the Green function "inside" the material, while $\underline{\check{g}}$ is the Green function "outside". If the outside is to the left of the interface, we use the plus sign, and the minus sign is used when the outside is to the right of the interface. The length of the inside is L, and $\zeta = R_B/R$ is a dimensionless interface parameter describing the ratio of the barrier resistivity R_B to the bulk resistance R of the inside material.

4 The distribution function

4.1 General form

Earlier we encountered the normalization condition $\check{g}\circ\check{g} = \check{1}$. Writing this out in terms of the retarded, advanced and Keldysh components gives the condition

$$\hat{g}^R\circ\hat{g}^K + \hat{g}^K\circ\hat{g}^A = 0. \tag{4.1}$$

An ansatz solution for $\hat{g}^K$ is

$$\hat{g}^K = \hat{g}^R\circ\hat{h} - \hat{h}\circ\hat{g}^A, \tag{4.2}$$

and $\hat{h}$ is known as *the distribution function*. The retarded, advanced and Keldysh Green functions have symmetries discussed in section 3.5.2, and from these symmetries one can show that the distribution function has the symmetry

$$\hat{h} = \begin{pmatrix} h_1 & h_2 \\ -\tilde{h}_2 & -\tilde{h}_1 \end{pmatrix}. \tag{4.3}$$

Equation (4.2) does not uniquely define $\hat{h}$, which is seen by $\hat{h} \to \hat{h} + \hat{g}^R\hat{y} + \hat{y}\hat{g}^A$. This means that we have some freedom to choose $\hat{h}$. Usually, h_2 is set to zero so that the distribution function becomes block diagonal.

The distribution function has earned its name because it is related to the occupation numbers of particles and holes. The particle number n is given by

$$\begin{aligned} n(\mathbf{r_1}, t_1) =& \langle \psi_\uparrow^\dagger(\mathbf{r}_1, t_1)\psi_\uparrow(\mathbf{r}_1, t_1) + \psi_\downarrow^\dagger(\mathbf{r}_1, t_1)\psi_\downarrow(\mathbf{r}_1, t_1) \\ & - \psi_\uparrow(\mathbf{r}_1, t_1)\psi_\uparrow^\dagger(\mathbf{r}_1, t_1) - \psi_\downarrow(\mathbf{r}_1, t_1)\psi_\downarrow^\dagger(\mathbf{r}_1, t_1)\rangle \\ =& \frac{i}{2}\operatorname{Tr}\Big\{\hat{G}^R(\mathbf{r}_1, t_1; \mathbf{r}_1, t_1) - \hat{G}^A(\mathbf{r}_1, t_1; \mathbf{r}_1, t_1) - \hat{G}^K(\mathbf{r}_1, t_1; \mathbf{r}_1, t_1)\Big\}. \end{aligned} \tag{4.4}$$

Going back to the definitions of $\hat{G}^R$ and $\hat{G}^A$, we see that

$$\hat{G}^R(\mathbf{r}_1, t_1; \mathbf{r}_1, t_1) - \hat{G}^A(\mathbf{r}_1, t_1; \mathbf{r}_1, t_1) = 2i\operatorname{Im}\Big\{\hat{G}^R(\mathbf{r}_1, t_1; \mathbf{r}_1, t_1)\Big\}.$$

Fourier transforming the relative time in the Green functions gives

$$\begin{aligned} n(\mathbf{r}_1, t_1) = \frac{i}{2}\int \frac{\mathrm{d}E}{2\pi} \operatorname{Tr}\Big(2i\operatorname{Im}\Big\{\hat{G}^R(R = \mathbf{r}_1, T = t_1; \mathbf{r} = 0, E)\Big\}\Big) \\ - \operatorname{Tr}\Big(2i\operatorname{Im}\Big\{\hat{G}^K(R = \mathbf{r}_1, T = t_1; \mathbf{r} = 0, E)\Big\}\Big). \end{aligned} \tag{4.5}$$

The Keldysh Green function satisfies the same ansatz solution as the quasiclassical Keldysh Green function, $\hat{G}^K = \hat{G}^R \circ \hat{h} - \hat{h} \circ \hat{G}^A$. Therefore,

$$\begin{aligned} n(\mathbf{r}, t) &= \frac{i}{2}\int \frac{\mathrm{d}E}{2\pi} \operatorname{Tr}\Big\{2i\operatorname{Im}\Big\{\hat{G}^R(\mathbf{r}_1, t_1; \mathbf{0}, E)\Big\}(1 - \hat{h}(E))\Big\} \\ &= \int \mathrm{d}E \operatorname{Tr}\left\{-\frac{1}{\pi}\operatorname{Im}\Big\{\hat{G}^R(\mathbf{r}_1, t_1; \mathbf{0}, E)\Big\}\left(\frac{1 - \hat{h}(E)}{2}\right)\right\} \end{aligned} \tag{4.6}$$

If the distribution function is diagonal, which it can be chosen to be when there are no spin-flipping terms in the Hamiltonian, the trace is simply the sum over the diagonal elements of the Green function multiplied by $(1 - h_\sigma(E))/2$. We recognize the expression for density of states $D_\sigma(E) = -\operatorname{Im}\{G^R_{\sigma\sigma}(E)\}/\pi$, and conclude that $(1 - h_\sigma(E))/2$ is the occupation function for either electrons or holes of spin σ. This is the reason $\hat{h}$ is called the distribution function. This shows that $h_\sigma^{e/h}(E) = 1 - 2f_\sigma^{e/h}(E)$, and that the full 4×4 distribution function is

$$\hat{h}(E) = \begin{pmatrix} 1 - 2f_e(E) & 0 \\ 0 & 1 - 2f_h(E) \end{pmatrix}. \tag{4.7}$$

In equilibrium, the distribution function $\hat{h}$ is obtained by inserting the Fermi-Dirac distribution function into the general form of $\hat{h}$, and the result is

$$\hat{h}(E) = \tanh\left(\frac{\beta E}{2}\right)\hat{1}. \tag{4.8}$$

This show that the equilibrium Keldysh Green function is

$$\hat{g}^K(E) = (\hat{g}^R(E) - \hat{g}^A(E)) \tanh\left(\frac{\beta E}{2}\right). \tag{4.9}$$

4.2 In the presence of a voltage

We now find the distribution function in the presence of a voltage. Consider a system with an applied voltage. On the left-hand side of the system, this rises the electron band with eV compared to the right side of the system. The Fermi level on the right side is still μ, while the Fermi level on the left side becomes $\mu + eV$. Energy is defined relative to the Fermi level on the right side. Before switching on the voltage, the probability of finding an electron at energy ϵ' on the left side was $f(\epsilon')$. After switching on the voltage, the electron has energy $\epsilon = \epsilon' + eV$, but the probability of finding this electron is still $f(\epsilon') = f(\epsilon - eV)$. Therefore, the distribution function for electrons with energy ϵ on the left side is $f_e(\epsilon) = f(\epsilon - eV)$. The probability for the electron at energy ϵ' to be missing is $1 - f(\epsilon')$, which is equivalent to the probability of finding a hole at energy $-\epsilon'$. After switching on the voltage, the energy of the electron increases to $\epsilon = \epsilon' + eV$, while the energy of the hole decreases to $-\epsilon = -\epsilon' - eV$. The probability of finding a hole at $-\epsilon$ is $1 - f(\epsilon - eV) = f(-\epsilon + eV)$. The distribution function for holes with energy ϵ on the left side is therefore $f_h(\epsilon) = f(\epsilon + eV)$. Inserting $f_e(\epsilon) = f(\epsilon - eV)$ and $f_h(\epsilon) = f(\epsilon + eV)$ into (4.7) gives

$$\hat{h} = \begin{pmatrix} \tanh\left(\frac{\beta(\epsilon - eV)}{2}\right) & 0 \\ 0 & \tanh\left(\frac{\beta(\epsilon + eV)}{2}\right) \end{pmatrix}. \tag{4.10}$$

In the general case, one can apply spin-dependent voltages. If we take the spin-quantization axis to be the z-axis, the distribution function takes the form

$$\hat{h} = \begin{pmatrix} \tanh\left(\frac{\beta(\epsilon - eV_\uparrow)}{2}\right) & 0 & 0 & 0 \\ 0 & \tanh\left(\frac{\beta(\epsilon - eV_\downarrow)}{2}\right) & 0 & 0 \\ 0 & 0 & \tanh\left(\frac{\beta(\epsilon + eV_\uparrow)}{2}\right) & 0 \\ 0 & 0 & 0 & \tanh\left(\frac{\beta(\epsilon + eV_\downarrow)}{2}\right) \end{pmatrix}. \tag{4.11}$$

5 Parametrized equations and numerics

Not all components of the Green function are independent, so it is convenient to parametrize the Usadel equation. In this chapter, we derive parametrized versions of the retarded and Keldysh Usadel equation suitable for numerical calculations. Additionally, the self-consistent gap equation will be derived. Lastly, we describe how the parametrized equations are solved numerically and how the phase of the system is determined.

5.1 The Ricatti parametrization

In this section, we parametrize the retarded Green function and the retarded Usadel equation.

For simple calculations, the θ-parametrization of the retarded Green function is practical. The retarded Green function is parameterized with two scalar parameters θ_σ,

$$\hat{g}^R = \begin{pmatrix} c_\uparrow & 0 & 0 & s_\uparrow \\ 0 & c_\downarrow & -s_\downarrow & 0 \\ 0 & s_\downarrow & -c_\downarrow & 0 \\ -s_\uparrow & 0 & 0 & -c_\uparrow \end{pmatrix}, \tag{5.1}$$

where $s_\sigma \equiv \sinh\theta_\sigma$ and $c_\sigma \equiv \cosh\theta_\sigma$ [39]. However, there are several limitations to the θ-parametrization. It can only describe singlet pairing and short-range triplet pairing, the hyperbolic functions are multivalued, and θ_σ is unbounded. This can lead to convergence- and stability problems in numerical calculations. Therefore, we will use another popular parameterization called the *Ricatti parametrization*. It is single-valued and the parameters are bound to $[0, 1]$, so it is well suited for numerical calculations. Also, it is more general than the θ-parametrization in the sense that one can analyze singlet pairing and both short-range and long-range triplet pairings. The derivation of the Ricatti parametrized equations is a shortened version of the derivation done in [46].

The Ricatti parametrized retarded Green function is defined as

$$\hat{g}^R = \begin{pmatrix} N & 0 \\ 0 & -\tilde{N} \end{pmatrix} \begin{pmatrix} 1+\gamma\tilde{\gamma} & 2\gamma \\ 2\tilde{\gamma} & 1+\tilde{\gamma}\gamma \end{pmatrix} = \begin{pmatrix} 2N-1 & 2N\gamma \\ -2\tilde{N}\tilde{\gamma} & -(2\tilde{N}-1) \end{pmatrix}, \tag{5.2}$$

where γ is a 2×2 matrix, $N \equiv (1-\gamma\tilde{\gamma})^{-1}$ and 1 is the 2×2 identity matrix. With this parametrization, the symmetries of the retarded Green function are automatically satisfied.

Consider the retarded part of the Usadel equation including the self-energies for superconductivity and magnetism,

$$D\nabla(\hat{g}^R\nabla\hat{g}^R) + i\Big[E\hat{\rho}_4 - \hat{\Delta} + \hat{M}, \hat{g}^R\Big] = 0. \tag{5.3}$$

The two upper blocks of this matrix equation are used for deriving the equations of motion for γ and $\tilde{\gamma}$ because the lower two blocks of the equation are equivalent to the upper two blocks. We multiply the upper left block with γ from the right and subtract it from the upper right block, and then we multiply with $N^{-1}/2$ from the left. The first term in the Usadel equation becomes

$$\frac{1}{2}N^{-1}\left([\nabla(\hat{g}^R\nabla\hat{g}^R)]^{(1,2)} - [\nabla(\hat{g}^R\nabla\hat{g}^R)]^{(1,1)}\gamma\right) = \nabla^2\gamma + 2(\nabla\gamma)\tilde{N}\tilde{\gamma}(\nabla\gamma). \tag{5.4}$$

The same operation is performed on the commutator to obtain

$$\frac{1}{2}N^{-1}\left([iE\big[\hat{\rho}_4, \hat{g}^R\big]]^{(1,2)} - [iE\big[\hat{\rho}_4, \hat{g}^R\big]]^{(1,1)}\gamma\right) = 2iE\gamma \tag{5.5}$$

and

$$\frac{1}{2}N^{-1}\left([i\Big[\hat{M}, \hat{g}^R\Big]]^{(1,2)} - [i\Big[\hat{M}, \hat{g}^R\Big]]^{(1,1)}\gamma\right) = i\mathbf{h}\cdot(\boldsymbol{\sigma}\gamma - \gamma\boldsymbol{\sigma}^*). \tag{5.6}$$

The commutator between Δ and the retarded Green function is

$$\begin{aligned}\Big[\hat{\Delta}, \hat{g}^R\Big] = &\begin{pmatrix} \Delta i\sigma_2(-2\tilde{N}\tilde{\gamma}) & \Delta i\sigma_2(-2\tilde{N}+1) \\ \Delta^* i\sigma_2(2N-1) & \Delta^* i\sigma_2(2N\gamma)\end{pmatrix} \\ &- \begin{pmatrix} 2N\gamma\Delta^* i\sigma_2 & (2N-1)\Delta i\sigma_2 \\ (-2\tilde{N}+1)\Delta^* i\sigma_2 & -2\tilde{N}\tilde{\gamma}\Delta i\sigma_2\end{pmatrix},\end{aligned} \tag{5.7}$$

and this gives

$$\frac{1}{2}N^{-1}\left([i\Big[\hat{\Delta}, \hat{g}^R\Big]]^{(1,2)} - [i\Big[\hat{\Delta}, \hat{g}^R\Big]]^{(1,1)}\gamma\right) = \Delta\sigma_2 - \Delta^*\gamma\sigma_2\gamma. \tag{5.8}$$

This gives one equation of motion for the parameter γ and one for its tilde conjugate,

$$D\nabla^2\gamma + 2D(\nabla\gamma)\tilde{N}\tilde{\gamma}(\nabla\gamma) + 2iE\gamma - \Delta\sigma_2 + \Delta^*\gamma\sigma_2\gamma + i\mathbf{h}\cdot(\boldsymbol{\sigma}\gamma - \gamma\boldsymbol{\sigma}^*) = 0, \tag{5.9}$$

$$D\nabla^2\tilde{\gamma} + 2D(\nabla\tilde{\gamma})N\gamma(\nabla\tilde{\gamma}) + 2iE\tilde{\gamma} + \Delta^*\sigma_2 - \Delta\tilde{\gamma}\sigma_2\tilde{\gamma} - i\mathbf{h}\cdot(\boldsymbol{\sigma}^*\tilde{\gamma} - \tilde{\gamma}\boldsymbol{\sigma}) = 0. \tag{5.10}$$

The Riccati parametrized Kupriyanov-Lukichev boundary conditions for γ are

$$\begin{aligned}\partial_x\gamma_1 &= \frac{1}{L_1\zeta_1}(1-\gamma_1\tilde{\gamma}_2)N_2(\gamma_2-\gamma_1) \\ \partial_x\gamma_2 &= \frac{1}{L_2\zeta_2}(1-\gamma_2\tilde{\gamma}_1)N_1(\gamma_2-\gamma_1).\end{aligned} \tag{5.11}$$

The boundary conditions for $\tilde{\gamma}$ are found by tilde conjugation.

5.2 Parametrization of the distribution function

The goal of this section is to derive a linear ordinary differential equation for the distribution function using the formulation introduced in [47]. The starting point for deriving an equation of motion for the distribution function is the Keldysh part of the Usadel equation. Define the matrix current $\check{\mathbf{I}} \equiv D\check{g}\tilde{\nabla}\check{g}$ such that the Keldysh Usadel equation becomes

$$\tilde{\nabla} \cdot \check{\mathbf{I}}^K = -i\Big[E\hat{\rho}_4 - \hat{\Sigma}, \check{g}\Big]^K. \tag{5.12}$$

The distribution function is block diagonal and can therefore be parametrized by the eight basis matrices,

$$\begin{aligned}
\hat{\rho}_0 &= \begin{pmatrix} I & 0 \\ 0 & I \end{pmatrix}, \qquad \hat{\rho}_4 = \begin{pmatrix} I & 0 \\ 0 & -I \end{pmatrix}, \\
\hat{\rho}_1 &= \begin{pmatrix} \sigma_x & 0 \\ 0 & \sigma_x \end{pmatrix}, \quad \hat{\rho}_5 = \begin{pmatrix} \sigma_x & 0 \\ 0 & -\sigma_x \end{pmatrix}, \\
\hat{\rho}_2 &= \begin{pmatrix} \sigma_y & 0 \\ 0 & \sigma_y \end{pmatrix}, \quad \hat{\rho}_6 = \begin{pmatrix} \sigma_y & 0 \\ 0 & -\sigma_y \end{pmatrix}, \\
\hat{\rho}_3 &= \begin{pmatrix} \sigma_z & 0 \\ 0 & \sigma_z \end{pmatrix}, \quad \hat{\rho}_7 = \begin{pmatrix} \sigma_z & 0 \\ 0 & -\sigma_z \end{pmatrix}.
\end{aligned} \tag{5.13}$$

These matrices span the block-diagonal spin-Nambu space, and parametrizing $\hat{h}$ with these turns out to transform the equation of motion into a simple form. Using the Einstein summation convention, the distribution function in this basis is

$$\hat{h} = h_m \hat{\rho}_m \tag{5.14}$$

with coefficients

$$h_m = \frac{1}{4}\,\mathrm{Tr}\Big\{\hat{\rho}_m \hat{h}\Big\}. \tag{5.15}$$

Due to the symmetry of the distribution function, only four of these coefficients are independent. However, all eight coefficients will be treated as independent because they are related by tilde-conjugation, which switches the sign of the energy $E \to -E$. By keeping all the coefficients, it will be sufficient to solve the equations for $E \geq 0$. Numerically, h_m will be treated as a 8-vector, and in the equation of motion 8×8-matrices will operate on it. Using the parameterization $\hat{h} = h_m\hat{\rho}_m$, the definition of $\check{\mathbf{I}}$ and $\hat{g}^K = \hat{g}^R\hat{h} - \hat{h}\hat{g}^A$ gives the following expression for the Keldysh part of the matrix current:

$$\hat{\mathbf{I}}^K = D[(\hat{g}^R\tilde{\nabla}\hat{g}^R)\hat{\rho}_m - \hat{\rho}_m(\hat{g}^A\tilde{\nabla}\hat{g}^A)]h_m + D[\hat{\rho}_m - \hat{g}^R\hat{\rho}_m\hat{g}^A]\tilde{\nabla}h_m. \tag{5.16}$$

Multiply with $\hat{\rho}_n/4$ from the left and take the trace. Defining the quantities

$$\mathbf{I}_n = \frac{1}{4}\,\mathrm{Tr}\Big\{\hat{\rho}_n \hat{\mathbf{I}}^K\Big\}, \tag{5.17}$$

$$\mathbf{Q}_{nm} = \frac{D}{4}\,\mathrm{Tr}\Big\{\hat{\rho}_m\hat{\rho}_n(\hat{g}^R\tilde{\nabla}\hat{g}^R) - \hat{\rho}_n\hat{\rho}_m(\hat{g}^A\tilde{\nabla}\hat{g}^A)\Big\}, \tag{5.18}$$

$$M_{nm} = \frac{D}{4}\,\mathrm{Tr}\big\{\hat{\rho}_n\hat{\rho}_m - \hat{\rho}_n\hat{g}^R\hat{\rho}_m\hat{g}^A\big\}, \tag{5.19}$$

allows us to write

$$\mathbf{I}_n = \mathbf{Q}_{nm}h_m + M_{nm}\tilde{\nabla}h_m. \tag{5.20}$$

This quantity has a clear physical interpretation: $\mathbf{I}_n$ is proportional to the spectral currents in the system. For example, the charge current is proportional to $\int \mathbf{I}_4 \mathrm{d}E$, and the spin current when the z-axis is the spin quantization axis is proportional to $\int \mathbf{I}_7 \mathrm{d}E$.

Multiplying the Usadel equation by $\hat{\rho}_n/4$ from the left and take the trace gives

$$\tilde{\nabla}\cdot\mathbf{I}_n = -\frac{i}{4}\,\mathrm{Tr}\Big\{\hat{\rho}_n\big[\check{\Sigma},\check{g}\big]^K\Big\}, \tag{5.21}$$

After expressing the right-hand side in terms of the distribution function, this equation will be combined with (5.20) to find a second order differential equation for the distribution function.

In the case of a block-diagonal self-energy $\check{\Sigma} = diag(\hat{\Sigma},\hat{\Sigma})$ that does not depend on the Green function, which is the case for *e.g.* superconductivity and the magnetic field, the commutator in (5.21) is simply

$$\big[\check{\Sigma},\check{g}\big]^K = \Big[\hat{\Sigma},\hat{g}^K\Big]. \tag{5.22}$$

Substituting $h_m\hat{\rho}_m$ and $\hat{g}^K = \hat{g}^R\hat{h} - \hat{h}\hat{g}^A$ and using the cyclic property of the trace gives

$$\tilde{\nabla}\cdot\mathbf{I}_n = -V_{nm}h_m, \tag{5.23}$$

where

$$V_{nm} = \frac{i}{4}\,\mathrm{Tr}\Big\{\Big[\hat{\rho}_n,\hat{\Sigma}\Big](\hat{g}^R\hat{\rho}_m - \hat{\rho}_m\hat{g}^A)\Big\}. \tag{5.24}$$

In the case of a second-order self-energy $\check{\Sigma} = \hat{\Sigma}\check{g}\hat{\Sigma}$, such as the spin-flip scattering, the commutator in (5.21) is

$$\big[\check{\Sigma},\check{g}\big]^K = \Big[\hat{\Sigma},\hat{g}^R\hat{\Sigma}\hat{g}^K + \hat{g}^K\hat{\Sigma}\hat{g}^A\Big]. \tag{5.25}$$

Multiplying by $\hat{\rho}_n$ from the left, taking the trace and using the cyclic property of the trace, and substituting in $h_m\hat{\rho}_m$ and $\hat{g}^K = \hat{g}^R\hat{h} - \hat{h}\hat{g}^A$ gives

$$\tilde{\nabla}\cdot\mathbf{I}_n = -W_{nm}h_m, \tag{5.26}$$

where we defined

$$W_{nm} = \frac{i}{4}\,\mathrm{Tr}\Big\{\Big[\hat{\rho}_n, \hat{\Sigma}\Big] \times (\hat{g}^R\hat{\Sigma}\hat{g}^R\hat{\rho}_m - \hat{\rho}_m\hat{g}^A\hat{\Sigma}\hat{g}^A + \hat{g}^R\Big[\hat{\rho}_m, \hat{\Sigma}\Big]\hat{g}^A)\Big\}. \tag{5.27}$$

For an Usadel equation that contains only self-energy terms of the types described above, the equation for $\tilde{\nabla}\cdot\mathbf{I}_n$ is

$$\tilde{\nabla}\cdot\mathbf{I}_n = -(V_{nm} + W_{nm})h_m, \tag{5.28}$$

where each self energy of first-order has its own V_{nm}-term, and each second-order term has its own W_{nm}-term. Inserting (5.20) into (5.28) gives a second order differential equation for the distribution function:

$$M_{nm}\tilde{\nabla}^2 h_m = -(\tilde{\nabla}M_{nm} + \mathbf{Q}_{nm})\cdot\tilde{\nabla}h_m - (\tilde{\nabla}\cdot\mathbf{Q}_{nm} + V_{nm} + W_{nm})h_m. \tag{5.29}$$

Defining the vector $\mathbf{h} = (h_0, h_1, \ldots, h_7)^T$ and the matrices Q, M, V and W according to their elements (n, m), and setting $\mathbf{A} = 0$, gives the equation

$$\nabla^2\mathbf{h} = -M^{-1}(\nabla M + \mathbf{Q})\cdot\nabla\mathbf{h} - M^{-1}(\nabla\cdot\mathbf{Q} + V + W)\mathbf{h}. \tag{5.30}$$

We proceed with the parametrized boundary conditions for the distribution function. The Keldysh part of the boundary conditions is

$$(\check{g}\partial_x\check{g})^K = \pm\frac{1}{2L\zeta}\big[\underline{\check{g}}, \check{g}\big]^K. \tag{5.31}$$

Multiply by $\hat{\rho}_n/4$ from the left and take the trace. The left-hand side is recognized from equation (5.17) as $\mathbf{I}_n$. We calculate the right-hand side:

$$\begin{aligned}
\pm\frac{D}{2L\zeta}\frac{1}{4}\,\mathrm{Tr}\Big\{\hat{\rho}_n\big[\underline{\check{g}}, \check{g}\big]^K\Big\} &= \pm\frac{D}{8L\zeta}\,\mathrm{Tr}\big\{\hat{\rho}_n(\underline{\hat{g}}^R\hat{g}^K + \underline{\hat{g}}^K\hat{g}^A - \hat{g}^R\underline{\hat{g}}^K - \hat{g}^K\underline{\hat{g}}^A)\big\} \\
&= \pm\frac{D}{8L\zeta}\,\mathrm{Tr}\big\{\hat{\rho}_n(\underline{\hat{g}}^R(\hat{g}^R\hat{\rho}_m - \hat{\rho}_m\hat{g}^A) - (\hat{g}^R\hat{\rho}_m - \hat{\rho}_m\hat{g}^A)\underline{\hat{g}}^A)h_m\big\} \\
&\quad \pm\frac{D}{8L\zeta}\,\mathrm{Tr}\big\{((\underline{\hat{g}}^R\hat{\rho}_m - \hat{\rho}_m\underline{\hat{g}}^A)\hat{g}^A - \hat{g}^R(\underline{\hat{g}}^R\hat{\rho}_m - \hat{\rho}_m\underline{\hat{g}}^A))\underline{h}_m\big\} \\
&= \pm(\underline{T}_{nm}\underline{h}_m - T_{nm}h_m).
\end{aligned} \tag{5.32}$$

In the last line, we defined the matrices

$$\begin{aligned}
T_{nm} &= -\frac{D}{8L\zeta}\,\mathrm{Tr}\big\{\hat{\rho}_n(\underline{\hat{g}}^R(\hat{g}^R\hat{\rho}_m - \hat{\rho}_m\hat{g}^A) - (\hat{g}^R\hat{\rho}_m - \hat{\rho}_m\hat{g}^A)\underline{\hat{g}}^A)\big\} \\
&= \frac{D}{8L\zeta}\,\mathrm{Tr}\big\{\big(\underline{\hat{g}}^A\hat{\rho}_n - \hat{\rho}_n\underline{\hat{g}}^R\big)\big(\hat{g}^R\hat{\rho}_m - \hat{\rho}_m\hat{g}^A\big)\big\}.
\end{aligned} \tag{5.33}$$

$$\underline{T}_{nm} = \frac{D}{8L\zeta}\,\mathrm{Tr}\big\{\big(\hat{g}^A\hat{\rho}_n - \hat{\rho}_n\hat{g}^R\big)\big(\underline{\hat{g}}^R\hat{\rho}_m - \hat{\rho}_m\underline{\hat{g}}^A\big)\big\}. \tag{5.34}$$

5.3 The gap equation

Recall the definition of the superconducting order parameter,
$\Delta(\mathbf{r},t) = \lambda(\mathbf{r})\langle\psi_\downarrow(\mathbf{r},t)\psi_\uparrow(\mathbf{r},t)\rangle$. The order parameter can be expressed via one of the elements of the anomalous Keldysh Green function,

$$\hat{G}^K_{23}(\mathbf{r},t,\mathbf{R},T) = -i\langle[\psi_\downarrow(\mathbf{R}+\mathbf{r}/2,T+t/2),\psi_\uparrow(\mathbf{R}-\mathbf{r}/2,T-t/2)]\rangle \tag{5.35}$$

as

$$\Delta(\mathbf{r},t)/\lambda = \lim_{\mathbf{r},t\to 0}\frac{i}{2}\hat{G}^K_{23}(\mathbf{r},t,\mathbf{R},T). \tag{5.36}$$

Fourier transforming, using the integral approximation (3.108) and performing the integrals over the momentum gives

$$\Delta(\mathbf{r},t)/\lambda = \frac{N_0}{4}\int_{-\omega_c}^{\omega_c}\mathrm{d}E\,\hat{f}^K_{21}(\mathbf{R},T,E). \tag{5.37}$$

It turns out that the above integral diverges for a bulk superconductor if the integration is performed over all energies. Physically, however, we should only consider the energy spectra of the phonons that mediate attractive electron-electron interaction in the superconductor [48]. This is why the integration limits are set to $\pm\omega_c$.

We could also have chosen to express the order parameter with other components of the Keldysh Green function, for example

$$\Delta(\mathbf{r},t)/\lambda = \frac{i}{2}\left(\lim_{\Delta\mathbf{r},\Delta t\to 0}\hat{G}^K_{41}(\Delta\mathbf{r},\Delta t,\mathbf{R},T)\right)^* = \frac{N_0\lambda}{4}\int_{-\omega_c}^{\omega_c}\mathrm{d}E[\tilde{f}^K_{21}(\mathbf{r},t,E)]^*. \tag{5.38}$$

These two expressions for the order parameter can be combined to make an expression where the integral is evaluated for positive energies,

$$\Delta(\mathbf{r},t) = \frac{N_0\lambda}{4}\int_0^{\omega_c}\mathrm{d}E[f^K(E)+(\tilde{f}^K(E))^*]_{21}. \tag{5.39}$$

The coupling constant λ and the cut-off energy ω_c are related through the order parameter Δ_0 at zero temperature because Δ must converge to Δ_0 when the temperature goes to zero in a bulk superconductor [46]. The retarded Green function in a bulk superconductor is given by (3.69), and in equilibrium the Keldysh Green function is

$$\hat{g}^K(E) = \begin{cases} 2sgn(E)\frac{E\hat{\rho}_4-\hat{\Delta}}{E^2-|\Delta|^2}\tanh\left(\frac{\beta E}{2}\right) & E^2 > |\Delta|^2 \\ 0 & E^2 < |\Delta|^2 \end{cases}. \tag{5.40}$$

At zero temperature, $|\Delta| = |\Delta_0|$ and $\tanh(\beta E/2) = sgn(E)$, meaning that $f_{21}^K(E) = 2\Delta_0/\sqrt{E^2 - |\Delta_0|^2}$ when $E^2 - |\Delta_0|^2 > 0$ and zero otherwise. Inserted into (5.37), this gives the zero-temperature self-consistent equation

$$\Delta_0 = N_0\lambda \int_{|\Delta_0|}^{\omega_c} \mathrm{d}E \frac{\Delta_0}{\sqrt{E^2 - |\Delta|^2}}. \tag{5.41}$$

Dividing by Δ_0 and performing a change of variables according to $E = |\Delta_0|\cosh(u)$, we find the relation between the coupling constant, the cut-off energy and the zero-temperature order parameter Δ_0:

$$\omega_c = |\Delta_0| \cosh\left(\frac{1}{N_0\lambda}\right). \tag{5.42}$$

The self-consistent gap equation finally reads

$$\Delta(\mathbf{r}, t) = \frac{N_0\lambda}{4} \int_0^{|\Delta_0|\cosh(1/N_0\lambda)} \mathrm{d}E[f_{21}^K(E) + (\tilde{f}_{21}^K(E))^*]. \tag{5.43}$$

5.4 Numerical determination of the state of a system

The self-consistent equation for the order parameter has the form $\Delta = F(\Delta)$, and the simplest way to solve such an equation is by fix-point iteration. The solution strategy is the following: Choose an initial guess $\Delta = \Delta_1$ which is inserted into the retarded Usadel equation to find the retarded Green function $\hat{g}^R$. After that, solve the equation of motion for the distribution function given Δ_1 and $\hat{g}^R$, and use the retarded Green function and the distribution function to calculate the successive $\Delta_2 = F(\Delta_1)$. This is repeated until $|\operatorname{Re}\{\Delta_{n+1} - \Delta_n\}|$ and $|\operatorname{Im}\{\Delta_{n+1} - \Delta_n\}|$ is less than some threshold value for all positions, and the system is then said to have converged to a fixed point for the gap. A weakness in using the absolute convergence criteria instead of the relative criteria $|\operatorname{Re}\{\Delta_{n+1} - \Delta_n\}/\operatorname{Re}\{\Delta_n\}|$, and similarly for the imaginary part, is that it will not be accurate when the actual solution for the gap is very small, but finite. Nevertheless, when the gap is zero the relative change in the gap can be very large, so in systems where the gap is zero for at least one position the relative criteria alone cannot be used alone. Therefore, it is more convenient to use the absolute convergence criteria.

In some systems, the gap will always converge towards the same fixed point for any initial guess $\Delta_1 \neq 0$. For superconducting systems, the fixed point is non-zero, while for normal state systems, the gap always converges to zero. These are stable solutions. There also exist unstable solutions, in which any perturbation from the solution will lead to a divergence away from that point. This is for example the case

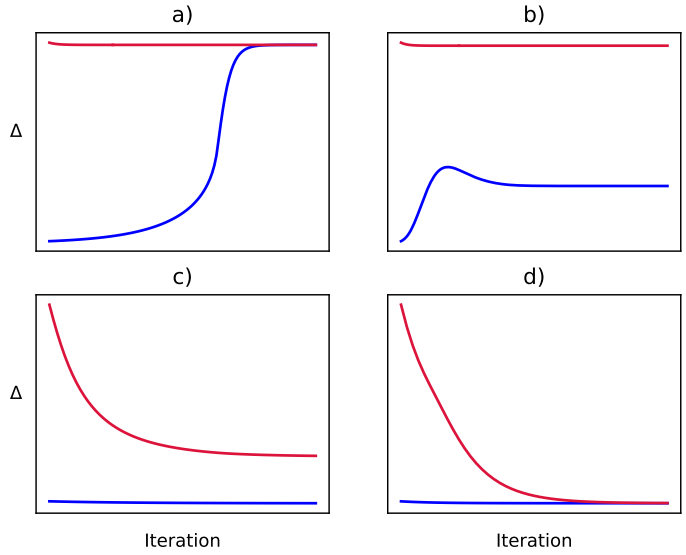

Figure 2: Demonstration of how the gap develops through the self-consistency iterations for a system in the superconducting phase (a and b), the bistable phase (c) and the normal phase (d). The red lines show the development when the initial guess is $\Delta = \Delta_0$, and the blue lines when the initial guess $\Delta = 0.01\Delta_0$.

for the normal state solution $\Delta = 0$ in a superconductor. Unstable solutions are physically uninteresting and will be discarded.

Some systems have distinct, locally stable solutions for the gap, meaning that the solutions are robust to small perturbations. These solutions correspond to different local minima in the free energy, and the system will eventually collapse into the state corresponding to the lowest free energy. A system that resides in a global minimum can be adiabatically varied by tuning the magnetic field or voltage until the system no longer is in the global minimum. It is now in a local minima in the free energy, but there is an energy barrier that prevents the system from jumping into the global minima. Therefore, it can remain in the local minimum for a while and a superconducting hysteresis effect can be observed.

In practice, the phase of a system is determined by solving with a low initial guess $\Delta = 0.01\Delta_0$ and a high initial guess $\Delta = \Delta_0$. Regions where both branches converge to a non-zero value, either to the same solution or to different superconducting solutions, are termed superconducting. If both solutions converge to zero, the system is in the normal state. Regions where one finds one superconducting solution and one normal solution are termed bistable. The categorization of the phase is depicted in figure 2, and is consistent with the definitions in [47].

The exact transition lines from the normal state to the superconducting state are not straightforward to calculate in the Usadel formalism, because there is no simple way to calculate the free energy out of equilibrium using quasiclassical theory. However, the transition lines are assumed to be in the bistable regions.

6 The effect of a spin-voltage on a spin-split superconductor

6.1 Introduction

It is established that superconductivity can co-exist with spin-splitting fields well beyond the Chandrasekhar-Clogston limit by spin-triplet or FFLO pairing, by the introduction of spin-orbit coupling to the system [49], by modification of the band structure in the superconductor [50], and by driving the superconductor out of equilibrium [47, 51]. This insight is applicable to the field of superconducting spintronics [7], where stabilizing superconductivity in the presence of magnetic elements is of great importance.

Bobkov and Bobkova [51] found that superconductivity can be recovered by sandwiching a superconducting film between two half metals and voltage bias the junction. A spin-splitting field m was applied to the superconductor. The half metals can be thought of as fully polarized ferromagnets with magnetizations pointing in opposite directions. Say the left half metal is polarized in the $+z$-direction, and that a voltage $+V$ is applied in the left half metal and $-V$ is applied in the right half metal. Then there is a voltage drop V for spin-up particles at the left interface, and a voltage drop $-V$ for spin-down particles at the right interface. There is no voltage drop for spin-up particles at the right interface or spin-down particles at the left interface. We therefore have a spin-dependent voltage, also known as a spin accumulation. Inside the film, the distribution of spin-up electrons is identical to the distribution in the left half metal and the distribution of spin-down electrons is identical to the distribution in the right half metal, so the distribution function is

$$\hat{h} = \begin{pmatrix} h_+ & 0 & 0 & 0 \\ 0 & h_- & 0 & 0 \\ 0 & 0 & h_+ & 0 \\ 0 & 0 & 0 & h_- \end{pmatrix}, \tag{6.1}$$

where $h_\pm = \tanh \beta(E \pm |e|V_s)/2$. Hence, at zero temperature the distribution function has a one-step form in each of the spin subbands. Such a one-step form was essential for the recovery of superconductivity. Inserting the one-step distribution function and the Green function for a bulk, spin-split superconductor into the gap equation revealed that $m = |e|V_s$ is equivalent to $m = |e|V_s = 0$, explaining why superconductivity is recovered under the simultaneous influence of a spin-splitting field and a spin-dependent voltage. It is also mentioned, though not further explored, that a spin-dependent quasiparticle distribution can lead to the occurrence

of an FFLO state for some parameter ranges.

Superconductivity is also recovered when applying a purely electric voltage $eV = m$, as reported by Ref. [47]. In this article, the superconductor was in contact with normal reservoirs where the chemical potentials were shifted by $\pm eV$ compared to the superconductor. The recovery of superconductivity was motivated analytically by considering the gap equation when applying a voltage and a spin-splitting field in a similar manner as explained above, and also numerically by calculating the phase diagram for a system with a varying voltage and spin-splitting field. This phase diagram, which displays the regions of superconductivity, bistability, and the normal state, was symmetric under exchanging $eV \leftrightarrow m$. Another setup where the chemical potentials in both reservoirs were shifted by $+eV$ was also suggested, but the phase diagrams for the two setups should be identical. To see why, we show that the gap $|\Delta|$ at a superconductor/normal metal interface has the same value regardless of whether the chemical potential in the normal reservoir is shifted by plus or minus eV. The distribution function at the interface is approximately identical to the distribution function in the reservoir,

$$\hat{h} = \begin{pmatrix} h_+ & 0 & 0 & 0 \\ 0 & h_+ & 0 & 0 \\ 0 & 0 & h_- & 0 \\ 0 & 0 & 0 & h_- \end{pmatrix}. \tag{6.2}$$

Inserting this into the gap equation gives

$$\Delta = \int_{-\infty}^{\infty} \mathrm{d}E f_{21}(E) \tanh\left(\frac{E - |e|V}{2T}\right) + f_{12}(-E) \tanh\left(\frac{E + |e|V}{2T}\right), \tag{6.3}$$

where f is the anomalous retarded Green function. At zero temperature, this reduces to

$$\Delta = \int_{|e|V}^{\infty} \mathrm{d}E \left(f_{21}(E) - f_{12}(E)\right) - \int_{-\infty}^{|e|V} \mathrm{d}E \left(f_{21}(E) - f_{12}(E)\right). \tag{6.4}$$

Switching the sign of V gives

$$\Delta = -\int_{|e|V}^{\infty} \mathrm{d}E \left(f_{21}(-E) - f_{12}(-E)\right) + \int_{-\infty}^{|e|V} \mathrm{d}E \left(f_{21}(-E) - f_{12}(-E)\right). \tag{6.5}$$

This may induce a phase shift to the order parameter, but we disregard it because we are only interested in $|\Delta|$. Restricting our attention to real order parameters, the bulk Green function for a spin-split superconductor satisfies $f(-E) = -f^*(E)$. Inserting this into (6.5) shows that the gap is unaffected by the sign of eV.

In the case of a spin-dependent voltage in the presence of a spin-splitting field, the gap equation at zero temperature takes the form

$$\begin{aligned}\Delta = &-\int_{-\infty}^{|e|V_s} \mathrm{d}E f_{21}(E) + \int_{-|e|V_s}^{\infty} \mathrm{d}E f_{12}(E) \\ &+\int_{|e|V_s}^{\infty} \mathrm{d}E f_{21}(E) - \int_{-\infty}^{-|e|V_s} \mathrm{d}E f_{12}(E).\end{aligned} \tag{6.6}$$

Switching the sign of the voltage is equivalent to switching $f_{12} \leftrightarrow f_{21}$, but in a bulk spin-split superconductor they are related by $f_{12}(E) = -f_{21}(-E)$. This substitution changes the value of the gap, and therefore the gap is not necessarily symmetric in position when a spin-dependent voltage is introduced to the system. We know that superconductivity is recovered when the spin-dependent voltage is close to the value of the spin-splitting field, but the full phase diagram showing the regions of superconductivity, bistability and the normal state is unknown. An emerging question is therefore how the phase diagram looks when applying a spin-dependent voltage.

A spin-dependent voltage also opens up the possibility for the spatially inhomogeneous gap, indicating the presence of an FFLO state. An oscillating order parameter divides the superconductor into domains with phases 0 and π. It has been suggested that superconducting phase domains can be used for memory applications [52]. The idea behind this is that the resistance of a superconducting layer with two phase-domains is higher than the resistance of a layer with one single phase, and therefore the critical current is lower. By tuning the layer to have phase domains one effectively can write 1, while tuning the layer to have a single phase corresponds to writing 0. Setups leading to a dominating FFLO state have therefore the potential to be used for storing information if the FFLO state remains when the spin voltage is switched off. Motivated by this, we apply normal reservoirs instead of half metals like Bobkov and Bobkova, let the spin-dependent voltage drops be nonzero at both interfaces, and we see if this leads to the appearance of an FFLO state.

If the chemical potentials are shifted in the same way in both reservoirs, the order parameter has to be symmetric because the system looks the same if the two reservoirs are swapped. The phase diagram could therefore look quite different from the voltage-biased system described above. Motivated by this, we are interested in how the phase diagram looks for a system where the spin-accumulation potential is the same in both reservoirs.

6.2 Model

The system we look at is a normal metal/superconductor/normal metal system. The superconductor is a thin film with an in-plane spin-splitting field pointing in the z-direction. This could be realized by growing the superconductor on top of a ferromagnetic insulator which induces a spin-splitting field in the superconductor. The normal metals are assumed to be reservoirs, unaffected by the inverse proximity effect. The normal metals have a spin accumulation, and the spin-quantization axis in the reservoirs is taken to be parallel to the direction of the spin-splitting field.

A spin accumulation can be created and detected with a structure consisting of a normal metal N connected to two ferromagnets F1 and F2 with either parallel or antiparallel magnetizations [53]. F1 is the injector and F2 is the detector. A current passes through F1 into the normal metal, forming a closed circuit at the left part of N. The current is spin-polarized due to the ferromagnet and when the current enters the normal metal, the spin diffuses into the right side. The voltage between F2 and N then depends on the relative orientations of the magnetizations of F1 and F2.

Note that a spin accumulation in the reservoirs is not the same as having ferromagnetic reservoirs. In a ferromagnet in equilibrium, the density of states is different for particles with different spins, but the chemical potential is the same regardless of spin. Therefore, the distribution function is unchanged. On the contrary, a spin accumulation changes the chemical potential but not the density of states, which will drive spin-up electrons to move from the left reservoir to the right reservoir and spin-down electrons in the opposite direction. This is illustrated in figure 3.

Two setups are considered: First, we consider setup A as shown in panel a) of figure 4, where the quasiparticle distributions are oppositely shifted in the reservoirs. Second, we consider setup B where the distribution functions in the reservoirs are identical. This is shown in panel b) of figure 4. The distribution functions used in setup A in the left and right reservoirs are

$$\hat{h}_L^a = \begin{pmatrix} h_+ & 0 & 0 & 0 \\ 0 & h_- & 0 & 0 \\ 0 & 0 & h_- & 0 \\ 0 & 0 & 0 & h_+ \end{pmatrix} \quad \hat{h}_R^a = \begin{pmatrix} h_- & 0 & 0 & 0 \\ 0 & h_+ & 0 & 0 \\ 0 & 0 & h_+ & 0 \\ 0 & 0 & 0 & h_- \end{pmatrix}. \tag{6.7}$$

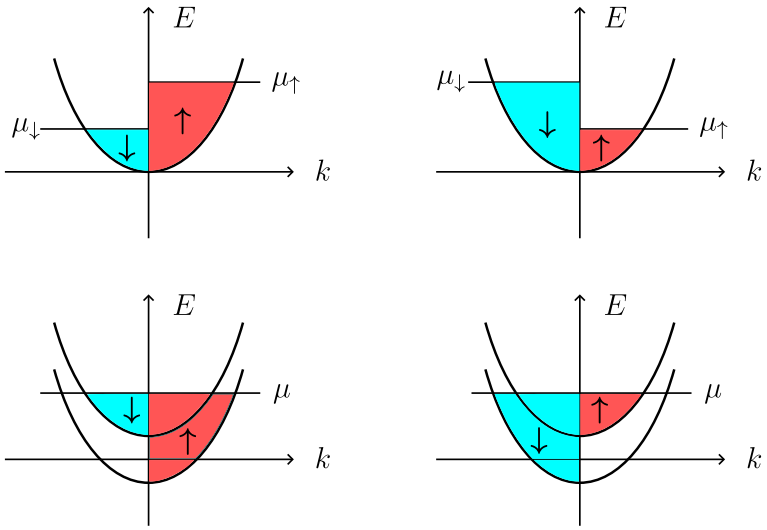

Figure 3: An illustration of the difference between a non-equilibrium spin accumulation in the normal metal reservoirs (upper graphs) and equilibrium ferromagnetic reservoirs (lower graphs). The colored areas represent the number of electrons with spin up and down. The graphs in the left part of the figure represent the left reservoir, and the right part represents the right reservoir.

In setup B, the distribution functions in the left and right reservoirs are equal,

$$\hat{h}_L^b = \hat{h}_R^b = \begin{pmatrix} h_+ & 0 & 0 & 0 \\ 0 & h_- & 0 & 0 \\ 0 & 0 & h_- & 0 \\ 0 & 0 & 0 & h_+ \end{pmatrix}. \tag{6.8}$$

This can be expressed in terms of the matrices ρ_0 and ρ_7 by noting that $(\rho_0+\rho_7)/2 = \mathrm{diag}(1,0,0,1)$ and $(\rho_0-\rho_7)/2 = \mathrm{diag}(0,1,1,0)$.

The superconductor is thin enough to be considered effectively 2D and to suppress the orbital effect for an in-plane magnetic field. Edge effects at the interfaces not bordering to the normal reservoirs are neglected, such that the superconductor can be effectively treated as 1D.

The parameters were chosen close to Ref. [47] to make the comparison of the phase diagrams easier. The length of the superconductor was set to $L = 8\xi$, where $\xi = D/\Delta_0$ is the bulk superconducting coherence length. Inelastic scattering was modeled using the Dynes approximation $E/\Delta_0 \to E/\Delta_0 + 0.01i$ in the retarded Usadel equation. The temperature in the reservoirs was $T = 0.01T_c$, which essentially is zero. The interface parameter ζ is set to 3, corresponding to a high barrier resistance compared to the normal state resistance. The self-energies included in the Usadel equation were superconductivity $\hat{\Delta}$ and the magnetic exchange field $\hat{M}$.

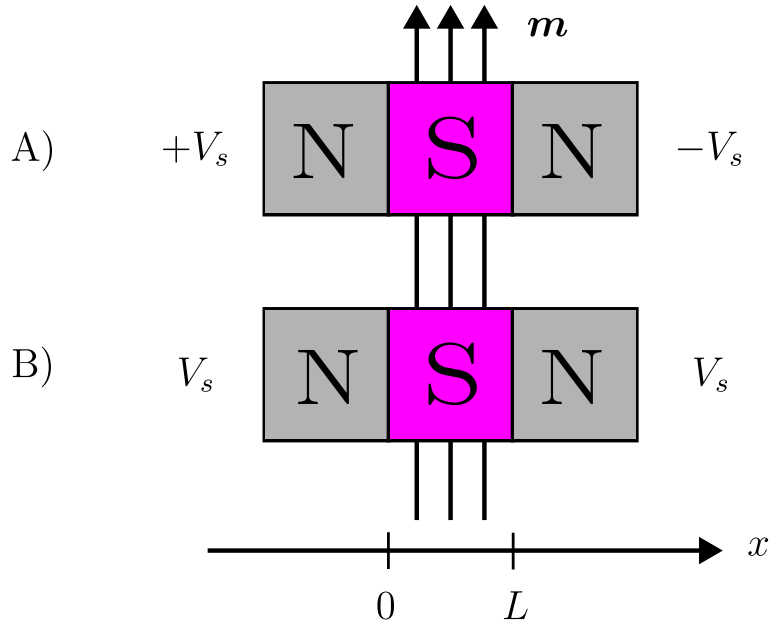

Figure 4: The two setups considered in this thesis. In setup A, the spin voltage V_s is opposite in the normal reservoirs. In setup B, the spin voltages in the normal reservoirs are the same. The superconductor is penetrated by the spin-splitting field **m**. The left side of the superconductor refers to the position $x = 0$, and the right side refers to $x = L$.

The 1D Usadel equation together with the Kupriyanov-Lukichev boundary conditions were then solved for 19×20 values for m and $|e|V_s$ in the interval $[0, 2\Delta_0]$ in setup A with initial guesses $\Delta_1 = \Delta_0$ (superconducting branch) and $\Delta_1 = 0.01\Delta_0$ (normal branch) to construct figure 7. In setup B, the equations were solved for 19×39 values for m and $|e|V_s$ in the intervals $[0, 2\Delta_0)$ and $[-2\Delta_2, 2\Delta_0]$ respectively. The result was the phase diagram for setup B in figure 5.

Calculations were performed on resources provided by UNINETT Sigma2.

6.3 Results and discussion

The numerical calculations required using supercomputer simulations which were time-consuming, as the equations had to be solved self-consistently for every parameter set. This is the reason for not having an abundant number of plots with results. We start by explaining the results for setup B, as these results are easier to interpret than the results for setup A.

Figure 5 shows the phase diagram in setup B. The colors on the background show the average value of $|\Delta(x)|/\Delta_0$ in the normal branch, while the dots display the average value of the gap in the superconducting branch. Dark purple regions are in the normal state, while yellow regions are superconducting. Yellow dots on top

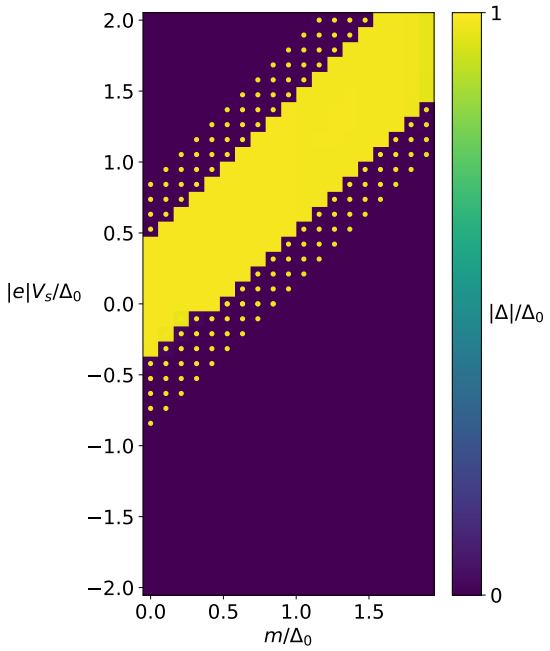

Figure 5: Phase diagram for setup B. The background shows the average value of the gap in the normal branch, and the dots show the average value of the gap in the superconducting branch. Dark purple regions are categorized as the normal state, yellow regions are superconducting, and dark purple regions with yellow dots are bistable.

of dark purple background means that the gap in the normal branch converged to zero, while the gap in the superconducting branch converged to a value close to the bulk value. These regions with dots on dark purple background are bistable. We see that at zero voltage, superconductivity exists for $m < \Delta_0$. In the region $0.5\Delta_0 < m < \Delta_0$, the system is bistable. This is reasonable considering the Chandrasekhar-Clogston limit at $m \approx 0.7\Delta_0$, which means that we expect a transition from the superconducting state to the normal state in this region. The same is seen for a zero spin-splitting field when varying the spin voltage.

From the phase diagram, it is seen that the gap either converges to some value close to Δ_0 or to the normal metal solution at zero, but never to something in between. This is reasonable considering the low temperature. In a bulk superconductor at zero temperature, the gap is Δ_0 for spin-splitting fields lower than the Chandrasekhar-Clogston limit. When applying a spin-splitting field larger than this limit, the gap immediately drops to zero. Therefore, the system with the same spin accumulations in the reservoirs behaves like a zero-temperature, bulk superconductor with an effective spin-splitting field m_{eff}.

In the figure, there is a superconducting band with width Δ_0 following the line $m = |e|V_s$, and a region of width $0.5\Delta_0$ outside this band is bistable. The phase diagram

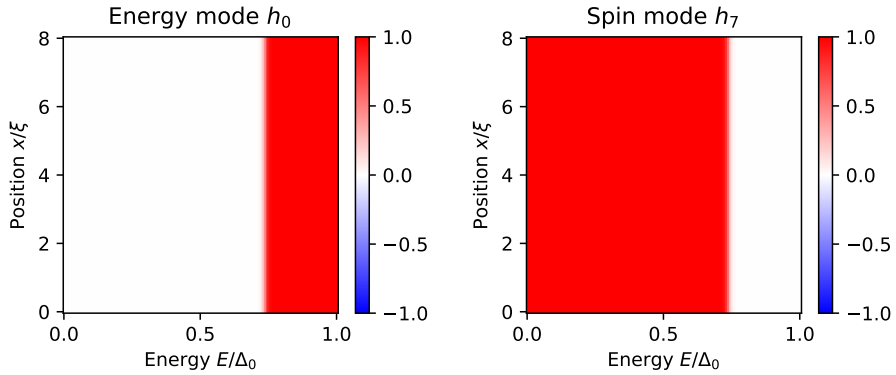

Figure 6: Distribution function modes in setup B case with $m = |e|V_s = 0.737\Delta_0$. All other modes are zero.

is symmetric around the line $m = |e|V_s$. This indicates that the simultaneous effect of a spin-splitting field m and a spin voltage $|e|V_s$ is an effective spin-splitting field $m_{eff} = m - |e|V_s$. The modes of the distribution function in setup B are plotted in figure 6. For negative energies, $h_0(-E) = -h_0(E)$ and $h_7(-E) = h_7(E)$ due to the symmetry of the distribution function. The shape of the distribution function is identical to the distribution functions in the reservoirs, $\hat{h} = t_+(\rho_0 + \rho_7)/2 + t_-(\rho_0 - \rho_7)/2$ where $t_\pm = \tanh((E \pm |e|V_s)/2T)$. This is equivalent to saying that the distribution function for electrons with spin up and holes with spin down is t_+, and the distribution function for electrons with spin down and holes with spin up is t_-. The distribution function therefore has a one-step form in each of the particle subbands. We already concluded that the system behaves like a bulk, spin-split superconductor, so if we insert the bulk expression for the retarded, spin-split Green function and the distribution function into the gap equation we find

$$\Delta = \int_{-\infty}^{\infty} \mathrm{d}E \frac{-2\Delta}{\sqrt{(E-m)^2 - \Delta^2}} \tanh\left(\frac{E - |e|V_s}{2T}\right). \tag{6.9}$$

Defining a new integration variable $E' = E - |e|V_s$ shows that the spin-splitting field and the voltage show up only in the combination $m - |e|V_s$. This demonstrates that the effect of the voltage and the spin-splitting field indeed is the equilibrium system with an effective field $m - |e|V_s$.

For the phase diagram to be fully symmetric, there should have been four extra yellow squares at the edge of the superconducting region for $V_s < 0$. Physically, at $m = 0$ the phase diagram should have been symmetric because at zero magnetic field, switching the direction of the spins in the reservoirs should not have any effect. It also turned out that the gap evolved differently for voltages ± 0 when the strength of the spin-splitting field was close to the limit for the normal state to become locally

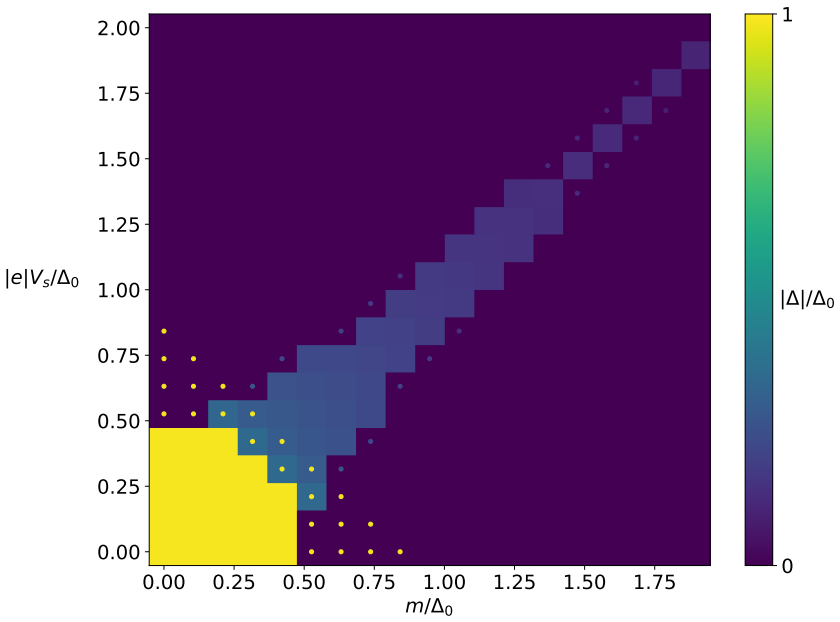

Figure 7: Phase diagram for setup A. The background shows the average value of the gap in the normal branch, and the dots show the average value of the gap in the superconducting branch. Dark purple regions are categorized as the normal state, and dark purple regions with yellow dots are bistable. Yellow regions and regions with visible dots on a background that is not dark purple are superconducting.

stable. The asymmetry in the phase diagram is therefore attributed to numerical inaccuracy close to the transition lines from the superconducting to the normal state.

Figure 7 shows the phase diagram in setup A. Again, the colors on the background show the average value of $|\Delta(x)|/\Delta_0$ in the normal branch, while the dots display the average value of the gap in the superconducting branch. Dark purple regions are in the normal state, yellow regions are superconducting, and regions with dots on dark purple background are bistable. The regions with visible dots on a background that is not dark purple are defined as superconducting. Compared to the phase diagram in [47], this phase diagram looks quite similar. It is maybe surprising that the phase diagram looks the same regardless of the spin dependence of the applied voltage, but there are important differences in the systems.

An important difference from the system with a spin-independent voltage is that the distribution function and the gap are not symmetric, they are spatially inhomogeneous. Figure 9 shows the spatial profile of the superconducting order parameter for different parameter choices in the region $m + |e|V_s > \Delta_0 < m - |e|V_s$. On the left-hand side, the gap is nonzero, while on the right-hand side the gap is small. This can be understood by recalling the discussion of the effective field m_{eff} in

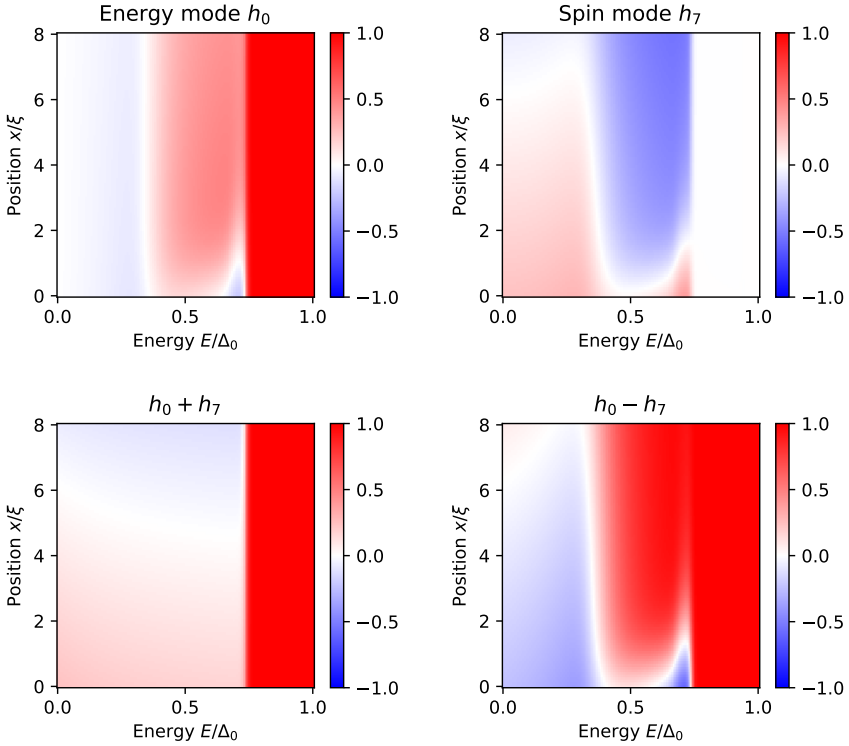

Figure 8: Distribution function modes in setup A with $m = |e|V_s = 0.737\Delta_0$. All other modes are zero.

setup B. On the left-hand side in setup A, $m_{eff} \sim m - |e|V_s$ while on the right-hand side $m_{eff} \sim m + |e|V_s$. The effective spin-splitting field is therefore increasing throughout the superconductor. An increase in the spin-splitting field leads to the suppression of the order parameter because of the proximity effect. At zero temperature in a bulk superconductor, the gap is not affected until the spin-splitting field reaches the Chandrasekhar-Clogston limit. Therefore, the suppression of the gap is due to Cooper pairs leaking out of the increasingly hostile superconductor for increasing spin-splitting fields. This shows that it is reasonable that the gap is larger on the left-hand side than on the right-hand side, and it also explains why superconductivity is recovered.

Using the gap equation to explain the recovery of superconductivity in setup A is not straightforward. The contribution from the modes h_n of the distribution function in setup A is more complicated than in setup B due to the modes being inhomogeneous, as seen in figure 8. The part of the distribution function that shows up in the gap equation is $h^e_\downarrow = (h_0 - h_7)/2$, which is the distribution function for spin-down electrons. For negative energies, $h^e_\downarrow(-E) = -(h_0(E) + h_7(E))/2$. Therefore, $h^e_\downarrow(E) = \mathrm{sgn}(E) = t_-$ for $|E| > |e|V_s$ as in setup B, but for energies $|E| < |e|V_s$

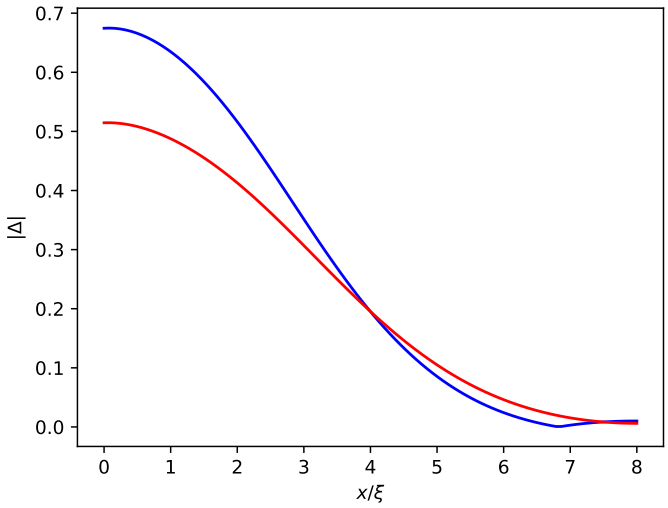

Figure 9: Typical shape of the gap in setup A in regions where $m + |e|V_s > \Delta_0 < m - |e|V_s$. The blue line has a phase shift from 0 to π at $x/\xi \approx 7$, while the phase of the red line is zero everywhere.

the distribution function varies both with position and energy. We can write this as $h^e_\downarrow(E) = t_- + \eta(x, E)$ where $\eta(x, E)$ is zero for $|E| > |e|V_s$. Inserting this into the gap equation makes it clear that the spin-splitting field and the voltage do not show up as $m - |e|V_s$ in η. Thus, claiming that there is an effective spin-splitting field $m - |e|V_s$ in setup A is not justified from the gap equation, so it cannot fully explain the recovery of superconductivity. However, another option for surviving beyond the Chandrasekhar-Clogston limit was encountered earlier, namely the FFLO state. The asymmetry in the gap indicates the existence of an FFLO-like state. Conclusively, there are two effects responsible for allowing superconductivity to exist with a spin-splitting field in setup A: the spin-accumulation counteracting the spin-splitting field and the occurrence of an FFLO-like state.

The inhomogeneity due to the FFLO-like state could have practical applications. For some of the parameter sets, the FFLO-like state is prominent enough to generate a π phase shift inside the superconductor at the position where the derivative of $|\Delta|$ is discontinuous. The jump in the phase gives two superconducting phase domains: the left domain has phase 0, while the right domain has phase π. This could potentially be used in memory applications, as briefly discussed earlier. Another option is to utilize that the gap is non-zero on one side of the superconductor, and close to zero on the other side. Due to parts of the film being pushed to a near-normal state, the spin resistivity of the film is smaller than that of a superconducting film because the region with a finite gap is smaller. Therefore, the probability for tunneling and

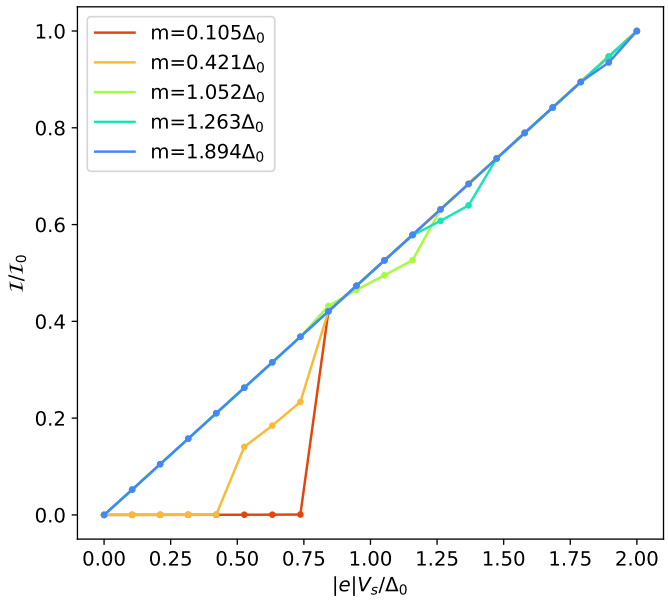

Figure 10: Spin current $\mathcal{I}$ as a function of spin voltage $|e|V_s/\Delta_0$ for various spin-splitting field strengths in setup A. The current was calculated in the superconducting branch and normalized to the normal state current $\mathcal{I}_0$ at $|e|V_s/\Delta_0 = 2$.

crossed Andreev reflection increases. The charge resistivity also decreases compared to the homogeneous superconducting state because the probability for tunneling increases. The spin- and charge resistivities of the film will still be higher than that of a normal state film where the gap is zero. By tuning the film to be either superconducting or inhomogeneous, or alternatively normal state or inhomogeneous, it can be read as either zero or one. It therefore has the capacity to store information. In dirty equilibrium superconductors, the FFLO state can only exist for vanishingly small temperatures. It would be interesting to see if the FFLO-like state persists for higher temperatures out of equilibrium, but this is left for future work.

Figure 10 shows the spin current in the superconducting branch of setup A as a function of voltage for various spin-splitting field strengths. The charge current in the system is zero. For $m = 1.894\Delta_0$, $I(|e|V_s/\Delta_0)$ (blue) is linear up to $m = |e|V_s$. Looking at the phase diagram, we see that this region corresponds to the normal state. This makes sense; it is Ohm's law but for spin currents and spin voltages. At $m = |e|V_s$, the system is superconducting and there is a small dip in the current. The superconducting state therefore has higher spin-resistivity than the normal state, which is reasonable due to the superconducting gap. An incoming electron with energy lower than the superconducting gap cannot be transmitted into the superconductor. Andreev reflection gives no net contribution to the spin current because

the reflected hole has the same spin as the incoming electron. The only processes that can contribute to the spin current in the superconducting state are therefore tunneling and crossed Andreev reflection. This represents a higher resistivity compared to the normal state, where the electron can simply be transmitted through the interface. The same is seen for $m = 1.052\Delta_0$ (green) and $m = 1.263\Delta_0$ (turquoise). At the two lowest spin-splitting fields $m = 0.105\Delta_0$ (red) and $m = 0.421\Delta_0$ (orange), the spin current is zero up until some critical voltage. The spin current is zero in the regions where the systems are superconducting, again indicating higher resistivity in the superconducting state. The spin-current is conserved throughout the superconductor. This is reasonable because there are no terms in the Hamiltonian flipping spins. If we had included spin-flipping terms, for example scattering on magnetic impurities, the spin current would decay towards the center of the superconductor. The absence of a charge current in the system is reasonable because spin-up particles are moving from the left side of the system to the right side, while the spin-down particles move in the opposite direction. The magnitude of voltages is the same for both spins, so the number of spin-up particles moving right is the same as the number of spin-down particles moving left. This gives a net spin current, but no net charge current.

In setup B, all currents are zero. We can explain this if we go back to figure 4 and let the y-axis be parallel to $\mathbf{m}$. Setup b) is invariant over a π rotation around the y-axis. However, a current flowing in the x-direction would change direction when rotating the system around the y-axis. Therefore, there cannot be any currents in setup B.

7 Summary and outlook

In this thesis, we have solved the quasiclassical and diffusive Usadel equation numerically in 1D and demonstrated that superconductivity can be recovered for spin-splitting fields exceeding the Chandrasekhar-Clogston limit when applying a spin voltage V_s to the system. The reasons for the recovery are the emergence of an effective spin-splitting field proportional to the spin-splitting field minus the spin voltage and the appearance of an FFLO state.

Having developed the framework for solving the Usadel equation numerically, other non-equilibrium phenomena in superconducting films can be studied. One such phenomenon is the process known as crossed Andreev reflection. An electron coming in from the left in a normal metal/superconductor/normal metal junction pairs up with an electron from the right normal metal, leaving a hole propagating away from the right interface. The hole and the incoming electron are entangled, meaning the superconductor creates entanglement between electrons on the left side and holes on the right side. Quantum entanglement is needed for quantum computation and teleportation of quantum states, and finding ways to generate entangled particles is highly relevant. Crossed Andreev reflection competes with other types of scattering at the interfaces, and there are currently research efforts focused on maximizing the crossed Andreev reflection signals [54–57]. A natural extension of this thesis will be to determine how using spin-split superconductors affects the probability for crossed Andreev reflection.

References

1. Onnes, H. K. Further experiments with liquid helium. C. On the change of electric resistance of pure metals at very low temperatures etc. IV. The resistance of pure mercury at helium temperatures. *Communications from the Physical Laboratory at Leiden* **120** (1911).
2. Meissner, W. & Ochsenfeld, R. Ein neuer effekt bei eintritt der supraleitfähigkeit. *Naturwissenschaften* **21,** 787–788 (1933).
3. Bardeen, J., Cooper, L. N. & Schrieffer, J. R. Theory of superconductivity. *Physical review* **108,** 1175 (1957).
4. Fossheim, K. & Sudbø, A. *Superconductivity: physics and applications* 15 (John Wiley & Sons, 2004).
5. Meservey, R. & Tedrow, P. M. Spin-polarized electron tunneling. *Physics reports* **238,** 173–243 (1994).
6. Andreev, A. F. The thermal conductivity of the intermediate state in superconductors. *Sov. Phys. JETP.* **19,** 1228 (1964).
7. Linder, J. & Robinson, J. W. A. Superconducting spintronics. *Nature Physics* **11,** 307–315 (2015).
8. Eschrig, M. Spin-polarized supercurrents for spintronics: a review of current progress. *Reports on Progress in Physics* **78,** 104501 (2015).
9. Ohnishi, K. *et al.* Spin-transport in superconductors. *Applied Physics Letters* **116,** 130501 (2020).
10. Amundsen, M. *Proximity effects in superconducting hybrid structures with spin-dependent interactions* PhD thesis (2020).
11. Baibich, M. N. *et al.* Giant magnetoresistance of (001) Fe/(001) Cr magnetic superlattices. *Physical review letters* **61,** 2472 (1988).
12. Binasch G.and Grünberg, P., Saurenbach, F. & Zinn, W. Enhanced magnetoresistance in layered magnetic structures with antiferromagnetic interlayer exchange. *Physical review B* **39,** 4828 (1989).
13. Kalenkov, M. S. & Zaikin, A. D. Crossed Andreev reflection and spin-resolved non-local electron transport. *Fundamentals of Superconducting Nanoelectronics,* 67–100 (2011).
14. Hemmer, P. C. *Kvantemekanikk* (Fagbokforlaget Vigmostad & Bjørke AS, 2005).
15. Bogoliubov, N. N. On a New Method in the Theory of Superconductivity. *Nuovo Cim* **7,** 794–805 (1958).
16. Birgani, A. G. *RKKY interaction and coexistence with magnetism in superconducting systems.* PhD thesis (2022).

17. Clogston, A. M. Upper limit for the critical field in hard superconductors. *Physical Review Letters* **9,** 266 (1962).
18. Chandrasekhar, B. S. A note on the maximum critical field of high-field superconductors. *Applied Physics Letters* **1,** 7–8 (1962).
19. Eschrig, M. Spin-polarized supercurrents for spintronics. *Physics Today* **64,** 43–49 (2011).
20. Fulde, P. & Ferrell, R. A. Superconductivity in a Strong Spin-Exchange Field. *Phys. Rev.* **135,** A550–A563 (3A 1964).
21. Larkin, A. I. & Ovchinnikov, I. U. N. Inhomogeneous state of superconductors (Production of superconducting state in ferromagnet with Fermi surfaces, examining Green function). *Soviet Physics-JETP* **20,** 762–769 (1965).
22. Saint-James, D., Sarma, G. & Thomas, E. J. *Type II superconductivity* (Pergamon Press, 1969).
23. Wosnitza, J. FFLO states in layered organic superconductors. *Annalen der Physik* **530,** 1700282 (2018).
24. Aslamazov, L. G. Influence of impurities on the existence of an inhomogeneous state in a ferromagnetic superconductor. *Sov. Phys. JETP.* **28,** 773–775 (1969).
25. Houzet, M. & Mineev, V. P. Interplay of paramagnetic, orbital, and impurity effects on the phase transition of a normal metal to the superconducting state. *Physical Review B* **74,** 144522 (2006).
26. Takada, S. Superconductivity in a Molecular Field. II: Stability of Fulde-Ferrel Phase. *Progress of Theoretical Physics* **43,** 27–38 (1970).
27. Lortz, R. *et al.* Calorimetric Evidence for a Fulde-Ferrell-Larkin-Ovchinnikov Superconducting State in the Layered Organic Superconductor κ-(BEDT- TTF)$_2$Cu(NCS)$_2$. *Physical review letters* **99,** 187002 (2007).
28. Bergk, B. *et al.* Magnetic torque evidence for the Fulde-Ferrell-Larkin-Ovchinnikov state in the layered organic superconductor κ-(BEDT- TTF)$_2$Cu(NCS)$_2$. *Physical Review B* **83,** 064506 (2011).
29. Matsuda, Y. & Shimahara, H. Fulde–Ferrell–Larkin–Ovchinnikov state in heavy fermion superconductors. *Journal of the Physical Society of Japan* **76,** 051005 (2007).
30. Kinnunen, J. J., Baarsma, J. E., Martikainen, J.-P. & Törmä, P. The Fulde–Ferrell–Larkin–Ovchinnikov state for ultracold fermions in lattice and harmonic potentials: a review. *Reports on Progress in Physics* **81,** 046401 (2018).
31. Morten, J. P. *Spin and charge transport in dirty superconductors* , M.Sc. thesis, (2003).
32. Usadel, K. D. Generalized diffusion equation for superconducting alloys. *Physical Review Letters* **25,** 507 (1970).

33. Keldysh, L. V. Diagram technique for nonequilibrium processes. *Sov. Phys. JETP* **20,** 1018–1026 (1965).
34. Matsubara, T. A new approach to quantum-statistical mechanics. *Progress of theoretical physics* **14,** 351–378 (1955).
35. Chandrasekhar, V. *Proximity-Coupled Systems: Quasiclassical Theory of Superconductivity* 279–313 (Springer Berlin Heidelberg).
36. Belzig, W., Wilhelm, F. K., Bruder, C., Schön, G. & Zaikin, A. D. Quasiclassical Green's function approach to mesoscopic superconductivity. *Superlattices and microstructures* **25,** 1251–1288 (1999).
37. Serene, J. W. & Rainer, D. The quasiclassical approach to superfluid 3He. *Physics Reports* **101,** 221–311 (1983).
38. Hugdal, H. G., Linder, J. & Jacobsen, S. H. Quasiclassical theory for the superconducting proximity effect in Dirac materials. *Physical Review B* **95,** 235403 (2017).
39. Jacobsen, S. H., Ouassou, J. A. & Linder, J. *Advanced Magnetic and Optical Materials* chap. 1. Superconducting Order in Magnetic Heterostructures (Wiley, 2017).
40. Eilenberger, G. Transformation of Gorkov's equation for type II superconductors into t ransport-like equations. *Zeitschrift für Physik A Hadrons and nuclei* **214,** 195–213 (1968).
41. Eckern, U. & Schmid, A. Quasiclassical Green's function in the BCS pairing theory. *Journal of Low Temperature Physics* **45,** 137–166 (1981).
42. Shelankov, A. L. On the derivation of quasiclassical equations for superconductors. *Journal of low temperature physics* **60,** 29–44 (1985).
43. Bergeret, F. S. & Tokatly, I. V. Manifestation of extrinsic spin Hall effect in superconducting structures: Nondissipative magnetoelectric effects. *Physical Review B* **94,** 180502 (2016).
44. Eschrig, M., Cottet, A., Belzig, W. & Linder, J. General boundary conditions for quasiclassical theory of superconductivity in the diffusive limit: application to strongly spin-polarized systems. *New Journal of Physics* **17,** 083037 (2015).
45. Kuprianov, M. Y. & Lukichev, V. F. Influence of boundary transparency on the critical current of dirty SS'S structures. *Zh. Eksp. Teor. Fiz* **94,** 149 (1988).
46. Jacobsen, S. H., Ouassou, J. A. & Linder, J. Critical temperature and tunneling spectroscopy of superconductor-ferromagnet hybrids with intrinsic Rashba-Dresselhaus spin-orbit coupling. *Physical Review B* **92,** 024510 (2015).
47. Ouassou, J. A. & Linder, J. Voltage control of superconducting exchange interaction and anomalous Josephson effect. *Physical Review B* **99** (21 2019).

48. Ouassou, J. A. *Density of States and Critical Temperature in Superconductor/Ferromagnet Structures with Spin-Orbit Coupling* , M.Sc. thesis, (2015), 33–34.
49. Bruno, R. C. & Schwartz, B. B. Magnetic field splitting of the density of states of thin superconductors. *Physical Review B* **8,** 3161 (1973).
50. Ghanbari, A., Erlandsen, E., Sudbø, A. & Linder, J. Going beyond the Chandrasekhar-Clogston limit in a flatband superconductor. *Physical Review B* **105,** L060501 (2022).
51. Bobkova, I. V. & Bobkov, A. M. Recovering the superconducting state via spin accumulation above the pair-breaking magnetic field of superconductor/ferromagnet multilayers. *Physical Review B* **84** (2011).
52. Bakurskiy, S. V., Klenov, N. V., Soloviev, I. I., Kupriyanov, M. Y. & Golubov, A. A. Superconducting phase domains for memory applications. *Applied Physics Letters* **108** (2016).
53. Takahashi, S. & Maekawa, S. Spin current, spin accumulation and spin Hall effect. *Science and Technology of Advanced Materials* **9,** 014105 (2008).
54. Brinkman, A. & Golubov, A. A. Crossed Andreev reflection in diffusive contacts: Quasiclassical Keldysh-Usadel formalism. *Physical Review B* **74,** 214512 (2006).
55. Falci, G., Feinberg, D. & Hekking, F. W. J. Correlated tunneling into a superconductor in a multiprobe hybrid structure. *Europhysics Letters* **54,** 255 (2001).
56. Liu, Y., Yu, Z., Liu, J., Jiang, H. & Yang, S. A. Transverse shift in crossed Andreev reflection. *Physical Review B* **98,** 195141 (2018).
57. Jakobsen, M. F., Brataas, A. & Qaiumzadeh, A. Electrically controlled crossed Andreev reflection in two-dimensional antiferromagnets. *Physical Review Letters* **127,** 017701 (2021).

Appendix A: Numerical code

Matrices, Green functions, observables and basic operations

```
import numpy as np
from scipy.integrate import solve_bvp, simpson
from scipy.interpolate import CubicSpline
import sys
from tqdm import tqdm
from time import time
np.set_printoptions(precision=14, floatmode='fixed')


# MATRICES

# Pauli matrices
sigma_x = np.array([[0,1], [1,0]])
sigma_y = np.array([[0, -1j], [1j, 0]])
sigma_z = np.array([[1,0], [0,-1]])

def dagger(g):
    """
    Dagger operator. np.complex128 conjugate and transpose.
    """
    return np.transpose(np.conjugate(g))

def comm(A, B):
    """
    Commutator between two matrices.
    """
    return A@B - B@A

def deltamatrix(dlta):
    """
    The anti-diagonal Delta self energy in the Usadel equation.
    :param delta: number
    :return: (4,4) matrix: antidiag(delta, -delta, delta^*, -delta^*)
    """
    selfenergy = np.zeros((4,4), dtype=np.complex128)
    selfenergy[0,3] = dlta
    selfenergy[1,2] = - dlta
    selfenergy[2,1] = np.conjugate(dlta)
    selfenergy[3,0] = - np.conjugate(dlta)

    return selfenergy

def sigmablock(sigma):
    """ Create the (4,4) equilvalent of the Pauli matrices. """
    zero = np.zeros((2,2), dtype=np.complex128)
    return np.block([[sigma, zero], [zero, np.conjugate(sigma)]])




# GREEN FUNCTIONS
def gR(rctti):
    """
```

```
    Constructs the retarded Green function matrix g from the Ricatti matrices a and b.

    :param rctti: (32,) array of matrices belonging to one single node.
    :return: The (4,4) retarded Green function belonging to that node.
    """

    vm = vector_to_matrices(rctti)
    a,b = vm[0],vm[1]
    N, tN = create_N_and_tN(a, b)
    I = np.identity(2)

    g11 = N @ (I + a @ b)
    g12 = 2 * N @ a
    g21 = - 2 * tN @ b
    g22 = - tN @ (I + b @ a)

    return np.block([[g11, g12], [g21, g22]])

def gA(g_R):
    """
    Constructs the Advanced Green function given the retarded green function.

    :param gR: (4,4) matrix, the retarded green function.
    :return: the (4,4) advanced green function.
    """
    return - rho[4] @ dagger(g_R) @ rho[4]

def gK(rctti, distr_fnc):
    """
    Construct the Keldysh green function from the retarded Green function
    and the distribution function.

    :param rctti: (32,) array. The retarded Green function
    (at one energy and one position).
    distr_fnc: (32,) array. The distribution function
    (at one energy and one position).
    :return: (4,4) array. The Keldysh Green function.
    """
    h, dh = h_and_dh_from_vec(distr_fnc)
    g_R = gR(rctti)
    g_K = g_R @ h - h @ gA(g_R)

    return g_K

def dgR(rctti):
    """
    Derivative of the retarded 4x4 Green function at one point: (d/dx gR) (x_n).
    :param rctti: (32,) array. The retarded Green function.
    :return: The derivative of the (4,4) retarded Green function
    """

    a, b, da, db = vector_to_matrices(rctti)
    N, tN = create_N_and_tN(a, b)

    dN  =  N @ (da @ b + a @ db) @  N
    dtN = tN @ (db @ a + b @ da) @ tN

    # blocks of d/dx g^R(x):
    ul = 2 * dN
```

```
    ur = 2 * (dN @ a + N @ da)
    ll = - 2 * (dtN @ b + tN @ db)
    lr = - 2 * dtN

    return np.block([[ul, ur], [ll, lr]])

def dgK(rctti, distr_fnc):
    """
    The derivative of the Keldysh Green function.
    :param rctti: (32,) array. The retarded Green function
    (at one energy and one position).
    distr_fnc: (32,) array. The distribution function
    (at one energy and one position).
    :return: (4,4) array. The derivative of the Keldysh Green function.
    """
    g_R = gR(rctti)
    dg_R = dgR(rctti)
    dg_A = gA(dg_R)

    h, dh = h_and_dh_from_vec(distr_fnc)

    dg_K = g_R @ dh - dh @ dg_A + dg_R @ h - h @ dg_A

    return dg_K

def rctti_and_drctti_from_FullretGF(full_retGF):
    """
    Extract rctti and d/dx rctti from a Full_RetardedGF object.

    :param full_retgf: Full_RetardedGF object
    :return: tuple - rctti, drctti. (e, 32, N) arrays.
    """
    E = full_retGF.energies
    x = full_retGF.xaxis
    rctti = full_retGF.rctti

    d_rctti = np.zeros(np.shape(rctti)) # derivative of rctti
    for e in range(E.size):
        full_retGF.energy_index = e
        d_rctti[e] = full_retGF.eom(x, rctti[e])

    return rctti, d_rctti



# OBSERVABLES

def delta(rctti, vect, E, ret_integrand=False):
    """
    Calculate delta (superconducting order parameter) given a retarded green function
    and a distribution function.

    Delta = - int_0^w dE [gK(E)]_21 + [gK(E)]_41

    :param rctti: (e, 32, N) array. The retarded Green function.
    :param vect: (e, 32, N) array. The distribuition function (parameterized).
    :param E: (e,) array. Energies.
    :param ret_integrand: True if the integrand
    should be returned.
```

```
    :return: (N,) array. Delta at each node.
             (e, N) array. Delta integrand at each node.
    """

    omega = E[0] # integration limit
    if E[-1] > E[0]:
        omega = E[-1]
    prefactor = 1/ (2*np.log(2*omega))

    N = rctti[0,0,:].size
    integrand_arr = np.zeros((E.size, N), dtype=np.complex128)
    for e in range(E.size):
        for i in range(N):
            g_K = gK(rctti[e,:,i], vect[e,:,i])
            integrand_arr[e,i] = -(g_K[1,2] + np.conjugate(g_K[3,0])) / 2

    dlta = -simpson(integrand_arr, E, axis=0) # integrate using Simpson's rule

    if ret_integrand:
        return integrand_arr
    return prefactor*dlta



# EQUILIBRIUM

def vector_to_matrices(rctti):
    """
    Extract the matrices a, b, da, db from the real vector rctti at *one* position.

    :param rctti: (32,) array. Contains the real and imaginary elements
    of a, b, da, and db.
    :return: (4,2,2) array: np.array([a, b, da, db])
    """

    vb = rctti[:16] + 1j*rctti[16:32]

    a  = np.reshape(vb[0:4], (2,2))
    b  = np.reshape(vb[4:8], (2,2))
    da = np.reshape(vb[8:12], (2,2))
    db = np.reshape(vb[12:], (2,2))

    return np.array([a, b, da, db])

def matrices_to_vector(M):
    """
    Make the real vector rctti from the matrices a, b, da, db at *one* position.

    :param M: (4,2,2) array: np.array([a, b, da, db])
    :return: (32,) numpy array. Contains the real and imaginary elements
    of a, b, da, and db.
    """
    Mr = np.real(M)
    Mi = np.imag(M)
    Mtot = np.array([Mr,Mi])
    return np.reshape(Mtot, (32,))

def v2m(v):
```

```
    """
    Similar function as vector_to_matrices, but for m positions instead of one position.
    :param v: (32, m). The ricatti parameterization at each position m.
    return: (4, 2, 2, m). a, b, da, db for each position m.
    """
    m = v[0,:].size
    M = np.reshape(v, (8, 2, 2, m)) # [Re(a), Re(b), Re(da), Re(db),
    #Im(a), Im(b), Im(da), Im(db)]
    M = M[0:4] + 1j * M[4:8] # [a, b, da, db] for each position
    return M

def m2v(M):
    """
    Similar function as matrices_to_vector, but for m positions instead og one.
    :param M: (4, 2, 2, m). a, b, da, db for each position m.
    return: (32, m). The ricatti parameterization vector at each position m..
    """
    m = M[0,0,0,:].size
    v = np.zeros((8,2,2,m))
    v[0:4], v[4:8] = np.real(M), np.imag(M)
    v = np.reshape(v, (32,m))
    return v

def create_N_and_tN(a, b):
    """
    Creates N and tN from the matrices a and b.
    :param a, b: (2,2). The matrices gamma and Tilde(gamma)
    :return: tuple, (2,2). N and tN=tilde(N).
    """
    I = np.identity(2)

    N  = np.linalg.inv(I - a @ b)
    tN = np.linalg.inv(I - b @ a)
    return N, tN

def full_equil_distrfnc(E, N, T, Vi=0):
    """
    Creates a (e,32,N) array containing the equilibrium distribution function.

    :param E: (e,) real array. Energies.
    :param N: number of nodes.
    :param T: temperature.
    :pram Vi: voltage.
    :return: (e,32,N) array. The distribution function in equilibrium.
    """

    distr_fnc = np.zeros((E.size,32,N))
    for e in range(E.size):
        for n in range(N):
            h = h_equil(T, E[e], Vi)
            dh = np.zeros(np.shape(h)) # the derivative is zero

            v, dv = coefficients_from_matr(h), coefficients_from_matr(dh)
            vec = make_vec(v, dv)

            distr_fnc[e,:,n] = vec

    return distr_fnc
```

```
def h_equil(T, Ei, Vi):
    """
    Equilibrium distribution function (matrix form).

    :param T: temperature/critical temperature
    :param Ei: energy
    :param Vi: voltage.
    :return: (4,4) array. The equilibrium distribution function at (T, Ei, Vi).
    """
    Ei = np.real(Ei)
    electron = np.tanh(1.76/T * (Ei-Vi)/2) * np.identity(2)
    hole = np.tanh(1.76/T * (Ei+Vi)/2) * np.identity(2)
    zero = np.zeros((2,2))
    return np.block([[electron, zero], [zero, hole]])

def mul(x, y):
    """
    Matrix multiplication of three dimentional arrays where the last dimension is
    position.
    Performs a 2x2 matrix multiplication x @ y for each position m.
    :param x, y: (2,2,m) arrays.
    :return: (2,2,m) = x @ y
    """
    return np.einsum('ijn,jkn->ikn', x, y)



# NON-EQUILIBRIUM

def make_basismatrices():
    """
    Create the basis matrices for (4,4) block diagonal matrix space.
    :return: rho = (8,4,4) array containing the eight (4,4) basis matrices.
    (rho0, rho1, rho2, ..., rho7)
    """
    rho4 = np.diag([1,1,-1,-1])

    # Pauli matrices
    sigma0 = np.identity(2)
    sigma1 = np.array([[0,1],[1,0]])
    sigma2 = np.array([[0,-1j], [1j, 0]])
    sigma3 = np.array([[1,0],[0,-1]])

    b0 = sigmablock(sigma0)
    b1 = sigmablock(sigma1)
    b2 = sigmablock(sigma2)
    b3 = sigmablock(sigma3)
    b4 = rho4 @ b0
    b5 = rho4 @ b1
    b6 = rho4 @ b2
    b7 = rho4 @ b3

    rho = np.array([b0, b1, b2, b3, b4, b5, b6, b7])

    return rho

rho = make_basismatrices()

def coeff_in_b_basis(M, n):
```

```
    """
    Find the projection of the matrix M on the n-th element rho_n of the rho-basis.

    :param M: (4,4) array.
    :param n: index of the basis matrix.
    :return: Mn. Number. Projection of M on bn.
    """
    return np.trace(rho[n] @ M) / 4

def coefficients_from_matr(M):# coefficients from matrix
    """
    Transform a (4,4) block diagonal matrix into the corresponding (8,)-array in
    rho-space.

    :param M: (4,4) block diagonal matrix.
    :return: (8,) vector. The matrix m expressed in the rho-basis.
    """

    M0 = coeff_in_b_basis(M, 0)
    M1 = coeff_in_b_basis(M, 1)
    M2 = coeff_in_b_basis(M, 2)
    M3 = coeff_in_b_basis(M, 3)
    M4 = coeff_in_b_basis(M, 4)
    M5 = coeff_in_b_basis(M, 5)
    M6 = coeff_in_b_basis(M, 6)
    M7 = coeff_in_b_basis(M, 7)

    v = np.array([M0, M1, M2, M3, M4, M5, M6, M7])

    return v

def matrix_from_coefficients(v):
    """
    Construct the full (4,4) block diagonal matrix from its coefficients in
    the rho-basis.

    :param v: (8,) array containing (M0, M1, ..., M7) = the coeffiecients in
    the rho-basis.
    :return: (4,4) matrix belonging to v.
    """
    M = np.zeros((4,4), dtype=np.complex128)
    for n in range(8):
        M += v[n] * rho[n]
    return M

def make_vec(v, dv):
    """
    From the two (8,m) arrays v and dv, create one real (32,m) array.
    If m=0, then there is no second dimension to the vectors involved.

    :param v: (8,m) array (np.complex128)
    :param dv: (8,m) array (np.complex128)
    :return: (32,m) array (real) = [Re(v), Re(dv), Im(v), Im(dv)]
    """
    vec = np.array([np.real(v), np.real(dv), np.imag(v), np.imag(dv)]) # (4, 8, m)
    if v.size == 8:
        return np.reshape(vec, (32,))
    else:
        m = v[0,:].size
```

```
        return np.reshape(vec, (32,m))

def split_vec(vec):
    """
    Extract the np.complex128 (8,m) vectors v and dv from vec.
    :param vec: (32,m) array. [Re(v), Re(dv), Im(v), Im(dv)].
    :return: v, dv. Both have shape (8,m)
    """
    k = 8
    v = vec[0:8] + vec[16:24] * 1j
    dv = vec[8:16] + vec[24:32] *1j

    return v, dv

def h_and_dh_from_vec(vec):
    """"
    Split the real, parametrized vector and construct the belonging matrices.

    :param vec: (32,) array
    :return: the 4x4 matrices belonging to vec
    """
    v, dv = split_vec(vec) # parameterized distribution fnc + derivative
    h_matr = matrix_from_coefficients(v) # distribution function
    dh_matr = matrix_from_coefficients(dv) # derivative of distribution function
    return h_matr, dh_matr

def mul_Mv(M, v):
    """
    Matrix times vector for multiple positions at once.
    The dinemsion of the matrices and vectors are 8 in the code, but in
    principle they could have any dimension.

    :param M: (8,8,m). Matrices of dimension (8,8) for each of the m positions
    v: (8, m). Vector of dimension (8,m) for each position
    return: (8,m). Mv for each position.
    """
    return np.einsum('ikn,kn->in', M, v)


def save_arraylist_to_file(lst, path):
    """
    A function for saving any number of flattened arrays into the same .npy-file.
    Each array needs a unique load_from_file()-function, because this function
    does not save the shape of the arrays nor their names.

    :param lst: list containing arrays. The arrays in lst has shape (m,)
    where m could be any number.
    :param path: the path to the place where we save the arrays.
    :return: None
    """

    L = len(lst) # number of arrays
    lengths = [] # lengths of arrays in lst

    tot = 1 # total numer of elements we want to save: for each array,
    #we save the number of elements and the elements.
    for el in lst:
        lengths += [el.size] # we need to save each element of the array
        tot += 1 + el.size # plus one because we also need the total
```

```
        #number of elements in the array

    # initialize the array we want to save.
    arr = np.zeros(tot, dtype=np.complex128)
    arr[0] = L

    c = L+1 # counter. The index for where the next array should be inserted in arr.
    for i in range(L):
        li = lengths[i] # lenght of array i in lst
        arr[i+1] = li
        arr[c:c + li] = lst[i]
        c += li

    # save arrays
    np.save(path, arr)

    return None

def append_to_file(arr, filename, overwrite=False):
    """
    Append an array to a .txt-file. The arrays are stores as two lists:
    Re(arr) and Im(arr).
    Different arrays are separated by #.

    :param arr: (m,) array to be written to file.
    :param filename: path to file
    :param overwrite: boolean. True if we do not want to overwrite the file:
    instead erase whatever is in the file
        from before and write the array into the empty file.
    """
    arr_str = str(np.real(arr)) + str(np.imag(arr)) + '#'
    m = 'a' # append mode

    if overwrite:
        m='w' # if filename is not empty, empty it and start writing.
        # print('Warning: do NOT open '+filename+' while the program is running!')

    file = open(filename, m) # open text file for appending the newly calculated delta
    file.write(arr_str)
    file.close()
    return 0
```

Solvers

```
class Full_RetardedGF:
    """
    This class contains the retarded Green function, and functions for solving the
    Usadel equation in equilibrium.
    """

    def __init__(self, l, N, r, T, E, q, exchange, rctti=np.empty(0),
                 delta=np.empty(0)):
        """
        This class contains the retarded Green function, and functions for solving the
        Usadel equation in equilibrium.

        :param l: system length / xi0
        :param N: number of nodes at the x-axis
        :param r: Interface parameters. Either a number or a (2,) array if the
        interface parameter is different at the left and right border.
        :param T: temperatures.  Either a number or a (2,) array if the temperature
        is different at the left and right border.
        :param E: (e,). Energies.
        :param q: inelastic scattering. Real number.
        :param exchange: (3,) array. Spin splitting field in directions x, y, z.
        :param rctti: (e,32,N) real array. The retarded green function at each
        energy and node.
        :param delta: (N,). The superconducting order parameter / gap at each node.
        """

        self.length = l
        self.N = N
        self.xaxis = np.linspace(0,l,N)

        self.energies = E
        e = self.energies.size

        self.q = q #  inelastic scattering term
        self.exchange = exchange # exchange field

        try: # is r an number or an array?
            dummy = int(r)
            self.interface_parameters = np.array([r,r]) # (rL, rR)
        except:
            self.interface_parameters = r

        try: # is T a number or an array?
            dummy = int(T)
            self.temperatures = np.array([T, T])
        except:
            self.temperatures = T # (TL, TR)

        if rctti.size: # if rctti is given
            self.rctti = rctti
            self.guess_prev_res = False # the guess for (e,n) is rctti(e,n)
            #- not the previously calculated value.
        else:
            self.rctti = np.zeros((e,32,N)) # guess: normal metal
            self.guess_prev_res = True # the guess for (e,n) is rctti(e-1,n).
```

```
        #Ie. use the previously calculated value as a guess.

    if delta.size: # if delta is given
        self.delta = delta
    else:
        self.delta = np.zeros(N, dtype=np.complex128)

    self.energy_index = 0

    # choose boundary conditions
    self.nxn = False
    self.nxn_transparent = False
    self.vxv = False

def save_to_file(self, path):
    """
    Save relevant information from the object to a file.
    The object can then be loaded from the file.

    :param path: path to the file where the object is saved. Ending with .npy.
    """
    # the arrays we save
    lst = [self.xaxis, self.energies, np.array([self.q]), self.interface_parameters,
    self.temperatures, self.rctti.flatten(), self.delta, self.exchange]
    # save
    save_arraylist_to_file(lst, path)

# ---- EOM AND BC ----------------------------------------------------------------------------------
def eom(self, x, rctti):
    """
    Equation of motion for the retarded Green function.

    :param x: (m,), the x-axis.
    :param rctti: (32, m), the retarded green function at each position m.
    :return: (32, m), derivative d/dx rctti at each position m.
    """

    m = x.size
    M = v2m(rctti) # (4, 2, 2, m)
    a, b, da, db = M[0], M[1], M[2], M[3] # (2,2,m)

    # create the matrices N and tilde(N)
    I = np.transpose(np.full((m, 2, 2), np.identity(2)), (1,2,0)) # (2,2,m)
    N_inv = I - mul(a, b) # (2, 2, m)
    tN_inv = I - mul(b, a)
    N = np.transpose(np.linalg.inv(np.transpose(N_inv, (2,0,1))), (1,2,0))
    # transposing due to np.linalg.inv taking inverse over the two last axes
    tN = np.transpose(np.linalg.inv(np.transpose(tN_inv, (2,0,1))), (1,2,0))

    # current energy including inelastic scattering
    Ei = self.energies[self.energy_index] + 1j * self.q

    # normal metal
    d_da = - (2 * mul(mul(da, tN), mul(b, da)) + 2j*a * Ei)
    d_db = - (2 * mul(mul(db, N),  mul(a, db)) + 2j*b * Ei)

    # superconductivity
    if np.count_nonzero(self.delta):
        if not np.array_equal(x, self.xaxis):
```

```
            d = CubicSpline(self.xaxis, self.delta)(x)
            # interpolate delta if the x-axis is not the original one
        else:
            d = self.delta

        delta_sigma = np.einsum('n,ij->ijn', d, sigma_y)
        # (2,2,m). sigma_y * delta(x) at each position
        deltacon_sigma = np.einsum('n,ij->ijn', np.conjugate(d), sigma_y)
        # (2,2,m). sigma_y * conjugate(delta(x)) at each position

        d_da += - (delta_sigma - mul(mul(a, deltacon_sigma), a))
        d_db += - (- deltacon_sigma + mul(mul(b, delta_sigma), b))

    # spin-splitting field
    if np.count_nonzero(self.exchange):
        h = ( np.transpose(np.full((m, 2, 2), sigma_x), (1,2,0)) * self.exchange[0]
            + np.transpose(np.full((m, 2, 2), sigma_y), (1,2,0)) * self.exchange[1]
            + np.transpose(np.full((m, 2, 2), sigma_z), (1,2,0)) * self.exchange[2] )


        d_da += - 1j * ( mul(h, a) - mul(a, np.conjugate(h)) )
        d_db += 1j * (mul(np.conjugate(h), b) - mul(b, h))

    return m2v(np.array([da, db, d_da, d_db]))

def bc_nxn(self, rctti_left, rctti_right):
    """
    Boundary conditions for a normal metal on both sides.

    :param rctti_left: (32,). Retarded Green function just inside the
    left border.
    :param rctti_right: (32,). Retarded Green function just inside the
    right border.
    :return: (32,). The residuals of the boundary conditions.
    """
    l = self.length

    # left
    rl = self.interface_parameters[0] # interafce parameter
    al, bl, dal, dbl = vector_to_matrices(rctti_left) # ricatti matrices
    res_al = dal - 1/(2 * rl * l) * al
    res_bl = dbl - 1/(2 * rl * l) * bl

    # right
    rr = self.interface_parameters[1]
    ar, br, dar, dbr = vector_to_matrices(rctti_right)
    res_ar = dar + 1/(2 * rr * l) * ar
    res_br = dbr + 1/(2 * rr * l) * br

    return matrices_to_vector([res_al, res_bl, res_ar, res_br])

def bc_transparent(self, rctti_left, rctti_right):
    """
    Transparent bc for NXN.
    rctti in N is zero.
    """
    al, bl, dal, dbl = vector_to_matrices(rctti_left)
    ar, br, dar, dbr = vector_to_matrices(rctti_right)
```

```
    return matrices_to_vector(np.array([al, bl, ar, br]))

def bc_vxv(self, rctti_left, rctti_right):
    """
    KL bc for VXV.
    """
    al, bl, dal, dbl = vector_to_matrices(rctti_left)
    ar, br, dar, dbr = vector_to_matrices(rctti_right)

    return matrices_to_vector(np.array([dal, dbl, dar, dbr]))

def bc_snn(self, rctti_left, rctti_right):
    l = self.length

    # left border: SX
    rl = self.interface_parameters[0]
    g_R = gR(rctti_left)
    dg_R = dgR(rctti_left)

    Ei = self.energies[self.energy_index]
    dlta = 1 # gap in S
    d = deltamatrix(dlta)
    q = self.q
    if Ei > dlta:
        pref = 1 / np.emath.sqrt((Ei + 1j*q)**2 - np.abs(dlta)**2)
    else:
        pref = -1j / np.emath.sqrt(np.abs(dlta)**2 - (Ei + 1j*q)**2)

    g_SC = pref * (Ei*rho[4] + d)

    kuprluki = g_R @ dg_R - 1/(2*l*rl) * comm(g_SC, g_R)

    res_al = kuprluki[0:2, 0:2]
    res_bl = kuprluki[2:4, 0:2]

    # right border: XN
    rr = self.interface_parameters[1]
    ar, br, dar, dbr = vector_to_matrices(rctti_right)
    res_ar = dar + 1/(2 * rr * l) * ar
    res_br = dbr + 1/(2 * rr * l) * br

    return matrices_to_vector([res_al, res_bl, res_ar, res_br])



# ---- SOLVE ----------------------------------------------------------------
def solve(self, e, guess):
    """
    Solve the retarded Usadel equation for a given energy.

    :param e: energy index. We solve the equation for Ei = energies[e]
    :param guess: (32,N) array. Initial gess on the retarded green function.
    :return: The return object of solve_bvp
    """
    self.energy_index = e # update energy index

    if self.nxn:
        bc = self.bc_nxn
    elif self.nxn_transparent:
```

```
            bc = self.bc_transparent
        elif self.vxv:
            bc = self.bc_vxv


        sol = solve_bvp(self.eom, bc, self.xaxis, guess) # solve

        if not sol.success:
            print(sol.message)
            sys.exit()

        # update the object's retarded green function at energy Ei.
        self.rctti[e] = sol.sol(self.xaxis)

        return sol

    def full_solve(self):
        """
        Solve the retarded Usadel equation for all energies.
        :param path: path to file where the result is saved.
        :return: None.
        """

        for e in tqdm(range(self.energies.size)):
            # make a guess
            if self.guess_prev_res: # use previous result as guess
                if e==0:
                    guess = self.rctti[0]
                else:
                    guess = self.rctti[e-1]
            else: # rctti is given: typically the a result that is already calculated
                guess = self.rctti[e]

            # solve
            sol = self.solve(e, guess)



class Full_DistrFnc:
    """
    The purpose of this class is to solve equations of motion for the distribution
    function for a collection of energies and voltage differences.
    """
    def __init__(self, l, N, r, T, E, V, q, rctti_in, d_rctti_in,
                 exchange, vect=np.empty(0)):
        """
        :param l: system length / xi0
        :param N: number of nodes at the x-axis
        :param r: Interface parameters. Either a number or a (2,) array if the
        interface parameter is different at the left and right border.
        :param T: temperatures.  Either a number or a (2,) array if the temperature
        is different at the left and right border.
        :param E: (e,). Energies.
        :param V: (v,). Voltage differences. Left side: +V/2, right side: -V/2.
        :param q: inelastic scattering. Real number.
        :param rctti_out_l: (e,32). The ricatti parameterized green function
        just outside the left border.
        :param rctti_out_r: (e,32). The ricatti parameterized green function
```

```
    just outside the right border.
    :param rctti_in: (e,32,N). The ricatti parameterized green function
    inside the material.
    :param d_rctti_in: (e, 32, N). Derivative of rctti.
    :param exchange: (3,) array. Spin splitting field in directions x, y, z.
    :param vect: optional. (v, e, N, 32), the solved distribution function.
        If not specified, vec will be a placeholder until the equations are solved.
    """

    # ------- Object attributes that never changes -------

    self.length = l
    self.N = N
    self.xaxis = np.linspace(0,l,N)

    self.energies = E
    e = self.energies.size

    self.q = q #  inelastic scattering term

    self.voltages = V
    v = self.voltages.size

    self.rctti_in = rctti_in
    self.d_rctti_in = d_rctti_in

    try: # is r an number or an array?
        dummy = int(r)
        self.interface_parameters = np.array([r,r]) # (rL, rR)
    except:
        self.interface_parameters = r

    try: # is T a number or an array?
        dummy = int(T)
        self.temperatures = np.array([T, T])
    except:
        self.temperatures = T # (TL, TR)

    # choose boundary conditions
    self.snn = False
    self.nxn = False
    self.nxn_transparent = False

    self.same = False
    self.opposite = False

    # -- Matrices in Usadel equation and boundary conditions --
    self.coeff_matrices = np.zeros((6, self.N, e, 8, 8), dtype=np.complex128)
    # M, dM, Q, dQ, V and W: this array is especially useful when interpolating
    self.T_in  = np.zeros((2, e, 8, 8), dtype=np.complex128)
    # Matrix for boundary conditions
    self.T_out  = np.zeros((2, e, 8, 8), dtype=np.complex128)
    # Matrix for boundary conditions

    self.exchange = exchange
    self.magnt_matrix = ( exchange[0]*sigmablock(sigma_x)
        + exchange[1]*sigmablock(sigma_y) + exchange[2] * sigmablock(sigma_z) )
```

```
        # ———— Object attributes that changes while solving the eqs ————

        self.voltage_index = 0
        self.energy_index = 0
        self.position_index = 0
        self.guess = np.zeros((32, N))

        # self.vect contains the parameterized distribution function in the material.
        if vect.size:  # if a solution is already given
            self.vect = vect # (v,e,N,32)
        else:
            self.vect = np.zeros((v, e, N, 32)) # (v,e,N,32) real array. Placeholder.

        self.distrFnc_out_l = 0
        self.distrFnc_out_r = 0

        self.delta=None

# —— FUNCTIONS ——————————————————————————————————————————————————————————————
    def save_to_file(self, path):
        """
        Save the Full_DistrFnc object to a file.
        :param path: path to the file with the .npy ending.
        """
        # List of arrays to be saved
        lst = [self.xaxis, self.interface_parameters, self.temperatures,
        self.energies, np.array([self.q]), self.voltages, self.rctti_in.flatten(),
        self.d_rctti_in.flatten(), self.vect.flatten(), self.exchange]
        save_arraylist_to_file(lst, path)

    def calculate_matrices(self, delta_new):
        """
        Calculate the matrices M, dM, Q, dQ, V, W and T, and putting them into the
        object property coeff_matrices.
        This function should be called only once per time the eqs are solved!

        :param delta_new: (N,) array containing the superconducting order parameter
        at each position.
        :return None.
        """
        # print('- calculating matrices -')
        for e in tqdm(range(self.energies.size)):

            for side in [0, -1]: # left and right side
                gR_in = gR(self.rctti_in[e, :, side]) # ret gf just inside
                #left/right border
                gA_in = gA(gR_in) # avd gf just inside left/right border

                gR_out = rho[4] # Assume N reservoirs on both sides
                gA_out = gA(gR_out)

                self.T_in[side, e] = ( np.einsum('ik,␣nkj,␣jl,␣mli␣->␣nm',
                gA_out, rho, gR_in, rho) - np.einsum('ik,␣nkj,␣mjl,␣li␣->␣nm',
                gA_out, rho, rho, gA_in) - np.einsum('nik,␣kj,␣jl,␣mli␣->␣nm',
                rho, gR_out, gR_in, rho) + np.einsum('nik,␣kj,␣mjl,␣li␣->␣nm',
                rho, gR_out, rho, gA_in))

                self.T_out[side, e] = (  np.einsum('ik,␣nkj,␣jl,␣mli␣->␣nm',
                gA_in, rho, gR_out, rho) - np.einsum('ik,␣nkj,␣mjl,␣li␣->␣nm',
```

```
        gA_in, rho, rho, gA_out)- np.einsum('nik,kj,jl,mli->nm',
        rho, gR_in, gR_out, rho) + np.einsum('nik,kj,mjl,li->nm',
        rho, gR_in, rho, gA_out))


    for n in range(self.N):
        g_R = gR(self.rctti_in[e,:,n]) # ret gf at energy Ei and position n
        g_A = gA(g_R) # adv gf at energy Ei and position n
        dg_R = dgR(self.rctti_in[e,:,n]) # derivative ret gf at Ei, n
        dg_A = gA(dg_R) # derivative adv gf at Ei, n

        a, b, da, db = vector_to_matrices(self.rctti_in[e,:,n])
        N, tN = create_N_and_tN(a, b)

        # Need to find (d/dx)^2 gR.
        da, db, d_da, d_db = vector_to_matrices(self.d_rctti_in[e,:,n])

        # dN/dx
        dN  =  N @ (da @ b + a @ db) @  N
        dtN = tN @ (db @ a + b @ da) @ tN

        # (d/dx)^2 N
        d_dN  =  (dN @ (da @ b + a @ db) @  N +  N @ (da @ b + a @ db) @  dN
        +  N @ (d_da @ b + 2* da @ db + a @ d_db) @  N)
        d_dtN =( dtN @ (db @ a + b @ da) @ tN + tN @ (db @ a + b @ da) @ dtN
        + tN @ (d_db @ a + 2* db @ da + b @ d_da) @ tN)

        # construct (d/dx)^2 gR.
        ul = 2* d_dN # upper left block
        ur = 2* (d_dN  @ a + 2* dN  @ da +  N @ d_da) # upper right block
        ll = - 2* (d_dtN @ b + 2* dtN @ db + tN @ d_db) # lower left block
        lr = - 2* d_dtN # lower right block

        dd_gR = np.block([[ul, ur], [ll, lr]]) # (d/dx)^2 gR
        dd_gA = gA(dd_gR) # (d/dx)^2 gA

        d_gRdgR = dg_R @ dg_R + g_R @ dd_gR # d/dx (gR d/dx gR)
        d_gAdgA = dg_A @ dg_A + g_A @ dd_gA # d/dx (gA d/dx gA)

        dltamatr = deltamatrix(delta_new[n])

        M = (np.einsum('kis,lsi->kl', rho, rho)
        - np.einsum('kit,ts,lsr,ri->kl', rho, g_R, rho, g_A))

        dM = (- np.einsum('kit,ts,lsr,ri->kl', rho, dg_R, rho, g_A)
        - np.einsum('kit,ts,lsr,ri->kl', rho, g_R, rho, dg_A))

        Q = (np.einsum('mit,nts,sr,ri->nm', rho, rho, g_R, dg_R)
        - np.einsum('nit,mts,sr,ri->nm', rho, rho, g_A, dg_A))

        dQ = (np.einsum('mit,nts,si->nm', rho, rho, d_gRdgR)
        - np.einsum('nit,mts,si->nm', rho, rho, d_gAdgA))

        V_super =  1j * (np.einsum('nit,ts,sr,mri->nm', rho, dltamatr,
        g_R, rho) - np.einsum('nit,ts,msr,ri->nm', rho, dltamatr, rho, g_A)
        - np.einsum('it,nts,sr,mri->nm', dltamatr, rho, g_R, rho)
        + np.einsum('it,nts,msr,ri->nm', dltamatr, rho, rho, g_A) )

        V_magnt = 1j * (np.einsum('nit,ts,sr,mri->nm', rho,
```

```
            self.magnt_matrix, g_R, rho)
            - np.einsum('nit,uts,msr,uri->nm', rho, self.magnt_matrix, rho, g_A)
            - np.einsum('it,nts,sr,mri->nm', self.magnt_matrix, rho, g_R, rho)
            + np.einsum('it,nts,msr,uri->nm', self.magnt_matrix, rho, rho, g_A) )

            W = np.zeros((8,8))

            self.coeff_matrices[:, n, e] = np.array([M, dM, Q, dQ,
                                                     V_super + V_magnt, W])

    return None


# ---- EOM AND BC ----------------------------------------------------------------
def eom(self, x, vec):
    """
    Equation of motion for the parametrized distribution function hvec at
    all positions and one energy.

    :param x: (m,) array. x-axis. NOT self.xaxis!
    :param vec: (32,m) array containing hv and dhv at each node.
    :return: (32,m) array containing d/dx vec.
    """
    if np.array_equal(x, self.xaxis):
        cm = self.coeff_matrices[:,:,self.energy_index,:,:] #(6,m,8,8)
    else: # interpolate the coefficient matrices if the x-axis is not the original.
        cm = CubicSpline(self.xaxis,
             self.coeff_matrices[:,:,self.energy_index,:,:], axis=1)(x)
    cm = np.transpose(cm, (0, 2, 3, 1))

    M, dM, Q, dQ, V, W = cm[0], cm[1], cm[2], cm[3], cm[4], cm[5] # (8, 8, m)
    M_inv =  np.transpose(np.linalg.inv(np.transpose(M, (2,0,1))), (1,2,0))

    hv, dhv = split_vec(vec)

    d_dhv = - mul_Mv(M_inv, mul_Mv(dM + Q, dhv) + mul_Mv(dQ + V, hv) )

    return make_vec(dhv, d_dhv)

def bc_transparent(self, vec_l, vec_r):
    """
    Transparent (continuous) boundary conditions.
    Demands that the distribution function inside the material is the equilibrium
    one.

    :param vec_l: (32,). The distribution function just inside the left border.
    :param vec_r: (32,). The distribution function just inside the right border.
    :return: (32,). The residuals of the boundary conditions.
    """
    hout_l = coefficients_from_matr(self.distrFnc_out_l) # the outside (equilibrium)
    #distribution function
    hl, dhl = split_vec(vec_l) # distribution function just inside left border
    res_l = hout_l - hl # residual

    hout_r = coefficients_from_matr(self.distrFnc_out_r)
    hr, dhr = split_vec(vec_r)
    res_r = hout_r - hr

    res = make_vec(res_l, res_r)
```

```
        return res

    def bc_NXN(self, vec_l, vec_r):
        """
        KL boundary conditions for normal metal on both sides.

        :param vec_l: (32,). The distribution function just inside the left border.
        :param vec_r: (32,). The distribution function just inside the right border.
        :return: (32,). The residuals of the boundary conditions.
        """
        e = self.energy_index
        rl = self.interface_parameters[0]  # interface parameter at left interface
        rr = self.interface_parameters[1]  # at right interface
        l = self.length

        # left border
        M_l, Q_l = self.coeff_matrices[0, 0, e], self.coeff_matrices[2, 0, e]
        Tin_l = self.T_in[0, e]
        Tout_l = self.T_out[0, e]

        hout_l = coefficients_from_matr(self.distrFnc_out_l)
        hl, dhl = split_vec(vec_l)

        res_l = M_l @ dhl + Q_l @ hl - 1/(2*l*rl) * (Tout_l @ hout_l - Tin_l @ hl)

        # right border
        M_r, Q_r = self.coeff_matrices[0, -1, e], self.coeff_matrices[2, -1, e]

        Tin_r = self.T_in[1, e]
        Tout_r = self.T_out[1, e]

        hout_r = coefficients_from_matr(self.distrFnc_out_r)
        hr, dhr = split_vec(vec_r)

        res_r = M_r @ dhr + Q_r @ hr + 1/(2*l*rr) * (Tout_r @ hout_r - Tin_r @ hr)


        res = np.array([np.real(res_l), np.real(res_r), np.imag(res_l), np.imag(res_r)])
        return res.flatten()


# ---- SOLVE ----------------------------------------------------------------------
    def solve(self, v, e):
        """
        Solve the equation of motion with KL boundary conditions for energy
        E[e] and voltage V[v]. The distribution function on the outside is the
        equilibrium distribution function.

        :param v: voltage index
        :param e: energy index
        :return: the object that solve_bvp returns.
        """
        self.voltage_index = v
        self.energy_index  = e

        # Equilibrium distribution functions on the outside.
        T = self.temperatures[0]
        Ei = self.energies[e]
```

```
        Vi = self.voltages[v]

        p = np.tanh(1.76/T * (Ei + Vi)/2)
        m = np.tanh(1.76/T * (Ei - Vi)/2)


        if e==0:
        self.distrFnc_out_l = np.diag(np.array([p, m, m, p]))
        # spin voltage Vi in z-direction
        # self.distrFnc_out_l = np.diag(np.array([m, m, p, p]))
        # ordinary voltage

        if self.same:
            self.distrFnc_out_r = np.diag(np.array([p, m, m, p]))
            # spin voltage Vi in z-direction
            # self.distrFnc_out_r = np.diag(np.array([m, m, p, p]))
            # ordinary voltage
        elif self.opposite:
            self.distrFnc_out_r = np.diag(np.array([m, p, p, m]))
            # spin voltage -Vi in z-direction
            #self.distrFnc_out_r = np.diag(np.array([p, p, m, m]))
            # ordinary voltage
        else:
            sys.exit('Choose same or opposite signs on voltages!')

        if self.nxn:
            bc = self.bc_NXN
        # elif self.nxn_transparent:
        #     bc = self.bc_transparent
        else:
            sys.exit('Choose a boundary condition')

        sol = solve_bvp(self.eom, bc, self.xaxis, self.guess)
        if not sol.success:
            print(sol.message)
            sys.exit()

        self.vect[v, e] = np.transpose(sol.sol(self.xaxis))
        # update vec according to the solution of the equation

        return sol

    def full_solve(self, path):
        """
        Solve the equation of motion for all energies and voltage differences.
        The result is saved to file for each energy and each voltage in case
        something crashes and the function is not able to finish.

        :param path: path to the file where the resulting object is saved,
        with ending .npy.
        """

        for v in range(self.voltages.size):
            for e in tqdm(range(self.energies.size)):
                self.guess = np.transpose(self.vect[v, e])
                sol = self.solve(v, e)

            self.save_to_file(path)
```

```
def absolute_convergence(new, old, tol):
    """
    Absolute convergence criteria.
    :param new: new array
    :param old: old array
    :param tol: tolerance
    :return: True if new and old are close enough. False otherwise.
    """
    F_real = np.max( np.abs( np.real(new - old) ) )
    F_imag = np.max( np.abs( np.imag(new - old) ) )

    if F_real<tol and F_imag<tol:
        return True
    else:
        return False



def solve(tol, V, exchange, filename, dltaguess, s, o):
    """"
    Solve the Retarded + Keldysh Usadel equation self consistently.
    """

    homepath = ''
    projectpath = ''


    # constants
    l = 8 # system length / xi0
    N = 100 # number of nodes
    x = np.linspace(0,l,N) # xaxis

    # Unevenly spaced energies
    E = np.zeros(500)
    E[0:50] = np.linspace(30, 3, 50, endpoint=False)
    E[50:500] = np.linspace(3, 1e-3, 450)

    q = 1e-2 # inelastic scattering in retarded Usadel equation
    r = 3 # interface parameter
    T = 1e-2 # temperature in reservoirs

    delta_new = CubicSpline(np.linspace(0,l,100),
                np.full(100, dltaguess, dtype=np.complex128))(x)
    delta_old = np.copy(delta_new) + 10 * tol  # the previous delta.
    # At the moment chosen in such a way that the while-loop starts

    # objects to solve for
    ret_gf = Full_RetardedGF(l, N, r, T, E, q, exchange)
    rctti, d_rctti = rctti_and_drctti_from_FullretGF(ret_gf)
    disfnc = Full_DistrFnc(l, N, r, T, E, np.array([V]), q, rctti, d_rctti, exchange)

    # choose boundary conditions
    ret_gf.nxn = True # KL bc, normal metal on the sides
    disfnc.nxn = True # KL bc, normal metal on the sides
    disfnc.same = s # V on both sides if same, V on left and -V on right if opposite
    disfnc.opposite = o

    counter = 0
```

```
while not absolute_convergence(delta_new, delta_old, tol):
    counter += 1
    it_time = time()
    # - - - - - - - - - - - - - - - - - - - - - - - - - - - -
    # update retarded equation according to the recently calculated delta
    ret_gf.delta = delta_new
     # Solve the retarded Green function
    ret_gf.full_solve()

    # update rctti and d_rctti in distribution_function according
    # to the solution for the retarded green function
    disfnc.rctti_in, disfnc.d_rctti_in = rctti_and_drctti_from_FullretGF(ret_gf)
     # calculate matrices belonging to new rctti and new delta
    disfnc.calculate_matrices(delta_new)
    # Solve the distribution function
    disfnc.full_solve(projectpath+'greenfunctions/DF_'+filename[1:-2]+'.npy')

    delta_old = np.copy(delta_new)
    # calculate delta from the calcualted green function and distribution function
    delta_new = delta(ret_gf.rctti, np.transpose(disfnc.vect[0], (0,2,1)), E)
    # - - - - - - - - - - - - - - - - - - - - - - - - - - - -

     # save delta
    append_to_file(delta_new, projectpath+'deltas/deltas_'+filename[1:-2]+'.txt')

return ret_gf, disfnc
```

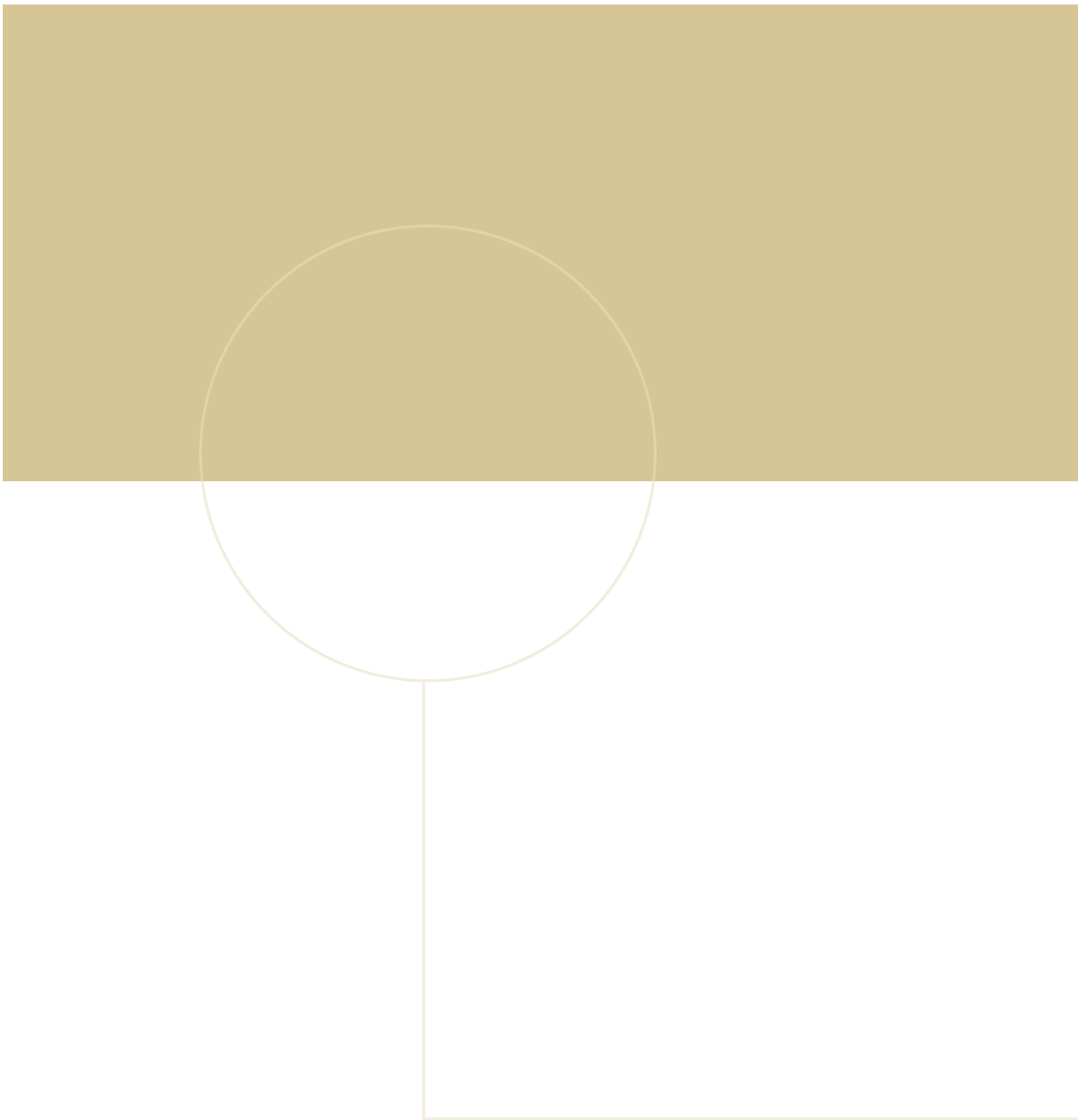

NTNU

Norwegian University of
Science and Technology